Biomaterials Science

ROYAL SOCIETY OF CHEMISTRY

REVIEW

View Article Online
View Journal | View Issue

Check for updates

Cite this: *Biomater. Sci.*, 2024, **12**, 4546

Tailoring of bioactive glass and glass-ceramics properties for *in vitro* and *in vivo* response optimization: a review

Elisa Piatti, * Marta Miola and Enrica Verné

Received 26th September 2023,
Accepted 5th March 2024

DOI: 10.1039/d3bm01574b

rsc.li/biomaterials-science

Bioactive glasses are inorganic biocompatible materials that can find applications in many biomedical fields. The main application is bone and dental tissue engineering. However, some applications in contact with soft tissues are emerging. It is well known that both bulk (such as composition) and surface properties (such as morphology and wettability) of an implanted material influence the response of cells in contact with the implant. This review aims to elucidate and compare the main strategies that are employed to modulate cell behavior in contact with bioactive glasses. The first part of this review is focused on the doping of bioactive glasses with ions and drugs, which can be incorporated into the bioceramic to impart several therapeutic properties, such as osteogenic, proangiogenic, or/and antibacterial ones. The second part of this review is devoted to the chemical functionalization of bioactive glasses using drugs, extra-cellular matrix proteins, vitamins, and polyphenols. In the third and final part, the physical modifications of the surfaces of bioactive glasses are reviewed. Both top-down (removing materials from the surface, for example using laser treatment and etching strategies) and bottom-up (depositing materials on the surface, for example through the deposition of coatings) strategies are discussed.

Open Access Article. Published on 06 Eost 2024. Downloaded on 2026-06-06 12:45:47.
This article is licensed under a Creative Commons Attribution 3.0 Unported Licence.

Introduction

Bioactive glasses (BGs) are a particular class of ceramics characterized by the well-known ability to interact and bond with hard tissues and, in some cases, also with soft tissues.[1,2] The term bioactivity means the ability of a material to be active biologically, evoking a specific biological response that results in a bond between the material itself and a tissue.[3] In particular, bioactive glasses fulfill their bioactivity through specific surface reactions that lead to the development of a silica gel layer that gradually promotes the formation of a layer of a biologically active mineral similar to hydroxyapatite (HA), generally called the HA-like layer, in the presence of body fluids *in vitro* or *in vivo*.[3] Thanks to its chemical and structural similarity to the mineral constituent of bone, the newly formed HA can bond firmly with living bone and surrounding tissues, providing an interfacial bond between the implant and the body tissue.[1] Moreover, while degrading at a controllable rate and converting to HA-like material, BGs release ions in a controlled manner.[4]

In recent years, regenerative medicine and tissue engineering (TE) have emerged as innovative promising approaches for the repair and regeneration of lost or damaged tissues and organs.[5] They have the potential to overcome the problems of the shortage of donor tissues and organs available for transplantation and possible donor site morbidity,[2,6,7] thanks to the development of new artificial materials and scaffolds, that are able to promote cell proliferation and tissue growth *in vitro* and *in vivo*.[6]

The clinical need for engineered bone tissue is still challenging in the field of orthopedic and craniofacial surgery, in direct relationship to the increasing human population and numerousness of traumatic injuries and pathological diseases, that can impair normal bone functions and lead to bone fractures non-unions, immobility, severe pain and deformity.[7] Nowadays, the demand for bone grafts is very high and represents the second most common tissue transplantation procedure after blood. Each year there are approximately 1 million cases of skeletal defects requiring bone graft procedures to achieve union, with significant socioeconomic consequences, and over 2.2 million bone graft procedures are conducted worldwide annually in orthopedics and dentistry.[7]

The human skeleton has exceptional healing ability, often with absolute functional and structural recovery, but in some cases, both external and biological factors can destroy the natural regenerative processes of bone.[7] Moreover, there is a critical size defect, beyond which a bone injury cannot be healed only by the natural bone healing capacity.[7] For example, in the case of extensive bone defects (such as bone fracture, that require the reconstruction of large bone segments), the bone self-healing mechanism is not feasible.[8]

Applied Science and Technology Department, Politecnico di Torino, Corso Duca degli Abruzzi 24, 10129 Torino, Italy. E-mail: elisa.piatti@polito.it

This journal is © The Royal Society of Chemistry 2024

Open Access Article. Published on 06 Eost 2024. Downloaded on 2026-06-06 12:45:47.
This article is licensed under a Creative Commons Attribution 3.0 Unported Licence.

Regeneration of large-size bone defects is clinically challenging and requires the use of multifunctional biomaterial, able to stimulate osteogenesis and angiogenesis and to obstacle bacterial infections.[9]

For a successful long-term implant, a good osseointegration is fundamental. This concept was first forwarded by Brånemark to describe a "direct structural and functional connection between ordered, living bone, and the surface of a load-carrying implant".[10] Osseointegration of implants is dependent on the attachment and proliferation of osteogenic cells on the implant surface, associated with the maturation and mineralization of their extracellular matrix (ECM).[11]

When an implant is inserted into the body, a complex series of events occur at its surface, leading to the adsorption of water molecules and proteins, that mediate the subsequent cellular adhesion and the activation and release of cytokines and other soluble growth/differentiation factors.[10] In the case of a bone implant, the activated osteogenic processes are very similar to those of bone healing,[10] involving multiple stimuli, both physical (such as substrate topography, stiffness, shear stress, and electrical forces) and biochemical (such as growth factors, cytokines, genes or proteins) factors.[7] Although the precise molecular mechanisms of osseointegration are still not totally understood, it is clear that the chemical and physical properties of the implant surface play a key role in the interactions between the implant and the host tissue, through the modulation of cell behavior, growth factor (GF) production and osteogenic gene expression.[10,12] Hence, to stimulate bone regeneration and osseointegration, BGs are designed to determine cell gene expression by four main mechanisms: (1) surface chemistry, (2) topography, (3) rate and type of dissolution of the released ions, and (4) shear stress at scaffold/bone interfaces (by *ad hoc* tailoring of their mechanical properties).[6]

Furthermore, the host immune system strongly interacts with the implanted biomaterial, producing various inflammatory and anti-inflammatory cytokines and exploiting strong paracrine effects that influence cellular activities, in a crosstalk between immune cells and all other cells involved in the bone regeneration process, although during bone tissue healing individual cell types play important roles even independently.[13] Therefore, the synthesis of BGs with anti-inflammatory properties could be useful to control post-implant inflammation and stimulate bone regeneration.

Recently, bioactive ceramics have been also applied in soft TE, in particular when regeneration of tissues at the interface with bone is required. Among these tissues, cartilage regeneration is widely studied[14,15] because the damage of the joints' articular cartilage such as the hip and knee is very common and can occur as a consequence of both degenerative diseases, such as osteoarthritis, and trauma, for example in sports injuries.[16] In these conditions, cartilage-engineered regeneration is of enormous benefit clinically.[16] Although, nowadays, there is no evidence of cartilage growth on a BG surface, the formation of a new subchondral bone layer seems to support cartilage-like tissue, at least at the extremities of osteochondral defects.[17] Therefore, for traumatic cartilage lesions and *osteochondritis dissecans*, the initial repair of subchondral bone could be a potentially advantageous approach for cartilage healing.[17] A solid surface or a support on which cartilage cells can spread is essential for the repair of cartilage in the case of large osteochondral defects.[17]

Pro-angiogenic properties are important not only in the case of soft TE and the regeneration of interfacial tissues but in tissue engineering in general, because a capillary/blood vessel network is a key requirement for blood supply and consequently oxygen and nutrient supply for the growing healing tissues, including bone tissue. Nowadays, the amount of oxygen required for cell survival in a tridimensional scaffold is limited to a diffusion distance between 150 and 200 μm from the supplying blood vessels.[18] For the *in vivo* survival of a tissue-engineered construct with a size larger than this oxygen diffusion limit, the tissue has to be vascularized and possess a capillary network for the delivery of oxygen and nutrients to the cells within the construct.[19] Thus, for a better regeneration of large bone defects, bioactive scaffolds must possess not only osteoconductivity (for the guidance of new bone growth), but also the ability to stimulate both osteogenesis (for promoting new bone formation) and angiogenesis (for inducing vascularization).[20] For example, in the case of highly vascularized bone, the lack of a functional microvasculature connected to the host blood supply has been identified as the culprit for implant failure.[6] In the case of large osseous defects, if nourishment and oxygen transport are insufficient, due to lacking angiogenesis, bone tissue can generally grow only up to a thickness of just 150–200 μm (corresponding to the diffusion limit of solutes and gases inside the tissue from the surface) before facing necrosis.[21,22]

Another critical issue related to bone implants is the risk of septic loosening. Unfortunately, despite the benefits of these artificial tissue substitutes and the strict antiseptic operative procedures, the problem of infections is still not solved[23] and the cells have to compete with bacteria to colonize the implant surface, in the so-called "race for the surface".[10] During the insertion of an implant, bacteria from the patient's own skin and/or mucosa enter the wound site, leading to implant-related infections, which are one of the most common reasons for surgical failure (14–29% of total failures), leading to implant removal.[23] This problem becomes even more critical when infections are caused by multidrug-resistant (MDR) pathogens.[10,24] Most infections occur in the form of biofilms, and hence they are extremely resistant to host defenses and therapy.[25] Hospital-acquired infections are, generally, considered to be the third-largest cause affecting public health.[10] Just a few data to highlight the gravity of this problem: in 2011, about 722 000 people in the United States (U.S.) were estimated to be involved in medical-device-related infections each year while residing in a U.S. hospital, and among them, about 75 000 patients died due to these infections;[26] whereas in Europe, each year more than 4.2 million patients are affected by bacterial infections acquired in hospitals.[26] Nowadays, the mortality rate of patients undergoing primary implant infections ranges from 10 to 18%. In the case of revised implants, this mortality rate can double or even

Open Access Article. Published on 06 Eost 2024. Downloaded on 2026-06-06 12:45:47.
This article is licensed under a Creative Commons Attribution 3.0 Unported Licence.

triple.[23] The phrase "race for the surface" was coined by Gristina in 1987 to describe the competition between bacteria and tissue cells for adhesion to and colonization of the implant surface.[10] The idea beyond this phrase was that a race takes place on the implant surface and it was believed that if this race is won by the bacteria, tissue cells will not be able to displace these primary colonizers to avoid biofilm formation and infection, whereas if the race is won predominantly by host tissue cells, the implant is protected from invading pathogens, allowing implant integration and tissue growth.[10] For example, the micro-environment of bone tissues can promptly become an excellent niche space for invading microbes thanks to their ability to adhere to both normal and necrotic bone surfaces, creating an ideal culture environment for continuous bacterial proliferation.[27] If the bacterial infection of an orthopedic prosthetic becomes chronic, it can serve as a septic focus leading to osteomyelitis, acute sepsis, and even death.[27] This approach has been recently improved by A. Cochis *et al.*[25] who have recently observed that co-cultures of cells and bacteria can be successfully used to simulate a competitive surface colonization, in addition to the ISO 22196 standard assays that use single-cell cultures or biofilm observation, demonstrating whether antibacterial surfaces are able to protect the adhered osteoblasts from the bacterial colonization as well as prevent the infection prior to the surface colonization by the osteoblasts.

Therefore, artificial implants have to be designed *ad hoc*, so that they can stimulate tissue regeneration and hinder bacterial colonization. In this context, for the fabrication of engineered biomaterials, it is important to point out that all types of cell (both mammalian and bacterial cells) are inherently sensitive to local chemical and topographical mesoscale, microscale, and nanoscale patterns, so that the topography, morphology, chemistry, surface energy, polarity, wettability and roughness of the implant strongly influence how the cells respond to the implant surface.[28–30] Moreover, the application properties of bioactive ceramics, including their biological influence on tissues and especially their biodegradation behavior, are determined by their chemical composition, morphology, and surface topography.

The aim of this review is to illustrate the main strategies by which bioactive ceramics (with particular attention to bioactive glasses) can be modified to enhance their interaction with cells and their antibacterial properties (Fig. 1). In particular, three approaches will be reviewed:

- doping with ions and drugs
- functionalization and coatings
- surface tailoring and internal nanostructures.

To write the actual review, a literature search was performed using PICO (the discovery tool of Politecnico di Torino), Google Scholar, and PubMed. These electronic databases were examined using different combinations of the following keywords: "glass", "ceramic", "bioactive", "bioceramic", "doping", "doped", "ion effect", "functionalization", "coating", "scaffold", "composite", "cell response", "infection", "osteomyelitis", "patterning", "structuring", "nanoscale", and different names of metallic and non-metallic ions.

Doping with ions and loading with drugs

Ion doping

On the basis of the network former, bioactive glasses can be classified into three categories – silicate, phosphate, and borate – with peculiar features and applications, as recently well reviewed by Baino.[31] The composition of bioactive glasses

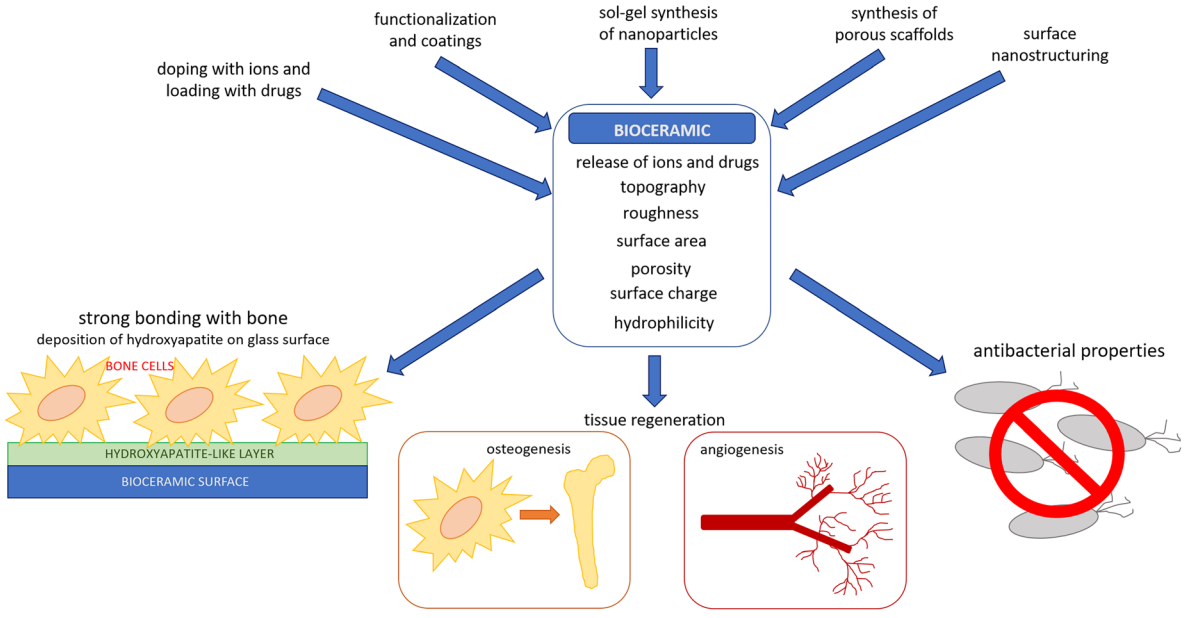

Fig. 1 Tailoring of bioceramics properties and consequent interaction of bioceramics with human and bacterial cells.

This journal is © The Royal Society of Chemistry 2024

Open Access Article. Published on 06 Eost 2024. Downloaded on 2026-06-06 12:45:47.
This article is licensed under a Creative Commons Attribution 3.0 Unported Licence.

can be successfully varied incorporating different ions in the glassy matrix by different synthesis methods.[6,32–34] Therefore, bioactive glasses are promising vehicles for the controlled delivery of therapeutic ions and could provide a robust alternative approach to the use of expensive growth factors for TE applications, because these ions are easier to handle and more cost-effective in comparison with GFs.[2,35]

Doping is defined as the incorporation of a low concentration of an element (ranging from a few ppm to a few percent) into the original material. There are different strategies to insert ions into the glass network, *i.e.* mixing with the raw materials and melting,[31] ionic exchange[31,36,37] on melt-derived BGs, as well as the sol–gel technique, which is very versatile and allows the facile incorporation of many ions in the glass composition.[38–41]

As the glass degrades *in vivo*, the incorporated ions are released at a biologically acceptable rate, in a tunable way. Indeed, the ion release capability, such as the degradation rate, of the BGs can be adjusted by modifying the glass composition according to the specific application.[40]

The released ions act as enzyme co-factors, either as coenzymes or prosthetic groups, influencing signaling pathways and stimulating metabolic effects involved in tissue formation.[4] Thus, they can induce intracellular and extracellular responses.[42] However, issues associated with the potential toxicity of these ions have to be taken into account.[43]

In the past several years a new type of bioactive glass has been developed: mesoporous bioactive glasses (MBGs) that possess a higher surface area and a mesoporous structure,[44] as pioneered by Yan *et al.*[45] who developed the first SiO_2–CaO–P_2O_5 MBGs. In addition, these glasses are characterized by a faster degradation rate; hence MBGs doped with metallic ions can release their therapeutic or antibacterial ions quicker than non-porous glasses[46] and show higher bioactivity.[34,45,47,48] MBGs can be used to fabricate very promising TE scaffolds whose physicochemical and biological properties can be further improved or modified by the incorporation of additional doping ions such as copper (Cu),[49] lithium (Li),[50] strontium (Sr),[51,52] or zirconium (Zr).[53]

An interesting review about the effect of ion release from bioactive glasses and glass-ceramics on human osteoblastic and osteoclastic cells, endothelial cells, and stem cells was published by Hoppe *et al.* in 2011,[4] whereas Lakhkar *et al.* in 2013[54] reviewed the role of the most significant ions playing a role in bone formation, and Sayed Mahmood Rabiee *et al.* in 2015 systematically reviewed the influence of the addition of aluminum (Al), magnesium (Mg), fluorine (F), potassium (K), silver (Ag), strontium, zinc (Zn), and zirconia (ZrO_2) on the chemical, physical and therapeutic properties of both BGs and glass-ceramics.[38] The effect of copper, cobalt (Co), lithium, manganese (Mn), magnesium, strontium, iron (Fe), and zinc on the physicochemical and structural properties, and consequently on the biological behavior *in vitro* and *in vivo* of silicate BGs doped with these ions, was reported in a review of Schatkoski *et al.*[55] In this review, we will further examine the therapeutic properties of the main doping ions for TE, especially for bone TE, and additionally provide an overview of their effects on bacterial cells, which are often an obstacle to tissue regeneration by causing severe infections.

The 45S5 Bioglass®, its effects and doping

The first bioactive glass that was developed (by Hench and coworkers in the 1970s) is the 45S5 Bioglass®, a Na_2O–CaO–SiO_2-based glass, but modified with a small amount of P_2O_5, allowing the synthesis of a chemically more labile material with enhanced bone-bonding ability.[54,56] The dissolution products of this glass upregulate the gene expression that controls osteogenesis and the production of related growth factors.[42,57] Indeed, the release of critical concentrations of soluble silicon (Si) (presumably in the form of $Si(OH)_4$), calcium (Ca), phosphorus (P), and sodium (Na) ions strongly affect the stimulation of osteogenesis and bone metabolism,[58] inducing the activation of a synchronized sequence of genes in osteoblasts, that undergo cell division and synthesize an extra-cellular matrix, which mineralizes to become bone,[3] as shown by *in vitro*[59] and *in vivo* results.[60] Moreover, when implanted into rabbit femurs, micrometric granules of 45S5 Bioglass® were found to promote more rapid bone growth than granules of synthetic HA.[61] The first investigation about the molecular interactions of the ionic dissolution products of 45S5 Bioglass® and their physiological environment was done in 2001 by Xynos *et al.*,[57] who observed for the first time that a solution containing Si, Ca, and P ions can stimulate gene transcription in human osteoblasts (including genes that (a) encode products that can induce osteoblast proliferation *e.g.*, RCL, (b) participate in the dynamic processes of ECM remodeling *e.g.*, metalloproteinases, (c) perform differentiated functions *e.g.*, CD44, and (d) promote cell–cell and cell–matrix attachment), and induce the secretion of GFs, such as insulin-like growth factor II (a key regulator of osteoblast homeostasis), and vascular endothelial growth factor (which belongs to the fibroblast growth factor family and has osteogenic potential).

To further enhance its properties, 45S5 Bioglass® has been modified by several research groups, incorporating several different doping ions.[62–66] It was observed that substitutions of 5–15 wt% B_2O_3 for SiO_2 or 12.5 wt% CaF_2 for CaO or inducing crystallization to form glass-ceramics have little influence on the bone-bonding ability of 45S5 Bioglass®, whereas the incorporation of small amounts (3 wt%) of Al_2O_3 prevents bonding to bone.[3] More details about how ions released from 45S5 Bioglass® influence the cell cycle are reported in an interesting review by Hench *et al.*[1]

Regarding the sodium release from 45S5 Bioglass® and similar glasses, under certain circumstances, this is very fast (initial burst release) and can cause a strong increase in pH, provoking an unwanted cytotoxic effect of these BGs, such as cell death at least under *in vitro* conditions. Thus, as a potential alternative, a new sodium-reduced fluoride-containing BG belonging to the CaO–MgO–SiO_2 system, namely BG1d-BG (with composition in wt%: 46.1 SiO_2, 28.7 CaO, 8.8 MgO, 6.2 P_2O_5, 5.7 CaF_2, 4.5 Na_2O), has been synthesized and already been evaluated *in vitro*, *in vivo* and in preliminary clinical trials.[67]

Open Access Article. Published on 06 Eost 2024. Downloaded on 2026-06-06 12:45:47.
This article is licensed under a Creative Commons Attribution 3.0 Unported Licence.

Besides the reduction of sodium content, the addition of magnesium (Mg) and fluorine has a positive effect on the biological properties of this novel BG,[67] as analyzed afterwards.

Osteogenic properties

In the case of silicate BGs, such as 45S5 Bioglass®, the mechanism for *in situ* tissue regeneration involves the up-regulation of seven families of genes that control the cell cycle, mitosis, and differentiation of osteoblasts and the high silicon concentration could be a major factor in stimulating the fast osteoblast growth.[6] Indeed, silicon has been found to play a fundamental role in the mineralization and gene activation of bone,[42] being shown *in vitro* to increase the intracellular activity of alkaline phosphatase (ALP) and the mineralization in MC3T3-E1 cells[68] and *in vivo* to affect skeletal development in chickens.[54]

Initially, the first hints that released ions could play a positive role in bone formation were suggested by preliminary results on calcium phosphate-based ceramics, which were modified by incorporating carbonate, magnesium, and fluorine.[54] Nowadays a wide number of publications have affirmed the ability of these and several other ions to stimulate bone regeneration, as here reported.

For example, calcium mediates numerous effects at the cellular and tissue levels, in particular in bone biology.[69] Calcium, indeed, is one of the most important components of the mineralized matrix, which acts as a reservoir for calcium and contributes to the maintenance of the homeostasis of calcium in the body.[54] Moreover, the appropriate concentration of calcium is fundamental for the appropriate calcification of the extracellular matrix, which is a critical step in the formation of mature bone. Furthermore, calcium plays an important role in bone homeostasis and bone remodeling *via* cell signaling pathways, influencing the proliferation and differentiation of both bone-forming osteoblasts and bone-resorbing osteoclasts, as well explained in the reviews written by Hoppe *et al.*[4] and Lakhkar *et al.*[54] Indeed, it is possible that the good osteogenic properties of 45S5 Bioglass® could be related to the calcium release more than to the release of silicon,[70] although Valerio *et al.* have observed that a higher Ca concentration did not increase the osteoblast activity of rat primary culture osteoblasts treated with the ionic products from the dissolution of a biphasic calcium phosphate (BCP), thus in the absence of Si release, but only in case of rat primary culture osteoblasts treated with the ionic products from the dissolution of a bioactive glass with 60% of silica (BG60S), so they suggested that the observed increase in osteoblastic proliferation and collagen secretion was related to Si contact.[71] Very high concentrations of calcium (>10 mmol) are cytotoxic for human osteoblastic cells, and therefore the proper therapeutic calcium concentration should be found. Maeno *et al.* demonstrated that medium (6–8 mmol) and low (2–4 mmol) concentrations of calcium are suitable for ECM mineralization and osteoblast stimulation, respectively.[72] Hench showed that a Ca concentration of 60–88 ppm (in combination with a Si concentration of 17–21 ppm) eluted from 45S5 Bioglass® is critical for the upregulation of several osteogenic genes, and consequently for the osteostimulation of human primary osteoblasts,[73] whereas other studies have shown that Ca concentrations of 88–109 ppm led to a reduction of Saos-2 osteoblast proliferation.[4]

Like calcium, strontium is a bone-seeking agent,[33] which can accumulate in high concentration in bone and substitute for calcium in hard tissue metabolic processes, thanks to the similarity between these two ions.[38] It is preferentially found in new bones rather than old and more in cancellous than cortical bones[33] and, in general, the amount of strontium in the skeleton is 0.335% of its Ca content.[38] Strontium has been shown to enhance *in vitro* and *in vivo* the replication of pre-osteoblastic cells and the cell osteogenic activity, and simultaneously to decrease the activity and the number of osteoclasts, leading to a local resorption of bone, by inhibiting the expression of receptor activator of nuclear factor kappa-B ligand (RANKL) in mesenchymal stem cells (MSCs).[33,74] Therefore, for its ability to prevent bone loss in osteoporotic patients, it has been used for many years for the treatment and prevention of osteoporosis, in the form of strontium ranelate (SrR), marketed as Protelos®, an approved drug in which strontium (Sr^{2+}) is the active component.[75] Sr ions are used as doping agents to fabricate bioactive ceramics with increased bone regeneration ability, as shown in many experimental works.[39,76–78] For example, using the melt-derived method, Kargozar *et al.* have synthesized four different glasses, in which Ca^{2+} ions were replaced with Sr^{2+} and Co^{2+} in different percentages, and have observed that the incorporation of Sr^{2+} ions into the glass structure promotes the activity of osteoblast cells through the induction of osteoblast markers like ALP, and the incorporation of Co^{2+} (0.5 mol%) does not have any toxic effect on cells.[74] Arepalli *et al.*[79] prepared new Sr-doped BGs, by partially substituting SrO for SiO_2 in the Na_2O–CaO–SrO–P_2O_5–SiO_2 system, and demonstrated that the substitution of SrO for SiO_2 is more beneficial than the substitution for CaO in the glass composition, in terms of mechanical properties, and viability and proliferation of human osteosarcoma U2-OS cells. Sr-doped Ca-substituting BGs with the composition SiO_2(75 wt%)–CaO(25–*X* wt%)–SrO(*X* wt%), with *X* = 0, 1, and 5 wt%, were synthesized also by Isaac *et al.*[80] through an acid sol–gel synthesis, obtaining similar results to the ones of Arepalli *et al.*, in particular in the case of 5 wt% Sr-doped glasses, which were shown to enhance ALP activity, OC secretion, and the up-regulation of RUNX2, OSTERIX (OSX), DLX5, collagen I, ALP, BSP, and OC mRNA levels, to a greater extent in comparison with undoped BGs and BGs with a lower Sr amount. Thus, according to these results, the optimum level of Sr incorporation is equal to 5 (mol%), but in general, the range of 2–10 (mol%) seems to be a reliable concentration of strontium. This was confirmed by Moghanian *et al.* who observed that the incorporation of 6 mol% of Sr in zirconium-doped BGs (60% SiO_2, 25% of CaO, 4% of P_2O_5, 5% of ZrO_2, and 6% of SrO) was statistically significant for stimulating cell proliferation, whereas the increase of Sr content up to 12 mol% reduced cell proliferation.[176] The successful healing

Open Access Article. Published on 06 Eost 2024. Downloaded on 2026-06-06 12:45:47.
This article is licensed under a Creative Commons Attribution 3.0 Unported Licence.

of large fractures of rat bone was, instead, achieved by Wei *et al.* using porous scaffolds doped with strontium.[77] Comparable results about the excellent bone regeneration ability of Sr-incorporating BGs were obtained by Zhao *et al.* who used mesoporous scaffolds composed of Sr-doped BGs (Sr-MBG scaffolds) to repair critical-sized rat calvarial defects,[52] after previous excellent *in vitro* results with MC3T3-E1 osteoblast cells (higher proliferation rates, ALP activity, and expression of osteogenic markers, type I collagen formation and bone nodule formation in comparison with Sr-free scaffolds).[78] For further information on Sr-doped silicate, borate, and phosphate glasses (including the synthesis methods, structure, reactivity and applications), a review by Kargozar *et al.* is available since 2019.[81]

Being the second most abundant mineral element in the human body and along with calcium a key component of the mineralized matrix, phosphorus plays many important roles in numerous body processes and the release of phosphate groups (such as orthophosphate PO_4^{3-}, linear species such as pyrophosphate ($P_2O_7^{4-}$) and tripolyphosphate ($P_3O_{10}^{5-}$) and cyclic species like cyclic trimetaphosphate $P_3O_9^{3-}$), from BGs, can enhance tissue regeneration.[54] The addition of 10 mmol inorganic phosphorus in a cell culture medium has been shown to stimulate the expression of key regulator agents for bone tissue formation, the matrix Gla protein (MGP), in osteoblastic cells.[82] Phosphate-based glasses are an ideal medium for the controlled release of therapeutic ions, because the weight loss and the related ion release are generally sustained over time and highly linear for a wide range of glass compositions and types, dissolving in a congruent and uniform way (due to acid- or base-catalyzed hydration of the polymeric phosphate network), differently from silicate glasses that dissolve mainly in an incongruent manner.[54] In any case, P could be not necessary for *in vitro* ECM mineralization, because even phosphate-free silicate glasses, such as the sol–gel derived 70S30C (mol%: $70SiO_2$–30CaO) synthesized by Jones *et al.*,[83] have been demonstrated to enhance osteoblasts to mature, differentiate and produce bone-like minerals. Anyway, the authors of the actual review agree with Hoppe *et al.*[4] that these last reported results should not underestimate the importance of phosphate glasses as therapeutic ion carriers and bone metabolism regulating agents.

Among others, the skeleton contains a significantly large amount of zinc, which plays an essential role in the formation and mineralization of bone,[54] as indicated by its accumulation in the growth plate and its concentration in a line along cancellous and cortical bone calcifying fronts. Remarkable for bone mineralization is also the fact that zinc is a key element in ALP, an enzyme that is central to the mineralization of bone matrix.[84] The importance of zinc for bone tissue formation is also confirmed by the negative effects of zinc deficiency, which is demonstrated to be associated with a retardation of skeletal growth and alterations in bone calcification.[85] In contrast, positive effects on bone metabolism have been obtained through dietary supplementation with zinc.[86] Moreover, the activities of matrix metalloproteinases that remodel the collagenous ECM of bone are dependent on zinc. Thus, it is clear that zinc can be potentially used as a bone regeneration therapeutic agent, as widely discussed in a recent review by O'Connor *et al.*[87] about the role of zinc in the growth, homeostasis, and regeneration of bone. Various BGs[88–91] for bone TE have been doped with zinc, taking advantage of its ability to influence the osteogenic differentiation of human bone marrow-derived mesenchymal stromal cells (hBMSC) and the osteoclastic differentiation of monocyte/macrophages *in vitro*, and to encourage the attachment and proliferation of osteoblasts, and to inhibit osteoclastic cells.[92]

Also, magnesium is very important in the bone matrix (which, in fact, contains 0.72 wt% of Mg[93]) and has stimulatory effects on the development, mineralization, and maintenance of bone.[38] It has been shown that the addition of magnesium in bioactive glasses is favorable for human osteoblast-like cell proliferation and function.[94] A review of the effect of Mg ions on glass properties and bone cell response (*in vitro* and *in vivo*) was published in 2012 by Diba.[93] Detailed information about glass compositions, Mg content (wt%), and the results of *in vitro* biological tests are reported in Table III of that review.[93] The applications of Mg-doped BGs in scaffolds, bone cements, and bioactive coatings are also reviewed.[93] The *in vivo* osteogenic ability of Mg-doped BGs (with composition $45SiO_2$–$3P_2O_5$–26CaO–$15Na_2O$–7MgO–$4K_2O$, mol%) has been further confirmed by implanting the BG-derived scaffolds into surgically created critical-size bone defects in rats, as published by Kargozar *et al.* in 2022.[95]

However, even ions not naturally contained in bone can positively affect bone tissue regeneration.

Cerium (Ce) was proved by Zhang *et al.*[96] to display a positive effect on the proliferation, differentiation, and mineralization of primary osteoblasts when cultured in a medium containing Ce^{3+} ions. Indeed, all tested concentrations (1×10^{-9}, 1×10^{-8}, 1×10^{-7}, 1×10^{-6}, 1×10^{-5}, and 1×10^{-4} mol L^{-1}) of Ce^{3+} promoted the proliferation of primary osteoblasts whereas their differentiation, adipocytic transdifferentiation and mineralization depended on the cerium concentration and on the culture time, with – for example – the differentiation promoted on the first and third day at concentrations of 1×10^{-9}, 1×10^{-7}, and 1×10^{-6} mol L^{-1}, but inhibited at higher concentrations.[96] The pro-osteogenic properties of Ce ions were also confirmed by Zheng *et al.*,[97] who observed the expression of osteogenesis-related genes in osteoblast-like Saos-2 cells cultured with Ce-containing BG particles.

Copper is mostly known for its antibacterial properties, but the reduction of osteogenesis and the lowered mechanical properties of bones in case of either dietary or genetic copper deficiency in both humans and animals are clues that copper could possess also interesting osteogenic properties. Copper is, in fact, essential for several enzyme-based processes for bone formation and bone maintenance. Anyway, this does not explain why the localized or systemic delivery of copper should be beneficial for the healing and correction of copper deficiency, but at the same time, it is not possible to deny this hypothesis without any opposite evidence, whereas results showing the stimulation of proliferation and differentiation of

Open Access Article. Published on 06 Eost 2024. Downloaded on 2026-06-06 12:45:47.
This article is licensed under a Creative Commons Attribution 3.0 Unported Licence.

MSCs cultured in osteogenic differentiation medium containing a Cu concentration around 0.1 mM have already been published.[98] These results have been confirmed by more recent results of Westhauser *et al.* who have cultured mouse bone marrow-derived mesenchymal stromal cells (BMSCs) in media containing the ion dissolution products of $70SiO_2$–25CaO–5X where X is CuO or MnO or ZnO (mol%),[91] and Rau *et al.* who have proved that the Cu-doping of 45S5 Bioglass® (with a composition in wt% of $45SiO_2$–$24.5Na_2O$–$6P_2O_5$–19.5CaO–5CuO) is effective in stimulating the early differentiation of MSCs to the osteoblast phenotype, through the over-expression of anti-inflammatory interleukins and the reduction of pro-inflammatory interleukins.[99] In addition, Lin Y. *et al.* have confirmed previous studies showing that the addition of 0, 0.4, 0.8, and 2.0 wt% CuO in silicate 13-93BG scaffolds (with a composition in wt% of $53SiO_2$–$6Na_2O$–$12K_2O$–5MgO–20CaO–$4P_2O_5$) enhance the migration and osteogenic differentiation of BMSCs.[100] However, it has been demonstrated that at high concentrations copper may inhibit osteogenesis *via* the down-regulation of osteogenic genes such as *RUNX2*, which is the main regulator of osteoblast phenotype, as well explained in the review by Kargozar *et al.*,[101] which contains an interesting overview of the effects and applications of Cu-containing BGs and bioactive glass-ceramics, with detailed information about glass compositions and dopant concentrations; therefore, the actual review will not provide further details.

Boron (B) interacts with the performance of several metabolic enzymes and its osteogenic properties are well known, as broadly reviewed by Balasubramanian *et al.*[58] and confirmed by various *in vitro*[102] and *in vivo* studies.[103–107] Indeed, impaired bone growth and abnormal bone development can be associated with boron deficiency, both in humans and animals.[58] Optimal levels of boron are, in fact, necessary for calcium metabolism, which is strongly related to the bone tissue metabolism process.[58] Different compositions of BGs containing boron, including boron-doped, borosilicate, and borate glasses, have been synthesized as promising suitable carriers of boron for bone TE applications.[58,108] Recently, it was shown that the incorporation of boron into BG scaffolds leads to a controllable release of boron ions with a significant improvement in the proliferation and bone-related gene expression (*Col* I and *RUNX2*) of osteoblasts.[109] Recently it has been shown that certain compositions of borate BGs enhance osteogenesis to a greater extent than 45S5 Bioglass®, although these borate glasses contain no Si.[2] However, a concern associated with the toxicity of borate ions, $(BO_3)_3$, released from borate has been recently raised, because some borate BGs have been demonstrated to be toxic to cells in *in vitro* cultures (especially in conventional "static" conditions, whereas in "dynamic" culture conditions the toxicity was diminished).[2]

The effect of fluorine on the regeneration of hard tissues such as bone and teeth is controversial. Concentrations of 25–500 ng ml^{-1} of fluoride ions have been demonstrated to stimulate osteoblast cells whereas concentrations of more than 500 ng ml^{-1} can suppress osteoblast activity.[110] In fact, high fluoride doses can be toxic for cells, causing oxidative cell damage[111] and leading to dental and skeletal fluorosis.[112] Alkasite, an alkaline calcium fluorosilicate BG without phosphate, based on the system SiO_2–CaO–Na_2O–CaF_2, can be used as an additive in resin composites for dentistry applications. Clinical trials confirmed that it offers better mechanical, aesthetic, and technical performance in comparison with resin-modified glass ionomer cements.[113]

For a decade, lithium has been suggested as a novel therapeutic ion for bone TE. In 2011 Khorami *et al.*[62] synthesized different lithium-containing Bioglass®-based glasses, by substituting 0–12 wt% Li_2O for Na_2O. They found that the proliferation rate and ALP activity of newborn rat calvaria-derived osteoblastic cells cultured on Li-substituted glasses were higher than those of Li-free glasses in a dose-dependent manner. Many other experimental results studies are now available, as well as reported by Durand *et al.*[114]

Manganese has been shown to support the proliferation of osteoblastic cells.[91,115] In 2014 Miola *et al.*[115] reported the synthesis of new BGs belonging to the system SiO_2–P_2O_5–CaO–MgO–Na_2O–K_2O doped with different amounts of manganese oxide (MnO) and their good osteogenic properties. Cellular tests performed on these Mn-doped BGs, up to a concentration of 50 μg cm^{-2} (μg of glass powders/cm^2 of cell monolayer), showed that the presence of Mn was not cytotoxic for MG-63 osteoblasts (cultured for up to 5 days with the synthesized Mn-doped glasses) and allowed a good proliferation, differentiation and spreading of osteoblasts on Mn-doped glasses, as shown by the ALP increase, expression of some bone morphogenetic proteins (BMPs), and calcium deposit.[115] However, in some compositions at high concentrations, Mn can have cytotoxic effects on bone MSCs.[91]

Niobium (Nb) is very biocompatible and has been shown to reduce the cytocompatibility of biomaterials.[116] It is also associated with an increase in ALP activity and enhanced calcification in bone defects.[117] Therefore, the incorporation of Nb in bioceramics is of great interest. Among the several incorporation methods, the sol–gel synthesis is the most promising in the case of niobium addition, because the adopted lower processing temperatures avoid the formation of strong bonding as in the case of the melting process, thus not causing a reduction in glass solubility and degradation, as shown by de Souza Balbinot *et al.*[116] who have synthesized sol–gel Nb-doped BG powders and scaffolds. An increase in cell mineralization related to the formation of a higher area fraction of mineralized nodule was observed after 14 days in the case of Nb-doped BG powders (in 5 mg concentration) when compared with BAG ($p < 0.05$).[116] The synthesized Nb-doped scaffolds presented an even higher mineralized area when compared with Nb-doped powders, probably because of increased interface interactions related to macroporosity,[118] and an increase in cell mineralization already after 7 days in comparison with undoped scaffolds, whereas no statistical difference was found in the cell proliferation rates between powders and scaffolds and in the case of the addition of niobium,[116] as instead found by Pradhan *et al.*[119]

45S5 Bioglass® doped with titanium (Ti) synthesized by Vrouwenvelder *et al.* has been shown to exhibit a higher pro-

 This journal is © The Royal Society of Chemistry 2024

Open Access Article. Published on 06 Eost 2024. Downloaded on 2026-06-06 12:45:47.
This article is licensed under a Creative Commons Attribution 3.0 Unported Licence.

liferation and expression of osteoblasts, if compared with 45S5 Bioglass® doped with B, Fe, and F and undoped 45S5 Bioglass®, probably because of the ion release from Ti-doped BG.[4,409] Therefore, these results seemed to suggest that also titanium possesses osteogenic properties.

Selenium (Se) was initially incorporated in bioceramics such as bioactive glasses,[120,121] HA,[122,123] and calcium carbonate[124] for its ability to induce apoptosis in bone cancer,[122] but Se-incorporated HA exhibited a significant improvement in cell proliferation.[125] The combination of antitumoral and osteogenic properties shown by Se ions is particularly relevant for bone tumor healing.

In contrast to many other ions, the aim of cobalt addition in bioceramics is generally not the direct stimulation of osteogenesis but rather has a pro-angiogenic purpose.[22] Although cobalt was shown to inhibit osteoblast proliferation and ALP gene expression, it can provide the required angiogenic environment to indirectly potentiate the inherent osteogenic properties of BGs.[22] When released from doped BGs, cobalt was shown to stimulate the expression of angiogenesis and osteogenesis genes, such as those regulated by several growth factors (such as vascular endothelial growth factor VEGF, fibroblast growth factor FGF, SDF-1, BMP-2, and RUNX2) of the cultured hBMSCs.[126] The pro-angiogenic properties of cobalt are already well known (as deeply discussed in the subsection "Pro-angiogenic properties"), but the above-reported results of Deng *et al.* showed that the addition of cobalt in BGs can promote also the osteogenic differentiation of hBMSCs.[126] The expression of osteogenic genes was upregulated as the culture time and the CoO amount in the BG increased.[126] In addition, when implanted in the calvarial defects of rats, Co-doped BGs showed an increase in the regeneration of new bone tissue and the formation of new blood vessels when compared with undoped BG scaffolds.[55] A study published in 2019 of PCL-HA membranes with localized Co^{2+} release showed that a cobalt ion concentration below 15 ppm was not significantly toxic to the MG-63 cells, which showed osteogenic activity, in detail the production of calcium deposition on the PCL–CoHA.[55] A doping concentration of 5 mol% was proved to be the threshold concentration for the potential use of cobalt in bone repair, due to the significant reduction in viability of hBMSCs and low cytotoxicity towards osteoblast-like Saos-2 cells.[22] Further details about the biocompatible dosage level of cobalt are available in a review by Baino *et al.*[22]

Zirconium does not possess osteogenic properties, because it does not influence osteogenesis by stimulating gene expression, but it facilitates the proliferation and differentiation of osteoblastic cells, as a consequence of the slower ion dissolution rate and the stabilization of the pH environment.[9]

Pro-angiogenic properties

Bioactive ceramics can also promote angiogenesis (or neo-vascularization), as already reported by Kargozar *et al.*[127] and here further reviewed. Various ions have been proved to promote angiogenesis, which plays a critical role in tissue regeneration and is highly beneficial in the case of large tissue-engineered constructs.[42] Thus, bioactive glasses and glass-ceramics releasing ions that activate genes promoting angiogenesis *in vivo* have been developed.[6,44] As angiogenesis is regulated by several growth factors (such as VEGF, transforming growth factor-β TGF-β and FGF) and especially conditions (such as hypoxia), in order to promote it, the use of ions that can stimulate angiogenic growth factors or induce hypoxic conditions, such as boron,[128,129] calcium,[130] cerium,[131] cobalt,[76,126,129,132] copper,[132–134] lanthanum (La), iron, lithium,[135] magnesium,[136,137] rubidium (Rb), strontium,[52,76,138] and zinc,[135] is widely investigated.

Hypoxia activates a series of processes mediated by the hypoxia-inducing factor-1α (HIF-1α) transcription factor. In addition, HIF-1α can initiate the expression of several genes associated with tissue regeneration and skeletal tissue development and enhance fracture repair.[9] The HIF-1α is hydroxylated by prolyl hydroxylase domain (PHD) proteins when ascorbate is present in the cell, counteracts the effect of reactive oxide species (ROS) and is rapidly degraded; so, it cannot upregulate VEGF.[22]

Cobalt is one of the most studied pro-angiogenic ions, because it can hinder the entrance of ascorbate into the cytosol, halting PHD function, leading to the upregulation of HIF-1α and finally increasing the secretion of VEGF, but it has been proved to be ineffective in concentrations below 5 ppm and cytotoxic, carcinogenic, and genotoxic to human cells at high concentrations, probably (a) interfering with cytoskeleton formation (in detail, inducing focal adhesion contact derangement formed by the integrins of microvascular endothelial cells, easily leading to apoptosis) or (b) increasing the production of ROS, causing DNA damage, or (c) inhibiting DNA repair.[22] A dose-dependent effect of Co was, indeed, observed for both *in vitro* biocompatibility and therapy.[22] It has been shown by a study by Hoppe *et al.*[139] that the maximum of the vital therapeutic ranges of Co ions released in physiological fluid seems to be lower than 5 wt% CoO. They found that the incorporation of 1 wt% CoO in the BG composition of 13–93, corresponding to Co^{2+} ion concentrations of 2 ppm, was found to be cytocompatible towards endothelial cells and osteoblast-like MG-63 cells, whereas the incorporation of 5 wt% of CoO with a Co^{2+} ion released concentration of 12 ppm, was cytotoxic to both cell types.[22] In any case, already above around 10 ppm, a reduction of 40% in the cells could be observed.[22] Therefore, the safety window can be set in the range of 2 to 12 ppm, but the therapeutic window was suggested to be even narrower (5 to 10–12 ppm).[22] These results are not surprising and confirmed the ones of Wu's research team, who synthesized the first Co-doped BGs by the sol–gel process in 2012, incorporating 2 to 5 mol% of cobalt into SiO_2–CaO–P_2O_5 mesoporous BGs to partially replace calcium. As a result of this Co doping a significant enhancement of VEGF secretion, HIF-1α expression, and bone-related gene expression (for ALP and osteocalcin) in bone BMSCs was observed, in comparison with Co-free MBG scaffolds, but the highest Co content led to a reduction of cell proliferation.[18] The therapeutic effect of Co ions released from the BGs could be triggered by a synergistic effect with other glass-derived ionic dissolution products.[22]

Open Access Article. Published on 06 Eost 2024. Downloaded on 2026-06-06 12:45:47.
This article is licensed under a Creative Commons Attribution 3.0 Unported Licence.

The research of Dai *et al.* has shown that copper can stimulate the expression of angiogenic GFs, not only activating the signaling pathway of hypoxia-inducible factor through the inhibition of the intracellular and extracellular degradation of HIF-1α, but also activating endothelial cells through the TNF-α pathway to produce an appropriate pro-inflammatory response, which in turns accelerates the degradation of the vascular base by inhibiting the expression of TIMP, and stimulates a beneficial inflammatory microenvironment, by recruiting inflammatory cells.[135,410]

Chen *et al.* have recently shown that boron possesses also angiogenic capability, promoting VEGF secretion, as demonstrated, for example, by borate glasses of the composition 1605 and 13-93B3, with and without CuO and ZnO.[128] Thus, borate glasses are optimal candidates for TE applications in which rapid and successful angiogenesis is required, considering not only bone scaffolding, but also soft TE applications such as skin regeneration and wound healing. In a study by Deliormanlı *et al.*,[131] the good angiogenic properties of borate BGs were further enhanced by adding cerium ions, whereas the incorporation of gallium (Ga) and vanadium (Va) caused a decrease in blood vessel formation.

Despite these interesting findings, few investigations have been carried out on this multi-target approach, based on the incorporation of different angiogenic ions to promote angiogenesis through the stimulation of several different signaling pathways, as further discussed in the subsection "Synergic effects and summary".

In recent investigations, 45S5 Bioglass® has also been shown to enhance the secretion of vascular endothelial growth factor *in vitro* and vascularization *in vivo*, suggesting that scaffolds containing controlled concentrations of 45S5 Bioglass® might stimulate neo-vascularization.[42]

Finally, it is interesting to point out that the expression of angiogenic GFs can eventually lead to a significant improvement in bone regeneration *in vivo* and *in vitro.*[135]

Magnetic, photothermal, and anticancer properties

Bioactive ceramics can also be doped with Fe ions to synthesize ceramics containing ferrimagnetic phases for potential use in cancer treatment through hyperthermia and the regeneration of osseous defects caused by bone cancer,[41] thanks to their ferrimagnetic properties and high apatite-forming ability.[41,140] Hyperthermia treatment is a clinical treatment based on the generation of heat in the tumor site under the application of an external magnetic field to an implanted magnetic material.[41] Moreover, if these ferrimagnetic ceramics are loaded with antitumoral drugs, it is possible to combine hyperthermia with chemotherapy, as suggested by Verné *et al.*[141] who have modified (through surface functionalization as reported in the section "Functionalization and coatings of bioactive glasses") a ferrimagnetic glass-ceramic belonging to the system SiO_2–Na_2O–CaO–P_2O_5–FeO–Fe_2O_3 into a carrier for antineoplastic agents such as cisplatinum and doxorubicin. A fascinating review of magnetic glass-ceramics for cancer treatment was published in 2019 by Miola *et al.*[142] and a review of bioceramics for magnetic hyperthermia was published by Sedighi *et al.* in 2022.[143]

Anticancer properties could be obtained in the case of Fe-doped glasses not only thanks to magnetic properties and hyperthermia, but also thanks to the ability of the dopant iron ions to absorb the near-infrared (NIR) light of a laser and convert it into heat, locally increasing the temperature (in so-called photothermal therapy).[144]

Both hyperthermia and photothermal therapy are based on the higher sensitiveness of tumor cells to temperature increments up to around 43 °C than healthy tissue cells.[22]

In addition, Fe ions can act as anticancer agents through Fenton's reaction, which results in catalytic H_2O_2 decomposition inside the tumor cells and the production of ROS.[144] Hence, Fe-releasing mesoporous BG nanoparticles (NPs) can be applied in ferroptosis-based bone cancer treatment.[144] Ferroptosis is a type of programmed cell death caused by ROS accumulation due to Fenton's or Fenton-like reactions.[144]

Another magnetic, photothermal, and ferroptosis-inducing doping element is cobalt.[22] However, the pro-angiogenic properties of cobalt could contribute to cancer development, leading to an opposite effect to the desired antitumoral therapy.[144] According to a recent review by Baino *et al.*,[22] nowadays, only two studies have been carried out on Co-doped BGs for anticancer applications. In the first one, 45S5 Bioglass®/HA composites containing Fe_2O_3 and CoO were synthetized for magnetic hyperthermia, but no evidence of the functional effect *in vitro* or *in vivo* has been reported yet.[22] The second one referred to sol–gel SiO_2–CaO–P_2O_5 mesoporous glasses, doped with Co, Cu, Mn, and Fe, for photothermal therapy.[144] *In vivo* results, after the subcutaneous injection of osteosarcoma Saos-2 cells into mice, showed that this Co-doped glass caused tumor tissue necrosis, but the necrosis rate was significantly lower compared with the other doped glasses and comparable to Co-free glass, suggesting that cobalt is not the best ion for this photothermal approach, but can offer better results when incorporated into implantable bioceramic systems (such as cobalt-ferrite nanoparticles) for other cancer treatment therapies like the above-described magnetic hyperthermia.[22]

However, anticancer properties can be also obtained by adding other ions, like Ag, B, Ca, Cu, chromium (Cr), Ga, germanium (Ge), Se, and Zn, that exploit their anticancer activity in a completely different way, with a peculiar antitumoral mechanism for each different ion.[144,145] For example, in the case of selenium, tumor cell death is caused by the generation of oxidative stress in the cells and the production of ROS.[144]

Finally, to carry out a comprehensive dissertation about antitumoral BGs, the possibility of synthesizing radioactive BGs using radioactive ions should be reported. In this case, tumor cells (including bone cancer cells) are killed by the beta radiation emitted by the radionuclides, which leads to radioembolization and a subsequent cut-off of the blood supply to the treated area.[144]

All the here-described anticancer procedures (hyperthermia, photothermal therapy, and local radiotherapy using

 This journal is © The Royal Society of Chemistry 2024

Open Access Article. Published on 06 Eost 2024. Downloaded on 2026-06-06 12:45:47.
This article is licensed under a Creative Commons Attribution 3.0 Unported Licence.

radioactive BGs) may be used together with chemotherapy or surgery, taking advantage of the synergistic therapeutic benefits of different antitumoral strategies. In addition, in this context, the regenerative properties of BGs should not be ignored, allowing them to successfully heal bone tumor defects.

For further information about the use of BGs and bioactive glass-ceramics in cancer therapy, the reader can refer to a review of Moeini, published in 2023.[144]

Bioactive properties

The ion exchange between the ions released from the glass matrix and the body fluids (or SBF solution, in the case of *in vitro* acellular bioactivity tests) can influence the bioactivity performance and HA deposition rate.

For example, a low amount of small fluoride ions seems to enhance the formation of apatite (in detail, fluorapatite) of higher crystallinity, even at low pH conditions (below 6), but more fluorine is not necessarily beneficial for apatite formation, leading to the formation of fluorite at the expense of apatite by increasing the fluoride content in the glass.[146] This ability of fluoride ions to increase glass bioactivity was also confirmed by studies on F-doped phosphate glasses.[147] Moreover, as fluoride is a small ion, if substituted with bigger ions, it allows the formation of a very ordered, highly crystalline apatite. Indeed, the formed HA is highly influenced by the size of the substituted molecules.

In contrast to fluoride ions, bigger carbonate ions, which substitute into two sites, tend to form a more disordered amorphous HA.[148]

As expected, since calcium is a main component of natural HA, a proper amount of calcium inside the BG network is essential for the ion exchange between glass and biological fluids, that is responsible for the HA deposition on the BGs,[31] and Ca-doped glasses showed an increased calcium deposition in *in vitro* cell cultures by increasing the release of Ca^{2+} ions into the culture medium.[74]

Other studies show an increase in glass bioactivity and bone mineralization in the presence of manganese in the BG,[115] although other studies reported that Mg has no effect or even a negative effect on apatite formation, not inhibiting, but retarding its deposition.[149]

It seems to be confirmed that bioactivity can be increased by incorporating boron ions in the bioactive glass, partially replacing the SiO_2 in silicate glasses with B_2O_3,[58,150] and the total substitution of silicon with boron has resulted in higher bioactive borate glasses, characterized by low chemical durability and a fast HA conversion rate.[151,152] It is interesting to notice that the bioactivity of borate BGs can be further increased by incorporating in the glass network fluoride ions, which render the glass network itself more soluble, as shown by ElBatal *et al.*, who compare the bioactivity of Na_2O–CaO–B_2O_3 and NaF–CaF_2–B_2O_3 glasses,[153] or strontium ions, as reported by Marzouk *et al.*[154] who observed an increase in the glass corrosion rate by increasing the SrO content, or even vanadium ions, which increase the degradation rate of the borate glasses.[155]

However, if borate glasses are doped with copper, their HA precipitation rate decreases,[156] but in general, the influence of copper on glass bioactivity is still under investigation and very argued. Most experimental works have shown a bioactivity reduction in the case of doping with copper, but there are even experimental results showing that Cu-doping does not alter the glass bioactivity; *e.g.* the bioactive glasses with a superficial *in situ* chemical and physical reduction of copper fabricated by Miola *et al.* maintained their bioactivity up to 14 days (the duration of the performed acellular bioactivity test),[134] or even accelerate apatite formation in case of Cu-doped BG nanoparticles containing 10–15 wt% Cu (10Cu-BGN and 15Cu-BGN) in comparison with 5Cu-BGN and undoped BG nanoparticles.[157]

Not only the effect of copper, but also the effect of magnesium on glass bioactivity is still unclear. Indeed, past studies showed that Mg did not inhibit the apatite-forming ability of BGs but Mg was believed to retard the time of apatite deposition, because of the negative effect of MgO that suppressed calcium release and thus hindered silica-gel layer formation,[93,158] although new results (published in 2020[159]) on sol–gel Mg-doped SiO_2–CaO–P_2O_5 have shown that the amount of apatite crystals increased in samples doped with 8 mol% of magnesium, whereas a lower Mg content was not effective in increasing glass bioactivity. These results have been also confirmed by recent studies (published in 2020[160]) on innovative magnesium–lanthanum dual-doped BGs, showing an increase in apatite formation and glass bioactivity in all five synthesized glass compositions (1 wt% lanthanum with 0, 1, 2.5, 5, and 10 wt% magnesium), especially in the BGs with the higher Mg content.

Gallium, instead, has been shown to delay the growth of a crystalline apatitic layer on Ga-modified glasses with respect to the Ga-free glass, probably because of the dramatic changes induced, at the glass/SBF interface, by the presence of the Ga_2O_3 component,[161] although gallium protects the formed HA matrix, thereby improving the biomechanical properties of the newly formed bone and in general of the skeletal system.[34]

Besides gallium, also cerium decreases HA formation,[65] and the higher its concentration, the lower the quantity of formed hydroxyapatite because the presence of these dopant ions leads to the formation of $CePO_4$ at the expense of HA.[65]

Comparing a SiO_2–CaO–P_2O_5 glass with SiO_2–CaO–P_2O_5 glasses modified with cerium, gallium, or zinc ions, Salinas *et al.* observed that zinc-doped BG shows the lowest bioactivity.[34]

Similar results were found in the case of 45S5 Bioglass®[63] and borate glasses[58] doped with zinc, confirming that Zn ions are inhibitors of HA crystal formation,[162] because of the ability of ZnO to act as an intermediate oxide (*i.e.* to act either as a network former ZnO_4 or as a network modifier like alkali oxides and alkaline earth oxides), forming tetrahedral species ZnO_4^{2-},[92,163] especially in the case of very high zinc concentration (above 20 wt%), that can cause a significant reduction

Open Access Article. Published on 06 Eost 2024. Downloaded on 2026-06-06 12:45:47.
This article is licensed under a Creative Commons Attribution 3.0 Unported Licence.

in dissolution behavior, leading to the incapability of the glass to form HA (as reported by Aina *et al.*[164]), although a few opposite results show an increase in glass bioactivity when a small amount of zinc is added to the glass composition. Abdelghany *et al.*[92] have shown that increasing the ZnO amount (from 2 mol% to 10 mol%) in soda lime borate glasses favors HA formation. Balamurugan *et al.*[165] have demonstrated that the incorporation of 5 mol% of zinc into a sol–gel $CaO–P_2O_5–SiO_2–ZnO$ system did not diminish the bioactivity and Salinas *et al.*[34] have observed a rapid *in vitro* bioactive response when the amount of ZnO is less than 4 mol%. However, in contrast, according to Shahrabi *et al.*,[166] the addition of 5 mol% of ZnO can cause the reduction of the number of non-bridging oxygen atoms, and so leads to a decreased bioactivity. Zn- and Ag-co-doped nano-sized glass particles[32] showed an initial increase of crystallized apatite deposition, followed by a delay in the HA formation, which was more pronounced in the case of the glasses incorporating zinc ions, in comparison with undoped glasses used as a control. In addition, MBGs are characterized by an extraordinary bioactivity which can be prevented anyway if zinc is added to the composition of a highly bioactive mesoporous glass, as recently reported by Neščáková *et al.*,[90] showing that the glass composition affects the glass bioactivity more than its surface area.

However, when Zn and Fe are added together, by increasing the combined Zn–Fe content, their combined effect leads to an increase in the glass bioactivity.[167] An enhancement in the growth of the apatite layer was also observed in the sol–gel BGs of an xZnO(22.4 − x)$Na_2O–46.1SiO_2–26.9CaO.2–6P_2O_5–2MgO$ system, probably due to the co-presence of magnesium ions and zinc ions.[168]

Another ion that has been shown to inhibit bioactivity is cobalt.[66] The presence of peaks attributable to HA was, indeed, not observed in the X-ray diffraction (XRD) patterns of the Co-doped BGs (BG.4Co) and B- and Co-co-doped BGs in the case of a higher concentration of doping cobalt ions (BG.2B4Co), whereas the XRD patterns of B- and Co-co-doped BGs in the case of a higher concentration of doping boron ions (BG.10B4Co) were characterized by the presence of the typical diffraction lines of hydroxy carbonated apatite (HCA), confirming the ability of boron to stimulate bioactivity.[66] However, opposite results were obtained in the case of BGs belonging to the $Na_2O–CaO–SiO_2–P_2O_5$ glass system by Vyas *et al.* In this study, bioactivity and mechanical behavior were enhanced by adding cobalt ions to the glass composition.[169] The *in vitro* apatite-forming ability of these Co-doped BGs was significantly improved by increasing Co amounts.[169] In the case of a moderate (2.5 mol%) incorporated amount of CoO, the effects on glass dissolution and apatite-forming ability became almost negligible, without a significant difference in comparison with the Co-free sol–gel BGs.[170] Further information about the dissolution rates and *in vitro* bioactivity of Co-doped BGs can be found in the already-mentioned review of Baino *et al.*[22]

It is interesting to point out that the incorporation of strontium can lead to a decrease in the glass dissolution and consequently in the kinetics of the ion release, causing a delayed bioactivity, because strontium has a large atomic radius that likely blocks the movement and release of other ions.[39,58,78,171] When Sr ions are substituted with smaller ions in the glass composition of sol–gel BG particles, the obtained BG particles are characterized by a higher surface area and lowered bioactivity, as demonstrated by Hoppe *et al.*,[172] who synthesized Sr-doped 1993 glass nanoparticles by substituting various amounts of CaO with SrO. However, when strontium ions are added to sol–gel-derived zirconium-doped BGs, leading to a glass ZS-BGs containing 60% of SiO_2, (36 − X)% of CaO, 4% of P_2O_5, 5% of ZrO_2 and X% of SrO (where X = 0, 3, 6, 9, and 12 mol%), the glass bioactivity is increased.[173] Indeed, the addition of Zr strengthens the connectivity of the glass network, reducing the release rate of Si, P, and Ca ions during the acellular bioactivity test, but in contrast, the addition of strontium has a weakening effect, which is stronger than the strengthening effect of zirconium.[173]

Surprisingly, even phosphorus could potentially hinder the bioactivity, because of the higher affinity of modifier Na and Ca cations for coordinating phosphate rather than silicate, leading (in combination with the formation of P–O–Si linkages) to an increase in the repolymerization of the silicate network with increasing P_2O_5 content, but practically this negative effect of P ions is counterbalanced by the increasing amount and related fast release of free orthophosphate groups. Indeed, increasing the content of phosphates has been shown to stimulate *in vitro* HCA deposition.[174] In this same study,[174] increasing amounts of CaO and SiO_2 inhibit the deposition of HCA during immersion in SBF.

Novel results on borate-substituted 45S5 Bioglass® with a basic composition (mol%) of $46.1B_2O_3–26.9CaO–24.4Na_2O–2.6P_2O_5$ [175] have shown that the sodium content has very little effect on the rate of conversion to HCA in SBF, because even with decreasing the amount of sodium, while maintaining the ratio of the other elements (until the synthesis of a sodium-free glass with a composition in mol% of $61.0B_2O_3–35.6CaO–3.4P_2O_5$), the formation of an HCA layer was observed within 2 h from immersion in SBF.

Finally, to provide a more complete possible analysis of ion effect on glass bioactivity, it should be also reported that small additions of Al_2O_3, Ta_2O_5, TiO_2, Sb_2O_3, or ZrO_2 in BG compositions have been shown to induce an inhibition of bone bonding.[3] Alumina and zirconia are, usually, added to the bioceramics composition to enhance the structural stability, the mechanical properties, and the corrosion resistance of the bioceramics, by eliminating some of the non-bridging oxygens and hence enhancing the network compactness.[38,176] Thus, it is remarkable that zirconium does not hinder the bioactivity of the bioceramics.[176] On the other hand, Al_2O_3 addition often significantly reduces the bioactivity, hindering the HCA formation. The concentration of alumina required to suppress the bioactivity depends on the composition or chemical durability of the glass. For example, if Al_2O_3 is added up to about 1.5 wt% in the case of modified 45S5 Bioglass® and 1.5 mol% in case of the $CaO–SiO_2–Al_2O_3$ system, no significant lowering of the bioactivity can be observed, whereas if $CaO–SiO_2–Al_2O_3$

 This journal is © The Royal Society of Chemistry 2024

Open Access Article. Published on 06 Eost 2024. Downloaded on 2026-06-06 12:45:47.
This article is licensed under a Creative Commons Attribution 3.0 Unported Licence.

glasses contained more than 1.7 mol% Al_2O_3, they did not form apatite.[38]

Recently, the effect of less common BG-doping ions, such as gadolinium (Gd), germanium (Ge), ytterbium (Yb), nickel (Ni), niobium, rubidium, and terbium (Tb) have been studied.

Germanium-containing glasses have been synthesized starting from the glass composition of $48SiO_2$–$6CaO$–$8SrO$–$36ZnO$–$2P_2O_5$ (mol%) and substituting 6 and 12 mol% of SiO_2 with GeO_2.[177] Immersion in simulated body fluid solutions has shown that the addition of Ge in the glass composition encouraged the deposition of crystalline HA on the glass surface.[177]

Niobium-incorporating glasses promoted an increased and faster mineralization of pre-osteoblastic cells *in vitro* when compared with bioactive glasses without niobium.[116,178] For example, niobium-containing (BAGNb) sol–gel glasses have been implanted in rat femurs, leading to higher mineral deposition in comparison with undoped BGs.[117] These doped BGs have been fabricated *via* a foaming surfactant-based sol–gel method in the form of powders (with the particle size ranging between 300 μm and 600 μm) and scaffolds, and differences in terms of the amount of mineralized tissue have been observed between the two types of implanted BAGNb; in particular, less mineralized tissue is formed in case of BAGNb scaffolds compared with BAGNb powders, showing that not only the composition, but also the structure may influence the bone formation. Anyway, both glass grafts (powders and scaffolds) showed lower trabecular formation when compared with autogenous bone; however, the newly formed bone was adequate and comparable to the autogenous bone at 60 days with a slower maturation. Generally, niobium acts as a network former bonding with the glass matrix, leading to the formation of Nb–O–Si and Nb–O–P and hence to an increase in chain stability and reduction of ion release, which are related to a decrease in the osteoinduction ability of the biomaterials, but if the synthesis temperatures are low, in the absence of bonding, niobium is released as a dissolution product in the form of Nb_2O_5 and the presence of Nb_2O_5 has been shown to have a positive effect on glass bioactivity. Therefore, these results are possible due to the lower temperatures involved in the sol–gel synthesis, because higher temperatures, such as in the case of the melt-quenched glass production, may increase the bonding formation[179] and lead to a reduction in solubility and degradation of the materials.[180]

Recent results of Zambanini *et al.*[181] have shown that even gadolinium and ytterbium are able to promote higher calcium phosphate deposition, despite the lower dissolution kinetics of glasses containing rare earth elements.

Rubidium-containing sol–gel BG nanoparticles have been shown to possess higher HA-forming ability in SBF in comparison with Rb-free BG nanoparticles.[182]

Terbium-doped BG nanoparticles have been synthesized using a template-assisted sol–gel method by Wang *et al.*[183] and their results have shown that the incorporation of Tb ions increased the bioactivity of the glasses.

Se-doped BGs have been shown to possess a good bioactive behavior.[120] These results suggested that selenium could be added to BG compositions to take advantage of the interesting properties of this ion (explained in other subsections – "Osteogenic properties", "Magnetic, photothermal and anticancer properties", "Antibacterial and antiviral properties" and "Antioxidant properties") without compromising the BG bioactivity.

Barium can also be added to the BG composition to improve the physico-mechanical properties (*e.g.* flexural strength and density) of the bioactive glass and it is remarkable to highlight that barium addition does not compromise glass *in vitro* bioactivity, as shown by Arepalli *et al.*[184] Furthermore, in 2021 Ba-containing BGs have been reported to possess an anti-inflammatory effect, significantly reducing the LPS-induced elevation of interleukin-6 (IL-6) and the tumor necrosis factor-α (TNF-α) in the C6 cell line (rat glioblastoma).[185]

The effect of other uncommon doping elements and further interesting experimental results about barium, gadolinium, lanthanum, manganese, niobium, rubidium, selenium, terbium, ytterbium, and zirconium are reported in a review by Pantalup *et al.*,[186] published in 2022.

Antibacterial and antiviral properties

It is well known that some metallic ions possess an antibacterial activity, such as silver,[25,32,36,187–194] copper,[133,134,140,195] gallium,[161,196–198] and zinc;[32,137,199] however, even bismuth (Bi),[145] boron,[145] bromide,[200] cerium,[198] cobalt,[201] fluorine,[147] iron,[140] lithium,[192,202,203] manganese,[204] strontium,[39,78] rubidium,[205] tantalum,[206] tellurium,[207] and titanium[208,209] have recently been shown to be antibacterial. Hence, various BG compositions containing antibacterial ions have been proposed.[32,188–190,192,196,206,207]

Different mechanisms have been suggested for the antimicrobial activities of silver, which is the most studied antibacterial ion:

(1) interference with electron transport:[38] Ag^+ ions strongly bind to electron donor groups on biological molecules containing sulfur, oxygen, or nitrogen;[210]

(2) binding to DNA:[38,194] it has been shown that Ag_2O BGs are bacteriostatic and elicit rapid bactericidal reactions; indeed released metallic silver is able to damage bacterial RNA and DNA, thus inhibiting replication,[188] by inhibiting the activity of respiratory enzymes through the generation of reactive oxygen species or catalyzing the oxidation of cellular components;[211]

(3) interaction with the cell components:[38] heavy metals such as silver can react with proteins by combining with thiol groups, which leads to the inactivation of the proteins[193] and a change in the membrane permeability (due to the combination between free Ag ions and the negatively charged functional groups on the bacterial cell), that causes a loss of the nutrients and entry of the free Ag ions into the bacteria;[194]

(4) attachment to the bacterial wall with consequent destruction of the lipid shell and penetration of free radicals on the bacteria surface, leading to the destruction of bacterial cells.[187]

Open Access Article. Published on 06 Eost 2024. Downloaded on 2026-06-06 12:45:47.
This article is licensed under a Creative Commons Attribution 3.0 Unported Licence.

In 2016, Miola *et al.* developed an innovative scaffold fabrication method based on a modified polymeric sponge replication technique, doping bioactive glass-ceramic scaffolds with silver directly during the scaffold synthesis.[190] These new synthesized Ag-doped scaffolds were demonstrated to be able to create a significant bacterial inhibition halo of about 2 ± 0.5 mm and their silver release kinetics were considered helpful to treat both the development of infections due to bacterial contamination (direct or indirect) of an implant throughout the surgery and the development of latent infections.[190] It is important to point out that, besides its high effective antibacterial properties, silver does not alter the mechanism and kinetics of glass ceramic bioactivity,[190] as confirmed by other recent studies on Ag-doped borate BGs.[212] However, it has been shown that glass containing 2 wt% of silver is toxic also to mammalian cells (whereas glasses containing 0.75 and 1 wt% silver are not toxic).[38]

The antibacterial and antimicrobial capability of silver has been compared with the effect of other ions. For example, nano-sized glass particles with a chemical composition of $60SiO_2–4P_2O_5–(x)Ag_2O–(31 - x)CaO$ and $60SiO_2–4P_2O_5–(x)ZnO–(31 - x)CaO$, where $x = 2$ or 4, were produced through a sol–gel synthesis by Shahrbabak *et al.*[32] An increase in the antibacterial effect of the glasses was recorded by increasing the Zn and Ag content, especially in the case of Ag-containing BGs, which have been shown to be more antibacterial than Zn-containing BGs. The glass containing 4% of silver (BA4 sample) showed the best antibacterial behavior. The pH rise and the ionic concentrations of species released by the glasses under investigation were monitored to determine whether differential changes in these factors between the different BGs could contribute to the antibacterial properties of AgBG, but the changes induced in pH and ionic content were similar to those provoked by AgBG and, therefore, the antibacterial effect of AgBG was attributed only to the released ionic silver.[188]

Another well-known antibacterial ion is copper. Among others, in 2005 Abou Neel *et al.* substituted calcium with variable copper amounts in the glass system $P_2O_5–CaO–Na_2O$, producing BG fibers with compositions (mol%) $50P_2O_5–30CaO–20Na_2O$, $50P_2O_5–30CaO–19Na_2O–1CuO$, $50P_2O_5–30CaO–15Na_2O–5CuO$ and $50P_2O_5–30CaO–10Na_2O–10CuO$.[195] Their results showed that the addition of CuO into the glass fibers was effective in reducing the number of bacteria attached to the fibers, in a Cu^{2+} dose-dependent manner, with higher antibacterial efficacy in the case of the higher CuO amount. Indeed, 10%Cu-doped BG was able to deliver a higher concentration of Cu^{2+}, preventing better bacterial colonization and reducing the number of viable bacteria in the local environment, an effect which may be due to either the reduction of bacteria in solution or the reduction in the viable bacteria attached to the fibers. In 2019, Miola *et al.* showed that a copper-doped glass through an ion-exchange technique (SBA3) was able to produce an inhibition zone of about 2–2.5 mm, 2 mm, and 1.5 mm ± 0.5 mm, respectively, as a consequence of the presence of free Cu^{++} ions in the glass network, alone or in synergy with Cu^0 nanoparticles.[134]

In 2020 the excellent antibacterial properties of Zr-doped sol–gel silicate BGs (in particular the one with a composition, in mol%, of 60% $SiO_2–31CaO–4P_2O_5–5ZrO_2$) have been reported, showing that the addition of zirconium enhances the antibacterial activity of BGs.[173]

Moreover, some of the abovementioned ions, such as boron, cobalt, gallium, lithium, and silver, possess not only antibacterial properties, but also antiviral abilities.[145]

Further details about antibacterial and antiviral ions (in detail, Ag, B, Bi, Ce, Co, Cu, Fe, Ga, Mn, Li, and Zn) and the concentrations required to obtain these effects can be found in the review published by Kargozar *et al.* in 2020[213] and in the one by Awais *et al.* in 2022.[145]

The antibacterial potential of doped mesoporous BGs has been recently reviewed by Kargozar *et al.*[214] and an interesting table recapping the biomolecular mechanisms behind the action of antibacterial ions released from BGs is available in another review.[215]

Antioxidant properties

Bioactive glasses have been also doped with elements with antioxidant behavior, such as cerium,[97,216] selenium,[217] and more recently tellurium.[207]

Cerium has been investigated in different biological applications due to its ability to switch between Ce^{4+} and Ce^{3+} oxidation states and protect cells against the damage resulting from ROS production.[216]

Recently, Miola *et al.*[207] investigated the possibility to dope a BG composition with a low amount of tellurium dioxide, to impart antibacterial and antioxidant properties. The authors demonstrated that Te-doped glasses protect the metabolic activity of cells from apoptosis induced by H_2O_2 treatment and at the same time that Te-doped glasses possess antimicrobial activity and preserve the bioactivity and the cytocompatibility.

Loading with drugs and natural extracts

Bioactive glasses and glass-ceramics can be loaded with various drugs, as demonstrated in many experimental studies.[120,218,219] Differently from ions, drugs cannot be incorporated into the glass during melting synthesis (because biomolecules suffer from thermal degradation in the case of high temperatures such as the ones involved in the melting of glass precursors),[220] but they can be mixed into the sol suspension during low-temperature sol–gel methods that do not need high temperature treatment to stabilize the formed gel, as shown by some experimental studies.[221] To enhance drug loading, the use of porous glasses (in particular, mesoporous glasses) is advantageous, as shown by various experimental investigations.[9,49,168,222,223] Mesoporous BGs offer also the advantage of slow drug release kinetics, which may be related to both the presence of many Si–OH groups in the internal part of MBG mesoporous channels and the hydrogen bonds and van der Waals forces that are formed between the MBG and the loaded drugs.[9]

Another way to prepare drug-releasing BGs, in particular porous BG scaffolds, is to coat them with a drug-loaded poly-

 This journal is © The Royal Society of Chemistry 2024

Open Access Article. Published on 06 Eost 2024. Downloaded on 2026-06-06 12:45:47.
This article is licensed under a Creative Commons Attribution 3.0 Unported Licence.

meric solution. For example, Li *et al.* fabricated vancomycin-releasing porous 45S5 Bioglass®-based glass-ceramic scaffolds by immersing the scaffolds into a solution consisting of PHBV and vancomycin.[224]

To cite a few examples (recapping the experimental studies of drug-loaded biomaterial mentioned in this review), on the basis of the final application, different drugs are available and have been already successfully loaded in BGs:

- dexamethasone and dimethyloxallyl glycine to enhance osteogenesis;[9]
- ampicillin,[18] ibuprofen,[9] and vancomycin[224,225] for conferring antibacterial properties;
- doxorubicin,[9,120,226] 5-fluorouracil,[225,227] and mitomycin C[228] for the inhibition of the viability of cancer cells.

In 2018 mesoporous sol–gel 58S nanoparticles were successfully loaded with propolis and cranberry, to impart antibiofilm properties to the BGs for potential bone healing and infection treatment procedures.[229] Information can also be found in the review published by Kaou in 2023.[230]

This review will not further enter into details of the used drugs, as a review about BGs as carriers for therapeutic drugs, growth factors, and proteins, for bone TE, has already been published by Hum and Boccaccini in 2012[220] and a rich overview table written by Baino *et al.* is available in their review.[44]

Applications of doped and loaded bioactive glasses

Among the possible applications of doped bioactive glasses and glass-ceramics, we can find the fabrication of multifunctional glass scaffolds,[41,49,231,232] and the use as fillers in polymeric matrix or bone cement to obtain composite scaffolds able to release therapeutic ions[6,8,42,163] or composite bone cement with enhanced osteogenic[233,234] and antibacterial properties,[235–237] respectively.

BGs releasing drugs with several therapeutic and/or antibacterial effects can be also added to bone cement.[226]

The use of BGs as fillers in degradable matrices might offer a promising strategy for the regulated *in situ* secretion/expression of angiogenic growth factors (*e.g.*, VEGF) and osteogenic markers (*e.g.*, ALP) in therapeutic levels, leading to successful vascularization and bone formation of TE scaffolds.[6] Composite scaffolds composed of bioactive glasses and polymers can be fabricated using different techniques such as electrospinning, 3D printing, salt leaching, and the slurry sponge method (just to cite a few examples), but the detailed description of these fabrication methods is out of the aim of this review. The interested reader can find more information about composite glass–polymer scaffolds in the following publications, for bone, dental,[238] and cartilage TE,[238] respectively, whereas for antibacterial PMMA-based bone cements a recent review by Bistolfi *et al.* is available.[239]

Not only solid scaffolds but also composite osteoconductive and antibacterial hydrogels can be fabricated by incorporating GFs and BG particles inside the hydrogels.[240–242]

Furthermore, composite bone cements incorporating magnetic BGs can be produced for hyperthermia treatment applications as done a few years ago by Miola *et al.*[243]

Doped bioactive ceramics are also useful to coat various surfaces and scaffolds, in order to impart multifunctionality (such as bioactivity and/or antibacterial properties) to the coated material, as shown by many experimental works.[244–250] Because of the well-demonstrated antibacterial property of silver, silver-containing BG powders have been largely used for coating polymeric scaffolds, resulting in a bioactive and bactericidal implant.[244,248] Many coating techniques are available, but atmospheric plasma spraying is probably the most popular one because of its good mechanical performance (bond strength and mechanical properties) and the excellent preservation of the amorphous structure of the sprayed BG powder.[246] For a comprehensive review of glass-based coatings on biomedical implants, see the review published in 2017 by Baino and Verné.[251]

Synergic effects and summary

In Table 1, the properties of doping ions are summarized. It is possible to observe that several ions realize opposite effects on eukaryotic and bacterial cells, promoting bone and blood vessel regeneration, but having an antibacterial behavior, thus inducing bacteria death.

As already reported, several ions possess more than one property. For example, boron, cerium, copper, lithium, and zinc show both osteogenic and antibacterial properties, as demonstrated by numerous experimental studies.[49,97,134,202] In addition, it should be reminded that boron[128,129] and copper[132–134] possess also angiogenic abilities. The multipotential ability of these ions makes them amazingly interesting for applications related to bone TE and bone surgery.

For example, the nano-sized glass particles produced by Shahrbabak *et al.*[32] (mentioned above in the subsection "Antibacterial and antiviral properties") were not only antibacterial, but also bioactive and enhanced G292 osteoblastic cell proliferation, being good candidates for bone TE applications.

Recently, in 2020, Zheng *et al.*[97] reported the synthesis of antioxidant, anti-inflammatory, and pro-osteogenic BGs containing cerium. A comprehensive review of Ce-containing BGs has been published in 2021 by Zambon *et al.*[252]

Besides its antibacterial and antioxidant properties, tellurium is well known for its high conductivity and piezoelectricity, a property that can help stimulate bone growth and regeneration. In fact, bone tissue is sensitive to electrical stimuli. For these reasons, new applications of Te-based glasses and glass-ceramics are emerging, not only thermoelectric applications[253] but also biomedical ones.[207,254]

Similar observations could be made on fluorine for dental surgery. Indeed, since long ago it has been well-known that fluorine can enhance apatite deposition and in recent years its antibacterial ability has been proved by Liu *et al.*[147] who demonstrated that the growth of sub-gingival bacteria (*Aggregatibacter actinomycetemcomitans* and *Porphyromonas gingivalis*) was significantly inhibited after incubation with F-doped BG particulates.

However, it should be also pointed out that recently there is an increasing interest in co-doping in tissue engineering,

Open Access Article. Published on 06 Eost 2024. Downloaded on 2026-06-06 12:45:47.
This article is licensed under a Creative Commons Attribution 3.0 Unported Licence.

Table 1 Properties of doping ions

	Properties					
Ion	Osteogenic	Angiogenic	Antibacterial/antiviral	Antitumoral	Antioxidant	Bioactive
Ag			Yes[32,36,145,188–190,192–194,213,215,244,245,248,255,257]	Yes[144,145]		Not modified[190,212] or delayed[32] depending on the Ag amount
Al	No, it prevents bone bonding[3]					Inhibited[3] or no effect if ions are incorporated in crystalline phases[38]
B	Yes[102–107,109,145,269,276]	Yes[66,128,129,145,213]	Yes[58,145,277]	Yes[145]		Enhanced[150,153]
Ba			Yes[186]			Not compromised[184] but diminished if co-doping with Fe[186]
Br			Yes[200]			
Ca	Yes[4,72,73]	Yes[130,213]		Yes[144]		Enhanced[74]
Ce	Yes[96,97,252]	Yes[97,131,252]	Yes[97,198,213,215,252,257]		Yes[97,216,252]	Lowered[65,216]
Co	Yes[126]	Yes[66,76,126,129,132,145,213]	Yes[145,201]	Yes[144]		Argued influence: enhanced[169] or inhibited[66]
Cu	Yes[49,91,98]	Yes[49,64,132–134,213,215,274,278]	Yes[49,133,134,140,145,195,213,215]	Yes[144,145]		Argued influence: enhanced[157] or lowered[156] or even no effect[134]
F	Yes[110]		Yes[147]			Enhanced[146,147,153]
Fe	Yes[9]		Yes[140,145]	Yes[41,141,144,243]		Enhanced if combined with zinc[167]
Ga	Yes[9]	No[131]	Yes[161,196–198,213,215]	Yes[144]		Delayed[161]
Ge						Enhanced[177]
Gd	Yes[186]					Enhanced[181]
La	Yes[186]	Yes[186]				Enhanced[160,186]
Li	Yes[62,114,202]	Yes[135]	Yes[145,192,202]			
Mg	Yes[94,95,145]	Yes[136,137,213]				Argued influence: enhanced[159,160,168] or not compromised[95] or delayed[149]
Mn	Yes[91,115,186]		Yes[145,186,204]	Yes[144]		Argued influence: enhanced[115,186] or delayed[149]
Na						Little influence[175]
Nb	Yes[116,117,119,186]	Yes[186]		Yes[226]		Enhanced if sol gel–sol BG,[116,117,178] whereas reduced if BG produced by melting–quenching[179,180]
P	Yes[54,82]	213				Enhanced[174,279]
Rb	Yes[186,205,280]	Yes[186,205]	Yes[205]	Yes[205]		Enhanced[182,186]
Se	Yes[125]		Yes[125,186,217,281]	Yes[123,144]	Yes[217]	Good[120,281]
Si	Yes,[68,71,138] however sometimes argued[70]	213				
Sb						Inhibited[3]
Sr	Yes[39,51,52,74,76–80,106,138,145,171,233,245,269]	Yes[52,76,138,282]	Yes[39,78,281]	Yes[281]		Argued influence: enhanced[58,154,173,249,255] or lowered[172] or delayed[39,58,78,171]
Ta			Yes[186,206]	Yes[206]		Argued influence: enhanced[186] or inhibited[3,186] depending on the added amount
Tb						Enhanced[183,186]
Te			Yes[207]		Yes[207]	
Ti	Yes[4]		Yes[208,209]			Inhibited[3]
Va		No[131]				Enhanced[155]

This journal is © The Royal Society of Chemistry 2024

Open Access Article. Published on 06 Eost 2024. Downloaded on 2026-06-06 12:45:47.
This article is licensed under a Creative Commons Attribution 3.0 Unported Licence.

Table 1 *(Contd.)*

Ion	Properties: Osteogenic	Angiogenic	Antibacterial/antiviral	Antitumoral	Antioxidant	Bioactive
Yb						Enhanced[181,186]
Zn	Yes[62,86,88,89,91,92]	Yes[135]	Yes[32,137,145,199,203,213,215,268]	Yes[144,256,283]		Argued influence: delayed[32,34,58,63,166,264] or even inhibited[3,34,90,92,162,163,247] or in contrast not diminished[165] or enhanced (depending on different amounts and co-doping with Mg or Fe)[34,92,167,168]
Zr	Yes[9,53,173,186]		Yes[173,186]			Argued influence: inhibited[3] or diminished[186] or in contrast not hindered[53] or even enhanced,[186] especially in synergy with Sr addition[176]

which allows multifunctionality to be reached by taking advantage of the different properties or different mechanisms of functioning of different doping ions. For example, co-doping with Ag and Li,[192] Ag and Sr,[255] Ag and Zn,[32,256] Ag and Ce,[257] B and Co,[66,129] B and Cu,[108,258,259] B and Zn,[260] Cu and Co,[261] Cu and Fe,[262] Cu and Sr,[263] Cu and Zn,[215,258,261,264] Si and Sr,[138] Sr and Co,[74] Sr and Li,[265] Sr and Zn,[266] Zn and Co,[267] and Zn and Mn[268] has been studied.

For example, Anand *et al.* fabricated multifunctional BGs by introducing amounts up to 2 mol% of Sr and Cu ions as co-dopants in the ratio 1 : 1 in MBGs and demonstrated that such novel BGs could be beneficial for bone tissue regeneration, ensuring also antibacterial properties against drug-resistant pathogen infection and, at the same time, promoting bone regeneration, *e.g.* solving the issues of bone deformities.[263] Similar multifunctional BGs were synthetized by Bano *et al.* by co-doping with silver and strontium.[255] These Ag- and Sr-co-doped BGs (named Ag–Sr MBGNs) were strongly antibacterial against *Staphylococcus carnosus* and *E. coli* bacteria and highly bioactive thanks to the addition of Sr.[255]

As vascularization is essential for osteogenesis and tissue formation in general, the combined stimulation of both osteogenic and angiogenic activities by strontium- and cobalt-substituted BGs have been shown to successfully promote *in vitro* bone regeneration when seeded with human umbilical cord perivascular cells (HUCPVCs),[76] which contain a subpopulation that shows common features of the MSC phenotype such as a high frequency of colony-forming unit-fibroblasts (CFU-F).[76] Thus, these BGs synthesized by Kargozar *et al.*[76] are optimal candidates as functional bone substitutes.

Angiogenesis was proved to be enhanced by the synergical effect of different couples of pro-angiogenic ions, such as boron and cobalt, cobalt and copper,[22] and copper and zinc.[215] The synergical effect of B and Cu has been reported in the case of B- and Co-doped 45S5 Bioglass® by Chen *et al.* in 2020, showing that the secretion of VEGF from bone marrow-derived stromal ST-2 cells was increased by the dual-doped BG in comparison with single (B or Co) doped BG.[66] The synergy of the ionic dissolution products (Cu^{2+} and Co^{2+}) from Cu- and Co-co-doped BGs has been shown to enhance wound healing ability, not only *in vitro*, but also *in vivo*. After being implanted, these microfibrous constructs induce better neovascularization, re-epithelization, and ordered deposition of ECM components (such as collagen and elastin) of damaged skin in the dorsum of rabbits, in comparison with commercial wound dressings.[22]

Preliminary studies of the bioactivity and cytotoxicity to Saos-2 cells of Cu- and Zn-co-doped BGs (1Cu1Zn–NaBG) have been also carried out, to evaluate the feasibility of co-doping with these two ions for potential use in bone regeneration thanks to the combination of the antibacterial properties and regenerative therapeutic effects of Cu (angiogenic agent) and Zn (osteogenic agent).[264]

Borate glasses have been doped with 6 mol% and 9 mol% of Sr, enhancing the cell growth rate, the ALP activity, and the bone sialoprotein (BSP) and osteocalcin (OCN) mRNA level of

Open Access Article. Published on 06 Eost 2024. Downloaded on 2026-06-06 12:45:47.
This article is licensed under a Creative Commons Attribution 3.0 Unported Licence.

MSCs, thanks to the combined effects of boron and strontium ions, that improved the osteogenic ability of these glasses.[269] In this context, it should be underlined that concentrations of boron above 0.65 mM may inhibit the growth and proliferation of MG-63 cells. The presence of SrO (0–9 mol%) in the composition (mol%) of borate-based 13-93B2 glass scaffolds ($18SiO_2$–$36B_2O_3$–$22CaO$–$6Na_2O$–$8K_2O$–$8MgO$–$2P_2O_5$) can accelerate the release of Si^{4+} and Ca^{2+} ions and suppress the rapid release of B^{3+}, thus significantly improving the cell proliferation and reducing the cytotoxicity of glass scaffolds.[55]

Khan *et al.*[265] demonstrated the synergical osteogenic effect of Sr and Li ions. Indeed, significant new bone formation, an abundant collagenous network, and a minimal or no interfacial gap between the bone and the implant were observed in Sr-doped and Li- and Sr-co-doped samples as compared with Li-doped samples.[265] In addition, Li- and Sr-co-doped (Li + r) samples led to an enhanced formation of peripheral cancellous tissue on the periphery and cortical tissues inside the implanted samples and to a higher degree of vascularity in comparison with the other tested glass compositions.[265]

Analogously, co-doping with cobalt and strontium has shown synergic osteogenic effects both *in vitro* and *in vivo*, showing *in vitro* calcium nodule formation and the expression of osteogenic markers and better bone healing when implanted in critical size defects of the distal femur in rabbits in the case of the group receiving Sr- and Co-co-doped glass constructs, compared with the Co-free groups, at both 4 and 12 weeks of follow-up.

In addition, it has been demonstrated that co-doping with two antibacterial ions like Ag and Li ions leads to an enhancement of the antibacterial properties of the modified BG. Four Li- and Ag-co-doped BGs (LA-BGs) with a fixed content of lithium (5 mol%) and a variable amount of silver (*i.e.*, $60SiO_2$–$31CaO$–$4P_2O_5$–$5Li_2O$–$0Ag_2O$, $60SiO_2$–$30CaO$–$4P_2O_5$–$5Li_2O$–$1Ag_2O$, $60SiO_2$–$26CaO$–$4P_2O_5$, $5Li_2O$–$5Ag_2O$, and $60SiO_2$–$26CaO$–$4P_2O_5$–$5Li_2O$–$10Ag_2O$) have been synthesized *via* a sol–gel technique, demonstrating that the BGs doped with 1 mol% of Ag and 5 mol% of Li realized the best cell proliferation and, at the same time, the best antibacterial properties.[192]

A synergistic antimicrobial efficacy of different antibacterial ions has been demonstrated also in the case of Cu- and Co-doped phosphate glasses at a concentration of 5 mg mL^{-1} against *E. coli* in comparison with single-doped glasses.[261]

In 2023 Taye *et al.* published the first (based on a literature overview of the work's authors) Ag- and Ce-co-doped BG (80S–Ag–Ce–MBG),[257] proving the antibacterial efficacy of this novel glass formulation against *E. coli*. These results confirmed the ones published by Raja *et al.* in 2022, showing a synergistic antimicrobial effect of Cu and Co against *E. coli* and Cu and Zn against both *E. coli* and *S. aureus*.[261]

The successful treatment of full-thickness injuries in rabbits by eggshell membranes coated with a Zn- and Co-co-doped glass demonstrated the synergistic effect of cobalt with zinc on wound closure efficacy as compared with the effect of single ions.[267]

Besides the abovementioned applications, the co-doping of BGs has been also studied to better control the sintering process. A study published in 2019 by Ben-Arfa about the effects of Cu^{2+} and La^{3+} doping on the sintering ability of sol–gel derived high-silica BGs revealed that copper promotes early densification, enhancing the density at lower sintering temperatures, and ultimately crystallization, whereas lanthanum offers beneficial effects at sintering temperatures higher than 1000 °C, inhibiting crystallization.

In the case of co-doping, an interesting novel method for the dual addition of doping ions was developed by Li *et al.*, as reported in 2022.[262] They employed the scalable reactive laser fragmentation in liquids method to produce 45S5 BG nanoparticles in the presence of light-absorbing Fe and Cu ions, successfully doping these nanosized BGs with two metal ions up to 4 wt%.

Another interesting approach to fabricating multifunctional BGs is to combine the doping with therapeutic and/or antibacterial ions with the loading with therapeutic and/or antibacterial drugs.

The synergetic effect of antibiotic drugs and antibacterial ions is, indeed, under investigation, as shown by several experimental works.[214,270]

Porous Li-modified BG nanoparticles were loaded with vancomycin or 5-FU to allow multiple deliveries of lithium ions with osteogenic properties and drugs with antibacterial or antitumoral properties.[225] So, these BGs could be used for curative and restorative bone treatment, in particular, bone regeneration as a consequence of the bioactive properties of the BG nanoparticles themself, osteoporosis treatment stimulated by the doping with Li ions, osteomyelitis treatment or cancer treatment in the case of vancomycin or 5-FU controlled release.[225]

Another promising candidate for bone tumor treatment is Se-doped and doxorubicin-loaded mesoporous sol–gel BG particles, because of their very good bioactivity (characterized by HA formation after only 3 days in SBF) and sustained and controllable drug delivery.[120] The addition of small amounts of selenium into the mesoporous BGs did not alter their mesoporous structure but enhanced both the drug-loading ability and the drug-release kinetics.[120]

Remaining in the application field of anticancer therapy, in particular for the therapy of osteosarcoma (a common malignant bone tumor, generally treated by surgical resection), Nd-doped mesoporous borosilicate bioactive glass-ceramic bone cement was developed for the repair of the bone defects caused by the surgery and the synergistic therapy of osteosarcoma recurrence through the combination of photothermal therapy and release of doxorubicin.[226] The sol–gel Nb-doped mesoporous bioactive glass-ceramics microspheres act both as a photothermal agent and a drug carrier, resulting in a bone cement with an enhanced killing effect on MG-63 osteosarcoma cells thanks to the synergistic effect of photothermal and chemical therapies.[226] The photothermal properties were given by the presence of Nd^{3+} whereas the drug-loading ability was by the mesoporous structure of the glass-ceramics.[226] It is interesting to point out that the increase in temperature (caused by the photothermal therapy) significantly accelerated

 This journal is © The Royal Society of Chemistry 2024

Open Access Article. Published on 06 Eost 2024. Downloaded on 2026-06-06 12:45:47.
This article is licensed under a Creative Commons Attribution 3.0 Unported Licence.

the release of doxorubicin from this drug-loaded bone cement.[226]

In 2020, copper doping has been demonstrated to influence the lattice of BGs, and consequently, their morphology and porosity, which influence the ionic dissolution (hence modulating glass bioactivity) and drug release in the case of porous Cu-doped BGs.[271] Due to the mesoporous network, 1.5% and 2.5% Cu-doped BGs showed an enhanced release of anti-inflammatory drugs such as acetaminophen and ibuprofen.[271] Thus, these Cu-doped BGs act as antibacterial drug carriers and are characterized by antibacterial properties amplified by the presence of copper, being potentially able to up-regulate the healing properties in dental applications and control oral microbial exposure.[271]

Also, cerium influences the porosity of mesoporous BGs; in particular, Farag *et al.* showed that the pore size diameter of MBGs decreased as the cerium content increased in all MBGs.[272] Doping with Ce ions was also proved to enhance drug adsorption (in detail, vancomycin).[272] Ce-free MBGS showed, in fact, the lowest drug absorption and the highest drug release percentage.[272] Thus, the actual MBGs were considered promising candidates for bone regeneration and bone cancer treatment, possessing the added value of being able to reduce the bacterial activity around the tumor site.[272]

The dependence of drug loading efficiency on the content of the doping ion was confirmed also by experimental studies of Mg-doped BGs,[55] which were modified to introduce amino groups on their surface, with the aim of loading negatively charged biomolecules such as amoxicillin.[55] It was proved that amoxicillin loading slightly decreased with an increase of Mg^{2+} content (from 0 mol% to 5 mol%) in the BG composition.[55]

The above-reported studies[271,272] demonstrated that drug loading and drug release could be controlled by the glass composition.

Drug release can be tracked and monitored using luminescent BGs on the basis of the change of the luminescence intensity, such as Eu^{3+}/Tb^{3+}-doped mesoporous electrospun BG nanofibers (MBGNFs) with an average diameter of 100–120 nm.[273] If loaded with ibuprofen, these luminescent nanofibers were shown to be able to release it in a sustained way *in vitro*, and biocompatibility tests on L929 fibroblast cells using the MTT assay have revealed the low cytotoxicity of MBGNFs.[273]

Finally, an interesting work on doping with different ions and its synergical use with the release of vitamin E was published by Hu *et al.*[274] Borate BGs were doped with copper to mitigate issues related to the uncontrolled release of borate glasses, which can lead to a very rapid degradation and transient biotoxicity;[274] in fact, the addition of Cu in borate glasses has been proved to render borate and borosilicate glasses more stable and to lower the release of other ions, such as Ca and B (although Cu-doped 13-93-BS glass showed an enhanced release of Si, probably because of the preferential connection of the modifier B ion in the network structure of borosilicate glasses to Si, making the Si–O–Si bonds more breakable).[258,275] They were used for the fabrication of a novel organic–inorganic dressing of BG/poly(lactic-*co*-glycolic acid), which was loaded with vitamin E (named VE-Cu BG/PLGA).[274] The *in vitro* cytotoxicity and angiogenesis of the VE-Cu BG/PLGA dressing were assessed using human fibroblasts and umbilical vein endothelial cells (HUVECs), showing positive pro-angiogenic effects in both cases: fibroblasts expressed higher levels of angiogenesis-related genes and HUVECs showed high migration, tubule formation, and VEGF secretion.[274] *In vivo*, in the case of full-thickness skin wounds in rodents, a significant improvement in the epithelialization of wound closure, and a clear enhancement in vessel sprouting and collagen remodeling was observed.[274] Thus, this dressing was considered very promising for the stimulation of angiogenesis and reconstruction of full-thickness skin defects, thanks to its controlled release of both Cu^{2+} and vitamin E.[274]

Functionalization and coatings of bioactive glasses

BG surfaces can be further chemically modified with various biomolecules (such as polymers, proteins, vitamins, and drugs), imparting or improving bioactive, mechanical, regenerative, and/or antibacterial properties.

Various strategies of chemical surface modification are available and the most suitable and effective in the case of BGs involve the use of coupling agents or pH changes; other approaches involving the deposition of coatings, the use of radiation, and the development of core–shell systems are also possible and widely investigated.[284] Moreover, the ion exchange method can be used to modify the bioceramic surface, as reported by J. H. Lopes *et al.* who adopted a molten salt bath ($Ca^{2+}_{\text{molten salt bath}}|Na^{+}_{\text{glass}}$) immersion ion exchange process to selectively change the surface reactivity and enhance the bioactivity of a melted 45S5 Bioglass® by accelerating some reactions in the early stages of Hench's mechanism.[285]

To improve the mechanical stability of highly porous glass and glass-ceramic scaffolds, many authors have coated the scaffolds with biodegradable polymers.[286–288] An ideal scaffold for bone TE should, in fact, offer suitable mechanical properties, adequate pore size, a high degree of porosity (to enable tissue ingrowth, vascularization, osteoconductivity, and osteoinductivity), and an adequate degradation rate, but most bioceramic scaffolds are too brittle and not suitable for load-bearing applications.[287]

Moreover, BG and bioactive glass-ceramics can be functionalized in order to enhance their biocompatible and bioactive properties[286] (referring in this case to the general meaning of the term bioactivity as the ability to induce or modulate biological activity[56] and not only their ability to bond to bone). Such coatings are able to provide a high degree of biocompatibility and promote cell adhesion[288] and tissue healing without causing severe reactions.[287]

Biologically active molecules and ECM proteins/peptides can be grafted on the BG surface to stimulate physiological

Open Access Article. Published on 06 Eost 2024. Downloaded on 2026-06-06 12:45:47.
This article is licensed under a Creative Commons Attribution 3.0 Unported Licence.

bone regeneration with both inorganic and organic signals.[286] For example, glass-ceramic scaffolds with very high mechanical properties and moderate bioactivity have been successfully functionalized with ALP, which is involved in bone formation and mineralization and is widely used as a marker of osteoblast differentiation in *in vitro* tests.[286]

Furthermore, the ECM possesses transmembrane integrin receptors with extracellular domains that can recognize motifs such as the sequence Arg–Gly–Asp (RGD) within ECM adhesion proteins, *e.g.* fibronectin and vitronectin, and cytoplasmatic domains that can interact with proteins like vinculin, paxillin, talin and actin, but also with other signaling molecules (such as FAK and c-Src) at the focal adhesion sites.[28,289] So it is possible to graft ECM adhesion proteins or derived peptides[28] and three main grafting techniques are available: simple adsorption, covalent bonding, or release from a degradable carrier.[290]

Growth factors such as bone morphogenetic proteins, insulin-like growth factors (IGF), TGF-β, and FGF can also be linked to the BG surface, imparting enhanced osteogenic properties to the bioactive glass.[291]

BGs and glass-ceramics are particularly reactive and prone to surface modifications, not only by direct anchoring, but also through functionalization with aminosilanes thanks to numerous silanol groups available on their surface.[286] Thus, the BG surface can be functionalized using several functional groups, that can act as active sites for specific properties or further molecular grafting, as recently well reviewed by Kargozar *et al.*[284] As shown by many experimental studies,[284,290,292–299] the functional group most commonly introduced on the surface of BGs is the amino group (NH_2); 3-aminopropyltriethoxysilane (APTES, $C_9H_{23}NO_3Si$), a nontoxic protein-coupling agent that can be easily introduced using silanization, was proposed by Verné *et al.*[300] as a successful agent for covalently bonding bone morphogenetic proteins (*e.g.*, BMP-2) to the BG surface, as confirmed by several experimental results (as reported below). For example, to improve their ability to bond with biomolecules, such as drugs, proteins, and peptides, gallium-containing BGs, characterized by the composition $45.7SiO_2$–$24.1Na_2O$–$26.6CaO$–$2.6P_2O_5$–$1.0Ga_2O_3$ (Ga1.0), were successfully functionalized with tetraethyl orthosilicate (TEOS) and APTES.[301] Novel highly porous 45S5 Bioglass®-based scaffolds have been fabricated by Rezwan *et al.*[292] using the polymer replica technique and later surface-functionalized with APTES and glutaraldehyde without the use of organic solvents, but it is worth noticing that these surface-modified BG scaffolds have shown an enhanced bioactivity only thanks to their more pronounced surface microroughness, which was believed to be caused by ion leaching during the functionalization aqueous heat treatment (at 80 °C). The influence of surface roughness on the behavior of bone cells and glass bioactivity will be further discussed in the section "Influence of topography on cell behaviour – superficial and internal nanostructure".

Despite Rezwan's results, Ferraris S. *et al.*[286] have successfully produced ALP-functionalized and highly bioactive scaffolds of SCNA (57% SiO_2–34% Ca–6% Na_2O–3% Al_2O_3 in mol%) bioactive glass-ceramic by introducing APTES on the glass surface after hydroxyl exposure and silanization of the glass surface itself and the higher bioactivity of these functionalized scaffolds was hypothesized to be related to the ability of the grafted homodimeric metalloenzyme ALP to attract phosphate ions utilizing its Zn cations and thus accelerate calcium ion precipitation and HA nucleation in SBF.[286]

Zhang *et al.*[302] have prepared amino-functionalized MBGs with the composition of 80% SiO_2–15% CaO–5% P_2O_5 (mol%), using the evaporation-induced self-assembly (EISA) method to synthesize the glasses and the reflux agitation method to successfully graft the 3-APTES by the silicon-alkylation reaction. The results indicate that the surface of N-MBG was positively charged, so that surface adhesion proteins with a negative charge could be easily adsorbed on the surface of the N-MBG, promoting the adhesion of mouse embryo osteoblast precursor cells (MC3T3-E1). Moreover, the functionalized MBGs showed an increased surface area and a more rapid release of Ca and Si ions. Therefore, these amino-functionalized ordered MBGs are more conducive to cell adhesion, proliferation, and differentiation compared with BGs and MBGs and so they could be potentially used as platforms for bone regeneration applications.

Furthermore, it is worth noticing that APTES functionalization has been shown to enhance the absorption of metallic ions on the glass surface.[297] Analogously, the surface modification of M58S glass with KH550 can improve the Ag^+ loading capacity (achieved using the dipping method).[193]

Moreover, only when gold is present in the glass composition is it possible to alternatively and selectively form two types of bond with either the amino or thiol groups of small organic biomolecules (*i.e.*, either Au–S or Au–N), by simply raising or lowering the temperature of the batch of functionalization, as demonstrated by Aina *et al.*, who have selectively functionalized mesoporous sol–gel silicate BGs containing AuNPs (SiO_2–CaO–P_2O_5–Au_2O), with 2-mercaptoethanol, 2-ethanolamine, and the SH-containing amino acid cysteine, carrying either/both amino or/and thiol groups.[303]

It is also possible to impart or improve the antibacterial properties of the implant; the BG scaffold can be coated with antibiotic drugs or antibacterial metallic ions, such as silver.[304–307]

Polyphenols are gaining a lot of attention thanks to their antioxidant, anti-inflammatory, antibacterial, bone-stimulating, and anticancer properties.[308–312] Among other studies, a few years ago, two silicate BGs – SCNA (57% SiO_2–34% CaO–6% Na_2O–3% Al_2O_3) and CEL2 (45% SiO_2–3% P_2O_5–26% CaO–7% MgO–15% Na_2O–4% K_2O, mol%) – have been successfully coupled with gallic acid and natural polyphenols extracted from red grape skins and green tea leaves by Zhang *et al.*[309,313] and Cazzola *et al.*,[308] after surface treatment for superficial –OH exposure. These studies showed that the amount of gallic acid was significantly higher on CEL2 than on SCNA (according to a preliminary test of the Folin & Ciocalteu assay) and that polyphenol-functionalized CEL2 was characterized by a faster HA kinetics deposition (if compared with non-functiona-

 This journal is © The Royal Society of Chemistry 2024

Open Access Article. Published on 06 Eost 2024. Downloaded on 2026-06-06 12:45:47.
This article is licensed under a Creative Commons Attribution 3.0 Unported Licence.

lized BG) because of the interaction between phenolic hydroxyls and Ca^{2+} ions.

It is also interesting to point out that the functionalization with polyphenols can trigger the *in situ* reduction of metallic nanoparticles on glass surfaces, as shown by various experimental studies.[134,312,314] Silver nanoparticles (AgNPs) were synthesized for the first time by Ferraris *et al.*[314] by *in situ* reduction on BGs (in detail, SCNA and SCN1, with the compositions in mol% of $57SiO_2$–$6Na_2O$–$34CaO$–$3Al_2O_3$ and $57SiO_2$–$9Na_2O$–$34CaO$, respectively) previously functionalized with gallic acid or with natural polyphenols extracted from red grape skin and green tea leaves, and, then immersed in an aqueous silver nitrate solution.

To sum up, chemical surface modification of BGs can be classified into two main categories:

1. to improve the surface bioactivity: functionalization with bioactive molecules, such as enzymes (like ALP), ECM proteins, growth factors, and drugs;

2. to impart or improve the antibacterial properties of BGs: coatings with antibiotic drugs or antibacterial ions, such as silver, or functionalization with antibacterial moieties, such as polyphenols and vitamins.

In the following table (Table 2), the main studies including experimental results about the bioactivity and osteogenic and antibacterial properties of functionalized bio-ceramics are reported.

Moreover, the BG surface and composition can be properly designed in order to induce the surface absorption of specific proteins after implantation. Indeed, protein signaling is influenced by the type, amount, and conformation of adsorbed proteins and regulates the adhesion, proliferation, and differentiation of cells and foreign body inflammatory processes.[292] The various parameters influencing protein absorption are largely discussed in a review by Zheng *et al.*[316]

Finally, it is remarkable that surface modification with organic groups allows a modulation of both the uptake and delivery of drugs in mesoporous materials, for example by tailoring the hydrophobicity of the glass surface with chemical groups.[223]

Influence of topography on cell behaviour – surface and internal nanostructure

Materials topography influences the behavior of cells attaching to the material surface, as demonstrated by an increasing number of experimental studies.[28,29,317] According to the specific topographical features of the surface and the type of cell, the material can promote the adhesion, proliferation, differentiation, migration, cell orientation, and gene expression of the attached eukaryotic cells[318,319] or, in the case of bacterial cells, the surface can show an antibacterial effect, as observed in many natural surfaces such as lotus leaf, cicada wings, gecko skin, and shark skin.[320–323]

The effect of surface topography on cells (both eukaryotic and bacterial cells) can be divided into two main groups: chemical and mechanical effects.

With chemical effects, we refer to the influence of chemical and wettability properties, that can be significantly altered by modifying and micro-/nanostructuring the surface topography.[324,325] Indeed, it is well known that by increasing or decreasing the surface contact angle (CA) up to 150° or down to 50°, it is possible to fabricate super-hydrophobic or super-hydrophilic surfaces and thus modulate how cells interact with the surface. For example, Ishizaki *et al.*[324] fabricated a superhydrophobic/superhydrophilic micropattern on a glass surface and used it as a scaffold for cell culture. On the micropatterned surface, the cells attached to the superhydrophilic regions in a highly selective manner, forming circular microarrays of cells corresponding to the pattern. On the micropatterned surface with pattern distances of 200 μm between superhydrophilic regions, the cells adhered to the superhydrophilic regions and partly extended to the neighboring cells. In contrast, when the pattern distances between the super-hydrophilic regions were more than 400 μm, the cells did not extend to the neighboring cells.

With mechanical effects, we refer to the combined influence of geometry and size of surface features, and forces such as gravitational force,[326,327] and shear stress.[317]

In this review, we will mainly focus on bone cells and bacterial cells, because bacterial infections are still very common in orthopedic implants, as reported in the "Introduction".

Influence of topography on tissue cells

Almost all cells in human tissues (aside from blood cells) are anchorage-dependent and influenced by surface topography. Eukaryotic cells can sense, interpret, and respond to environmental features at all length scales from the macro down to the molecular scale, reorganizing in function of topography.[28,328] Therefore it is possible to promote implant integration and tissue regeneration by fabricating implants with *ad hoc* topography.[29,329] For example, roughened implant surfaces have been shown to enhance osseointegration compared with smooth surfaces.[325]

Surface topography provides the adhered cells with mechanical signals, that are then converted intracellularly into biochemical signals through a process called mechano-transduction.[330] Two different mechanisms of mechano-transduction are possible:

1. the conversion of mechanical signals into biochemical signals through biomolecules (indirect mechano-transduction) and consequent gene expression modulation;

2. the propagation of mechanical signals (such as mechanical forces like traction stress that leads to a mechanical deformation and stretching of the cell membrane and so to a modification of the cell cytoskeleton) from outside the cell to the nucleus to directly alter the nucleus shape and possibly chromosome orientation (direct mechano-transduction), for example provoking the opening of stretching-activated channels (SACs).[10,330,331]

Open Access Article. Published on 06 Eost 2024. Downloaded on 2026-06-06 12:45:47.
This article is licensed under a Creative Commons Attribution 3.0 Unported Licence.

Table 2 Functionalized bio-ceramics

Ceramic	Ligand	Functionalization	Bioactivity	Cell response	Antibacterial properties	Ref.
45S5 Bioglass®	APTES and enzyme ALP	Both *via* silanization and through direct anchoring to hydroxylated surfaces	Enhanced, in particular in the case of direct anchoring of ALP			296
SCNA and CEL2 glasses	APTES and enzyme ALP	Both *via* silanization and through direct anchoring to hydroxylated surfaces	Enhanced, in particular in the case of direct anchoring of ALP	Stronger expression of one of osteocalcin, good cell viability, and proliferation		290 and 315
MBGs (85% SiO_2–15% CaO, mol%)	APTES	Amination and then chemical links with amino acid sequences of collagen, to synthesize collagen hydrogels incorporating NH_2-functionalized MBG NPs	Improved	Excellent viability, good proliferation, and osteogenic differentiation, enhanced cytoskeletal extensions of MSCs cultivated on Col–mBGn hydrogels		293
BG with composition (mol%) $80SiO_2$–$15CaO$–$5P_2O_5$	APTES	Amino functionalization by reflux agitation method	Good	Good platform for MC3T3-E1 cell adhesion		302
BGs belonging to the $56SiO_2{\cdot}(40-x)CaO{\cdot}4P_2O_5{\cdot}xAg_2O$ system (with x = 0, 2, and 8 mol%)	APTES and protein coupling agent glutaraldehyde	Before protein attachment, silanization with APTES, and surface functionalization with glutaraldehyde		Improved stability of the protein attachment, reduction amount of the adsorbed protein (balanced by silver presence), and good hemoglobin affinity		295
Ga1.0	TEOS and APTES	Silanization with APTES and then functionalization with TEOS	After a short SBF soaking time (4 days), separation of calcite favored by APTES functionalization whereas separation of HA favored by TEOS functionalization			301
Highly ordered mesoporous 58S Bioglass® (SM58S) and Ag-doped MBGs (Ag-SM58S)	γ-aminopropyl triethoxy-silane (KH550)	Direct grafting		*In vitro* osteoblast proliferation and differentiation	Against *E. coli* and *S. aureus* (thanks to the sustained release of Ag^+)	193
45S5 Bioglass®	Silver ions	Immersion into a silver nitrate solution, followed by the addition of formaldehyde and then 8% ammonia solution	Acceleration of the nucleation and growth of highly crystalline HA driven by the presence of AgNPs on the surface		Not tested, but supposed because of the presence of Ag^+	305
BG with composition $0.42SiO_2$–$0.15CaO$–$0.23Na_2O$–$0.20ZnO$	Silver ions	Immersion into a silver nitrate solution			Against *Staphylococcus epidermidis* and *E. coli*	306
SCNA (57% SiO_2, 34% CaO, 6% Na_2O, and 3% Al_2O_3)	Silver ions	Thermo-chemical treatment to induce ion exchange			Against *S. aureus* and *E. coli* with a zone of inhibition of about 2 mm	304
BG with composition $50SiO_2$–$18CaO$–$9CaF_2$–$7Na_2O$–$7K_2O$–$6P_2O_5$–$3MgO$	Silver ions	Ion exchange	Good	Good biocompatibility	Good	307

This journal is © The Royal Society of Chemistry 2024

Open Access Article. Published on 06 Eost 2024. Downloaded on 2026-06-06 12:45:47.
This article is licensed under a Creative Commons Attribution 3.0 Unported Licence.

Table 2 *(Contd.)*

Ceramic	Ligand	Functionalization	Bioactivity	Cell response	Antibacterial properties	Ref.
CEL2	Polyphenols from *P. pavonica* algae and AgNPs surface	*In situ* reduction			Against *S. aureus*, however, a certain specimen toxicity was observed toward human progenitor cells	312
Bioactive glass (similar to the 45S5 Bioglass®) in the system SiO_2–Na_2O–CaO–P_2O_5 was prepared, using a standard glass-forming process by mixing SiO_2, Na_2CO_3, $CaCO_3$, and $CaHPO_4$ in the following weight ratio 33.67 : 31.34 : 26.38 : 8.61	APTES and rhBMP-2	Exposure of –OH groups, functionalization with APTES, surface activation with carbonyldiimidazole, and finally immobilization of rhBMP-2 recombinant		Non-covalently immobilized rhBMP-2 is biologically highly active, whereas covalently bound protein is not, although juxtracrine stimulation is supposable		298
45S5 Bioglass®	APTES and collagen	Functionalization with APTES and then coating with collagen	Higher cell viability (MG-63 human osteosarcoma cell line) on cross-linked collagen-coated samples	Collagen offers many nucleation sites for HA formation		299
Silicate (S53P4) and phosphate (Sr50) BGs	APTES	Basic treatment and silanization for fibronectin absorption	Improved cell adhesion and promotion of cell spreading			289

Therefore, the extracellular matrix of cells provides structural support and bioactive cues to cells for the regulation of their activities. Adherent cells possess, indeed, thin ECM projections (called filopodia, lamellipodia, and nanopodia), that permit the cell itself to move and sense the surface topography during adhesion. These projections end with cell attachment molecules that serve as anchor points for movement. The most common are specific receptors called integrins, heterodimeric proteins constituted of two subunits, α and β, which cluster together and recruit cytoplasmic proteins to form a focal contact and adhere to the surface, developing a defined cytoskeleton.[332,333] Surface structure, in particular its nanoscale features (dimensionally comparable with the focal adhesions of the cells, whose size is in the range of 5–200 nm), influences cell adhesion affecting the recruitment of integrins (characterized by a size of 8–12 nm) and consequently cytoskeleton development. This in turn affects cell differentiation, proliferation, spreading, signal transduction pathways, and survival.[10,30] Integrins sense the biophysical and biochemical properties of the ECM and are linked to the nucleus directly through the cytoskeleton and indirectly through signal transduction, actuating the abovementioned mechano-transduction pathways. Thus, these receptors are involved in mechanosensing and bi-directional transmission of mechanical force, but if the spacing between the integrins is lower than 70 nm, the integrins cannot gather together and focal adhesion does not take place.

The organization of the ECM is frequently hierarchical from nano- to macro-features, with many proteins forming large-scale structures with feature sizes up to several hundred microns.[29] The nanoscale structure of the ECM, constituted by a natural intricate nanofibrous web, supports cells and presents an instructive background to guide their behavior, paving the way for cells to form complex tissues such as bone, liver, heart, and kidneys.[28] Engineered nanoscale features are orders of magnitude smaller than most mammalian cells, *e.g.* osteoblasts, and are comparable with the integrins, as discussed above, and can mimic the irregularities in the ECM (such as its undulations, bending, branching, *etc.*), and on the cell membrane.[334] Therefore, nanoscale patterning can influence the organization and type of the forming focal adhesions, either by disrupting their formation or by inducing specific integrin recruitment, influencing the morphology of the cells and allowing the formation of regions with or without cell colonization on a biomaterial surface,[28] whereas micro-features can regulate the cell behavior at the level of cell populations or at the level of a single cell.[28] For example, the implant's superficial roughness can affect the production of local growth factors and cytokines by osteoblast-like MG-63 cells and, consequently, modulate their cell activity.[11]

On the other hand, the macro features of the surface (in the range of hundreds of μm) do not influence the cell adhesion and spreading, because the cells usually spread only over distances of tens of μm, and thus they can spread both on the

Open Access Article. Published on 06 Eost 2024. Downloaded on 2026-06-06 12:45:47.
This article is licensed under a Creative Commons Attribution 3.0 Unported Licence.

side walls of the surface features and in the valleys among them, but they take part in the mechanical anchoring of the implant, supporting its primary stability.[334] If the surface features are rounded and relatively distant, they may have a beneficial or neutral influence on cell spreading and growth, while sharp and densely distributed features may have the opposite effect.[335]

Furthermore, recently the influence of nanostructured phase-separated morphologies on cell behavior has been evaluated. Kowal *et al.*[336] have observed that cells preferred to attach to and grow on surfaces with spinodal phase-separated morphology in comparison with droplet-like phase-separated ones.

In conclusion, topographical features can be sensed as a behavior stimulus, through the surface deformation, changing the behavior of cells, which respond to the changes of their microenvironment adaptively remodeling tissues, or can act as a barrier to the cells' movement, hindering the ability of cells to move on the substrate.[26,325] Thus, micro- and nano-patterned surfaces can be constructed as tissue scaffolds with specific functions related to cell adhesion and proliferation or potential bio-sensor applications.[326]

Osteoblasts are the largest of the mesenchyme-derived cells and require a high degree of intracellular tension to support the expression of a phenotype. The osteocytes of bone tissue are considered the main mechanosensing cells of bone, the cellular units responsible for the transduction of the mechanical or physiological stimuli into a differential cellular and tissue response.[9,104] Modification of the surface topography through micro-roughening has been shown to enhance the osseointegration of biomedical implants in orthopedics and dentistry, such as titanium implants and BG scaffolds.[10,11,337] Indeed, as shown by Pföss *et al.*[338] osteoblast-like MG-63 cells oriented in the direction of the grooves, which acted as contact guidance. Moreover, Karazisis *et al.*[339] have shown that the controlled nanotopography of titanium implants downregulated the expression of monocyte chemoattractant protein-1 (MCP-1), from day 1 of cell culture, and triggered the expression of osteocalcin at day 3, promoting higher osteogenic activity and a larger amount of early formed osteoid and woven bone. In the case of etched micro- or nanostructured BG surfaces, it was stated by Koort *et al.*[340] that the leaching of Na, K, Mg, P, and Ca ions and the enrichment of the glass surface with Si ions could have a significative positive effect on the bone regeneration caused by etched BGs due to the enhanced glass solubility. Moreover, they observed the growth of cortical bone in the interstices of the BG implant, which could lead to an accelerated osteointegration of the bone substitute.[340] Regarding the osteointegration, Wang *et al.*[341] have obtained good results *in vitro* in terms of the adhesion, spreading, and proliferation of HOB cells by covering the surface of orthopedic titanium implants with a nanostructured glass-ceramic coating (as described in Table 3). Moreover, the release of Ca and Si ions from the glass coating stimulated the expression of genes related to the bone tissue.[341] A strong bonding between the bone and implant can be further enhanced by the superior HA formation which can be stimulated by surface glass patterning. Indeed, Shaikh *et al.*[342] have obtained a superior growth of HA on laser-patterned 45S5 Bioglass® samples.

In this scenario, it is important to underline that the response of osteoblasts to nanostructured micro-rough surfaces is dependent on their current differentiation state, as observed by Gittens *et al.*[325] who found out that the addition of nanostructures to micro-rough Ti6Al4V surfaces, leading to the fabrication of combined micro/nanostructured surfaces, significantly enhanced MSC proliferation and osteoblast maturation, but, in contrast, suppressed the differentiation of MSC into osteoblastic cells.

Moreover, according to recent studies, nano-topography mediates the foreign body response in bone healing, reducing the overproduction of proinflammatory cytokines (IL-1b, IL-6), chemokines (CCL22), matrix enzymes (elastase), and other substances (PGE2) from the macrophages, that could lead to a large persistent and long-term inflammatory response.[27,329] Therefore, these results suggest that nanostructured orthopedic implants could modulate the immune response *in vivo* and prevent implant encapsulation.[329] This is a very interesting discovery because it is well-known that extensive and prolonged interactions of inflammatory cells (such as macrophages) with biomaterials at the host–implant interface can lead to the failure of orthopedic devices.[27]

Moreover, BG microroughed implants can have both a solution-mediated and a surface-controlled effect on osteogenic cell activity, releasing ions and simultaneously affecting cell behavior thanks to their surface microfeatures.[11] In 2016, Dobbengo *et al.*[330] published a systematic review of the effects of surface nanopatterning on the osteogenic differentiation of MSCs. In order to understand the effective role of nanopatterns, they distinguish the reviewed papers into two categories: cell culture on a nanopatterned surface in the presence or the absence of osteogenic factors. They concluded that the only pattern feature that affects MSCs' osteogenic differentiation, adhesion, cytoskeletal organization, and cell morphology is the nanopillar height.[330] Although no one of the reviewed papers refers to a glass substrate, this finding could be useful for the optimized design of nanopatterned bioactive glass with enhanced osteoinductive behavior.

Chasing this aim to fabricate nanostructured BG surfaces with enhanced bone tissue regeneration ability, the influence of hierarchical morphology should also be considered. Experimental results on laser-patterned Co–Cr–Mo implantable alloys have, indeed, demonstrated that the hierarchical combination of micro- (grooves) and nano- (ripples) roughness significantly enhances cell outgrowth.[343]

However, despite the intense experimental and theoretical investigation into understanding the physical, chemical, and biological aspects of cell–surface interactions, the knowledge of these phenomena is mostly limited to the interactions on the macro- and micro-length scales, with only limited information about cell behavior in contact with surface nanoscale features, and the mechanisms by which surface topography

 This journal is © The Royal Society of Chemistry 2024

Open Access Article. Published on 06 Eost 2024. Downloaded on 2026-06-06 12:45:47.
This article is licensed under a Creative Commons Attribution 3.0 Unported Licence.

Table 3 Nanostructured bioceramic surfaces

Glass composition	Nanostructuring method	Final material	Application	Ref.
60% SiO_2, 36% CaO, 4% P_2O_5 (mol%)	Acid-catalyzed sol–gel synthesis using citric acid (CA) as the catalyst and TEOS as the silica precursor, to control surface nano-morphology	Bioactive nanopatterned glass, with high *in vitro* bioactivity and the ability to promote adhesion and proliferation of MSCs (in particular three morphologies were obtained: (1) surface covered by particles in the size range 100–300 nm if CA/TEOS = 0.11, (2) nanoporous surface covered by nanoparticles if CA/TEOS = 0.22, (3) surface covered by dispersed particles if CA/TEOS = 0.33	Bone TE	356
Borosilicate glass with low alkali content	Combination of a physical vapor deposition method (radio-frequency magnetron sputtering) on a melted silica substrate with a metastable phase separation synthesis, followed by differential etching of the coating	Glass phase-separated nanostructured film with a spinodal structure	Optical field	357
Biocompatible glass belonging to the system $CaO–Na_2O–P_2O_5–SiO_2$	Melting, crystallization of different phases (spinodal decomposition and phase separation), and finally selective chemical leaching (depending on the variable SiO_2 content and the performed thermal treatment for glass crystallization)	Spinodal microstructured glass with multimodal porosity	Bone TE	358
Bioactive glass with the following composition: 24.4% Na_2O–26.9% CaO–2.6% P_2O_5–46.1% SiO_2 (mol%)	Melting; crystallization at the microscale level (spinodal decomposition and multiple phase separation), selective chemical leaching	Spinodal microstructured glass with multimodal porosity	TE scaffolds	359
Quartz	Wet chemical etching of a coating composed of a monolayer of perfluorodecyl trichlorosilane (previously deposited on a glass substrate using LPCVD at 620 °C, to create nanostructures on the substrate) and thermal oxidation of the formed silica nanostructures (no need for mask removal)	Nanostructured super-hydrophobic and transparent glass with anti-fog properties	Optical field	360
Optical glass (L-BAL42, OHARA)	Dry etching (reactive ion etching, RIE) with a nano-mask formed by ultrathin film (<10 nm of thickness) sputtered on the glass substrate, leading to the formation of pillars	Hierarchical micro- and nano-structured glass with anti-reflective and antifog properties	Optical field	361
Soda-lime glass	Non-lithographic, anisotropic etching: (1) deposition of a layer of SiO_2 on a sacrificial layer of glass by plasma-enhanced chemical vapor deposition (PECVD) using a mixture of N_2O and SiH_4, (2) CF_4 plasma treatment (so a super-hydrophilic nanostructure with a high aspect ratio nanopillar of SiO_2 that acts as a mask for etching), (3) selective etching (slow where there are pillars, faster in zones without pillars)	Nanostructured super-hydrophobic glass (after plasma etching higher roughness, from 0.095 nm to 1.849 after 60 min of CF_4 plasma etching)	Multifunctional glass surfaces with hydrophobic or super-hydrophilic, anti-fog and low-reflective properties	362
Antiglare glass	Laser-assisted nanoimprinting: (1) quartz layer, deposited using a bipolar-type plasma-based ion implantation and deposition (PBII&D) technique (2) layer able to absorb light (diamond-like carbon), used as a mask for etching followed by reactive ion etching (RIE): 1. deposition of a film of Al on the DLC mask 2. spin-coating of a resist on the film of Al 3. patterning using electron beam (BE) lithography 4. etching of the film of Al by RIE using CHF_3 gas 5. etching of the layer of DLC using a mixture of O_2 and Ar (the remaining Al acts as a mask) 6. HCl bath to remove residuals	Nanopatterned glass formed by concave and convex zones	Optical field	363
Silicon nitride, zirconia and 45S5 Bioglass®	High-energy laser treatment of surfaces of silicon nitride (β-Si_3N_4) and zirconia-toughened alumina (ZTA) to create a series of regular cylindrical cavities, which were subsequently filled with 45S5 Bioglass® powders, mixed with different fractions of Si_3N_4 powders (0, 5, and 10 mol%) – the addition of 45S5 Bioglass® was fundamental to render this material bioactive	Bioactive functionalized double ceramic microstructured surfaces formed by a series of regular, cylindrical cavities filled with 45S5 Bioglass® powders and Si_3N_4 powders due to the combined effect of laser patterning and Bioglass®/Si_3N_4 filling	Bone implants	364
Borofloat glass	Non-lithographic process: (1) deposition of a nickel film by electron beam evaporation (annealing at 600–650 °C per 5 min to form nickel nanoparticles on glass surface), (2) etching using these nickel NPs as a mask and SF_6 plasma in an inductively coupled plasma (ICP) etching system	Nanostructured glass with self-cleaning properties	Solar cell packaging	365
GDC/YSZ system	GDC sputtering using Discovery 18DC/RF magnetron sputter deposition system: (1) thin films of sputtered GDC on YSZ substrates, (2) annealing	Nanostructured hydrophilic surface, characterized by various nanopatterns depending on the annealing treatment: isolated isles, connected isles, and pits, with width variable in the range 75–250 nm and height variable in the range 100–2500 nm	Bone TE (*e.g.* orthopedic implants) and soft TE (*e.g.* corneal regeneration if printing on hydrogels)	318

Open Access Article. Published on 06 Eost 2024. Downloaded on 2026-06-06 12:45:47.
This article is licensed under a Creative Commons Attribution 3.0 Unported Licence.

Table 3 *(Contd.)*

Glass composition	Nanostructuring method	Final material	Application	Ref.
45S5 and 13-93	Direct mold casting	Periodical microtexture (groove of 10 μm)	Bone TE	338
Glass with low T_g	Imprint lithography using a mold of $Si_3N_4/SiO_2/Si$ and a glass with low T_g Steps: 1. molding in a silicon-based mold stamp produced by the VLSI process (a) deposition of a layer of SiO_2 on a substrate of Si (low-pressure chemical vapor deposition) (b) etching by reactive ion etching 2. mold pressed on the glass substrate	Glass with surface parallel gratings (some of them even in the micrometric range), forming a pattern of 1.0 mm of length 330 nm or 250 nm of width, and 300 nm of depth	Optical field (optoelectronics)	366
Powders of zirconia reinforced with alumina (ATZ) – composed of 3% of ZrO_2 stabilized with yttrium with circa 20% of Al_2O_3	Femtolaser for micro-structuring the surface of disks of powders of zirconia Steps: 1. preparation of zirconia powder disks, pressing powders of zirconia with 49 N, pre-sintering them at 1000 °C, polishing and sintering them at 1500 °C for 2 h 2. femtolaser	Microstructured zirconia	Load-bearing long-term applications in the maxillo-facial and dentistry field	329
45S5 Bioglass®	Melting-quenching of 45S5 Bioglass® and then laser treatment of the glass surface	Nanostructured 45S5 Bioglass® with an increased surface roughness, a bigger surface area, and a more hydrophilic behavior (the water contact angle of BG changed from 80° to 34° for untreated and laser-treated samples, respectively)	Bone TE	342
Powders of glass-ceramics HT ($Ca_2ZnSi_2O_7$) e SP ($CaTiSiO_5$)	Atmospheric plasma spray	Coating of HT and SP on disks of Ti–6Al–4V	Bone TE	341
3D bioactive glass-ceramic	Modification of the scaffold surface with (A) either buffered water (pH = 8) with APTES at 80 °C for 4 h (B) or just simply with the buffered water on its own under the same conditions	BG scaffold with nanostructured surface topography, in detail scaffold surfaces with: (A) cavities of almost 599 nm, which were formed by the remaining silicate glass matrix after leaching of the $Na_2Ca_2Si_3O_9$ crystals from the scaffold (B) uniformly distributed spindle-shaped submicron-scale crystallites (this indicated a continuous dissolution of both glass and crystalline phases)	Scaffold per TE	367
Three glasses: 19–93 1–98 3–98	Chemical etching with a solution of NH_4F (22 M) and $C_8H_{10}O_7$ (8.5 M) at 1 : 3 (vol%) ratio	Bioactive glass with surface microroughness	Bone and cartilage TE	340
45S5 Bioglass®	Liquid precursor plasma spraying (LPPS) Synthesis of the precursor: 1. mixing of TEOS and EtOH under magnetic stirring (molar ratio 1 : 2) 2. H_2O addition (TEOS : H_2O = 1 : 8) 3. addition of an ammonia solution, used as the catalyst for TEOS hydrolysis 4. addition of TEP after 40 min (followed by stirring for 20 min) 5. $Ca(NO_3)_2{\cdot}4H_2O$ and $NaNO_3$ dissolved in water and then added to the initial suspension 6. stirring for 1 h Plasma spraying using an Metco MN air plasma spraying system and AR2000 thermal spraying robot	Titanium disks coated with a nanostructured BG film	Bone TE	353
Bioactive glasses with compositions (wt%): 13–93, 1–98 and 3–98	Chemical etching with different solutions with pH varying in the range 1–13	Sintered microspheres characterized by surface roughness composed of microgrooves and small pits	Orthopedic implants	368
BG solid disks and BG porous scaffolds	Novel chemical etching method with a solution consisting of NH_4F (22 M) and $C_8H_{10}O_7$ (8.5 M) 1 : 3 (vol%)	Controlled micro-rough surface on BG solid disks and porous implants made of sintered microspheres	Bone TE	11
45S5 Bioglass®	Variation of melting temperatures and thermal treatments	45S5 Bioglass® with spinodal or droplet-like morphologies	Bone TE	336

This journal is © The Royal Society of Chemistry 2024

Open Access Article. Published on 06 Eost 2024. Downloaded on 2026-06-06 12:45:47.
This article is licensed under a Creative Commons Attribution 3.0 Unported Licence.

modulates cell behavior, in particular *in vivo*, is still not totally understood.[28] Interestingly, nano-topography seems to have a stronger influence on osteo-specific function *in vivo* when applied in combination with microscale features, indicating a possible synergy between the cellular and subcellular in directing re-generation.[320] Moreover, although many reviews have tried to summarize the available results about cell culture on nanostructured substrates and, therefore, to elucidate how cells interact with a surface at the nanoscale,[324] there is a lack of information about bioactive ceramics.

Effect of topography on bacterial colonization

Bacteria are prokaryotic cells with a cell membrane composed of phospholipids and an external prokaryotic peptidoglycan layer, that renders the bacterial membrane more rigid and less deformable if compared with eukaryotic cell membrane.[317,332] For this reason, usually, bacteria are not capable of accommodating to the surface nanofeatures and maintaining their shape during attachment to a surface whereas eukaryotic cells can stretch and distort, adequately adapting their shape to the nanofeatures without compromising their intracellular material.[12,317] This external layer of peptidoglycan is thicker in Gram-positive bacteria in comparison with Gram-negative bacteria, which have a thin peptidoglycan layer covered by an additional polysaccharide outer layer.[332] This dissimilarity explains the different responses of Gram-positive or Gram-negative bacteria to nanopatterned substrates. Moreover, in contrast to eukaryotic cells, bacteria do not adhere only to surfaces with ECM.[332]

Several reviews have been written about the effect of the various parameters affecting the bacterial adhesion and the different types of nanostructured architecture that have already been fabricated.[30,317,326,327]

For example, Shaikh *et al.*[344] have nanostructured a melted 45S5 glass by femtosecond laser-induced surface modification (Fig. 2), showing that the increased surface roughness enhanced the glass bioactivity and hindered the bacterial adhesion; in particular samples with the highest-achieved average surface roughness (~6.25 μm) completely inhibited the attachment of all the tested bacteria (*Staphylococcus aureus*, *Pseudomonas aeruginosa*, and *Escherichia coli*).

Despite extensive research on the parameters stimulating or inhibiting bacterial colonization, a clear correlation between surface roughness and bacterial adhesion has not been found yet. Some studies showed an increase in bacterial adhesion in the case of nanostructured surfaces characterized by nano-rough features, whereas others showed that surfaces with nanoscale roughness could have a bacteria-repellent effect.[345] Further studies stated that there is no correlation between surface roughness and bacterial adhesion.[346]

For the description of the surface roughness, the main parameter is R_a, "the average deviation of the roughness profile from the mean line".[334] However, recent studies showed that this parameter alone is insufficient for describing the size of the prominences and the depressions that characterized the surface topography.[334]

Patterned surfaces can exploit their antibacterial effect using different mechanisms, such as the contact-killing effect, anti-adhesive effect, and entrapment effect.[347]

The contact-killing antibacterial effect is based on the mechanical rupture of the bacterial membrane, as a consequence of (A) the stretching of the suspended parts of the bacteria adhered on distanced nanofeatures (caused by an adhesion force and gravity force)[317,326] or (B) the "fakir effect" (the bacteria lay on a "bed of nails", the nanofeatures, that destroy the bacterial membrane).[348]

Anti-adhesion ability can be exploited by patterned surfaces with a feature size close to 1 μm.[347]

In the third case, the concavity and convexity of the patterned surface can be an obstacle to the movements of adherent bacterial cells, that can remain entrapped in the valleys of the surface.[349]

Anyway, to maintain a critical point of view, it is necessary to mention the intrinsic limitation of these nanostructured

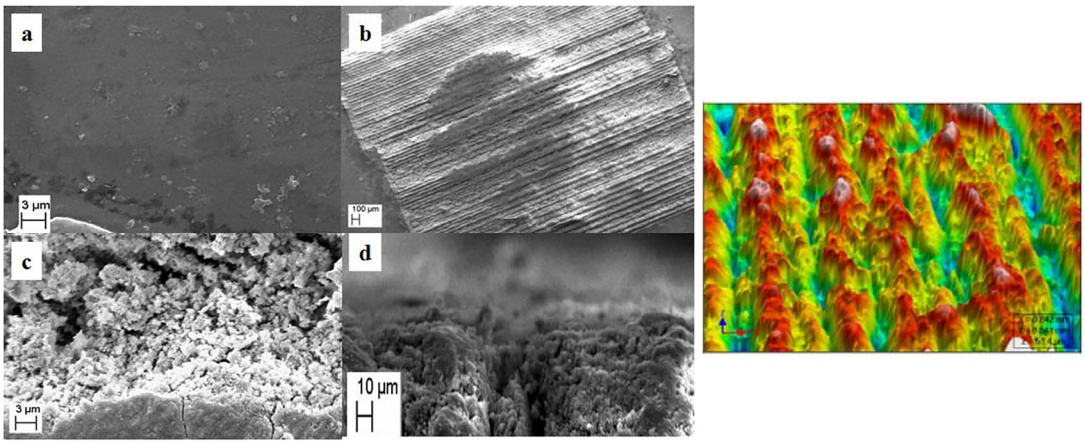

Fig. 2 45S5 Bioglass® samples treated with femtolaser, reproduced from ref. 342 with permission of the Laser Institute of America: left – SEM images of (a) the surface of untreated BG, (b, c) laser-treated region of BG at low (46X) and high (3KX) magnification and (d) cross-sectional view of laser-treated BG, with scale bars of 3 μm, 100 μm, 3 μm and 10 μm, respectively; right – 3D optical image of laser-treated BG.

Open Access Article. Published on 06 Eost 2024. Downloaded on 2026-06-06 12:45:47.
This article is licensed under a Creative Commons Attribution 3.0 Unported Licence.

antibacterial surfaces. Only bacteria that enter directly in contact with the surface interface will be inactivated; they can prevent bacterial proliferation on the surface of interest but cannot sterilize the bulk environment surrounding the surface.[317]

Recently, new surfaces with interswitchable functions are emerging: they can kill attached bacteria, release killed microbes, and either return to the initial killing state or maintain the final nonfouling state.[350] This is a very interesting research field, but up to now, no bioceramics with these functionalities are available.

Osteoblasts and bacterial cells differ greatly in size, with the former being roughly an order of magnitude larger than staphylococcal bacteria (~1 μm in diameter), which are commonly responsible for implant-associated infections. Bacteria also have a characteristic shape and are more rigid and less deformable than osteoblasts.[10] Thus, usually, bacterial cells are not able to adequate to the surface nanofeatures, whereas osteoblasts can stretch and distort, adapting their shape to the surface nanofeatures without compromising their intracellular material.[12,317]

Therefore, it is ideally possible to fabricate surfaces with *ad hoc* topography, able to promote bone regeneration and osteointegration while killing adherent bacteria cells. For example, using the glancing angle deposition technique (by magnetron sputtering), Izquierdo-Barba *et al.* have successfully fabricated a nanocolumnar Ti coating on aTi6Al4 V bone implant, which can strongly the reduce bacterial adhesion of *S. aureus* while maintaining a good osteoblast cell attachment.[351] Up to now, similar topographies have not been fabricated on bioceramics, so this remains another fascinating open research theme.

Fabrication techniques for patterned glass surfaces and glass-based materials with nano- and microscale features

Some techniques for the fabrication of nanostructured substrates have been reported,[29,322–324,332,352] but only a few of them are available and have been used for bioactive ceramics. Structural topography can be created by either depositing material on a surface or etching material from the surface, as well reviewed by Anselme *et al.* in 2010.[332] Ceramics can also be used to produce nanostructured coatings on metal implants.[341,353,354] Moreover, recently, nanofibrous BG scaffolds have gained much interest since their structure is similar to the ECM, enabling them to manipulate cell behavior by providing topographical cues.[46]

In Table 3, we report the main nanostructured bioceramic surfaces that we are aware of.

A widely investigated approach for removing material for ceramic nanostructuring is selective chemical etching. For example, Itälä *et al.*[11] adopted a novel chemical etching method with a solution consisting of NH_4F (22 M) and $C_8H_{10}O_7$ (8.5 M) 1 : 3 (vol%), to fabricate a controlled micro-rough surface on BG solid disks and porous implants made of sintered microspheres. It was shown that the BG surface micro-roughening accelerated the early formation of the silica-gel layer in both SBF and Tris solutions during the first few hours of immersion, probably due to the changes in the chemical composition of the outermost glass surface after the etching procedure. Moreover, the microrough BG surface was beneficial for the initial attachment of human osteoblast-like MG-63 cells (which were originally isolated from human osteosarcoma MG-63 cells and used to study the attachment of osteogenic cells on smooth and microrough bioactive glasses), although microroughening had no obvious effect on cell proliferation rate, that was less sensitive to the differences in the surface topography.

Parikh *et al.*[318] have fabricated random (pseudo-periodic) nanofeatures on a mechanically, thermally, and chemically stable ceramic system (Fig. 3), using an easy and cheap non-lithographic strategy, as reported in Table 3, that leads to the creation of self-assembled ceramic surfaces composed of an yttria-stabilized zirconia (YSZ) substrate, coated with a thin film of gadolinium-doped ceria (GDC). The fabricated features were able to mimic the ECM and influence the cell attachment behavior of SK-N-SH neuroblastoma cells, which are known to undergo morphological changes with culture density. Of the three engineered surfaces (islands, connected islands, and pits, shown in Fig. 3 [318]), connected islands demonstrated a better influence on cell spreading, polarization, and focal contact formation, whereas both islands and pits allowed cell attachment and cell polarization, but only pits permitted cell spreading, even if limited in comparison with the spreading on connected islands. These results suggested that cell attachment is most strongly influenced by feature area, rather than height, and disparity in cell behavior can be probably related to differences in the size of the features, which was greatest for connected islands. Indeed, the worst cell behavior was observed on islands that were shorter and smaller, when compared with connected islands and pit surfaces.

Boccaccini *et al.* have adopted a deposition method, depositing uniform CNTs on highly porous bioactive and biodegradable 45S5 Bioglass®-derived glass-ceramic scaffolds intended for bone TE by electrophoretic deposition, to stimulate osteoblast cell attachment and proliferation by providing a nanostructured surface consisting of pore walls and to confer biosensing properties to scaffolds by adding electrical conduction functions. They observed that CNTs can induce the orderly formation of a nanostructured CNT/HA composite layer when the scaffolds are in contact with biologically relevant media.[12]

The mold casting technique was adopted by Pföss *et al.*[338] who have remelted glass frits of 45S5 Bioglass® and 13-93 on microstructured PtAu5 substrates, in order to fabricate microstructured bioactive glasses characterized by grooves with a width of 30 μm and ridges with a width of 10 μm (Fig. 4 [338]).

In the above-reported works, micro- or nano-patterns were produced on the glass surface, but micro- or nano-topography can be also fabricated by depositing bioactive glasses on specific substrates, such as in the case of coatings of orthopedic implants.[337]

Another very interesting patterned deposition of bioactive glasses is the micropatterning of bioactive glasses on free-

 This journal is © The Royal Society of Chemistry 2024

Open Access Article. Published on 06 Eost 2024. Downloaded on 2026-06-06 12:45:47.
This article is licensed under a Creative Commons Attribution 3.0 Unported Licence.

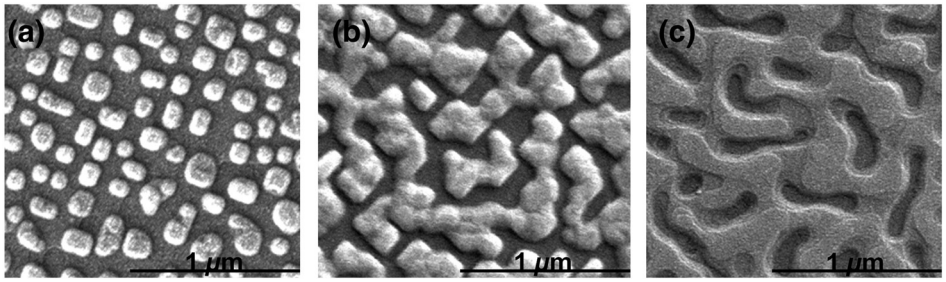

Fig. 3 Scanning electron microscopy of the patterns (nanofeatures) obtained from selectively chemically etching bioactive glass solid disks and porous scaffolds manufactured using the GDC/YSZ system: (a) islands, (b) connected islands, and (c) pits. Scale bar of each micrograph equal to 1 μm. Reprinted form ref. 318 (Copyright © 2012) with permission from Elsevier.

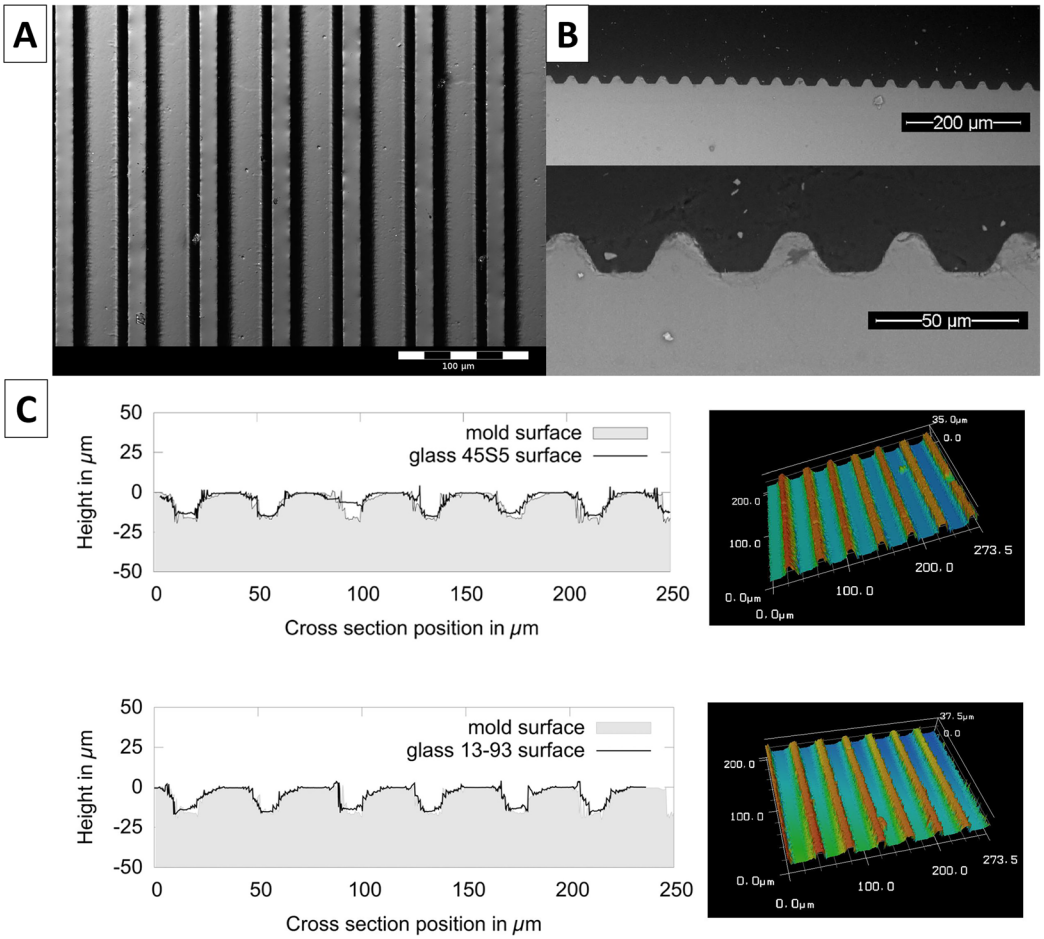

Fig. 4 Microstructured 45S5 Bioglass® and 13-93[338] with permission of DeGruyter: (A) surface of glass 13-93; (B) SEM micrographs of the cross-section of cast bioactive glass 45S5 showing the surface microstructure; (C) 2D laser scanning profile of the surface microstructure on bioactive glass 45S5 (top) and 13-93 (bottom) superimposed with a 2D scan of the mold surface, as well as 3D laser-scanning profiles of the glass surfaces of 45S5 and 13-93 (right).

standing chitosan membranes, achieved by Luz *et al.*,[355] who patterned BG sol–gel nanoparticles with a composition (mol%) $55SiO_2$–$40CaO$–$5P_2O_5$ on free-standing chitosan membranes by microcontact printing using a poly(dimethylsiloxane) (PDMS) stamp. Firstly, they inked the PDMS stamp in a glass substrate covered with a homogeneous layer of BG nanoparticles; then they pressed the PDMS stamp covered with BG nanoparticles on the surface of the chitosan membranes, which were used as a printing substrate (Fig. 5A[355]). Thus, they were able to spatially control the properties of biomaterials at the microlevel, inducing a patterned growth of hydroxyapatite on the chitosan substrates (Fig. 5B[355]), and their novel

Open Access Article. Published on 06 Eost 2024. Downloaded on 2026-06-06 12:45:47.
This article is licensed under a Creative Commons Attribution 3.0 Unported Licence.

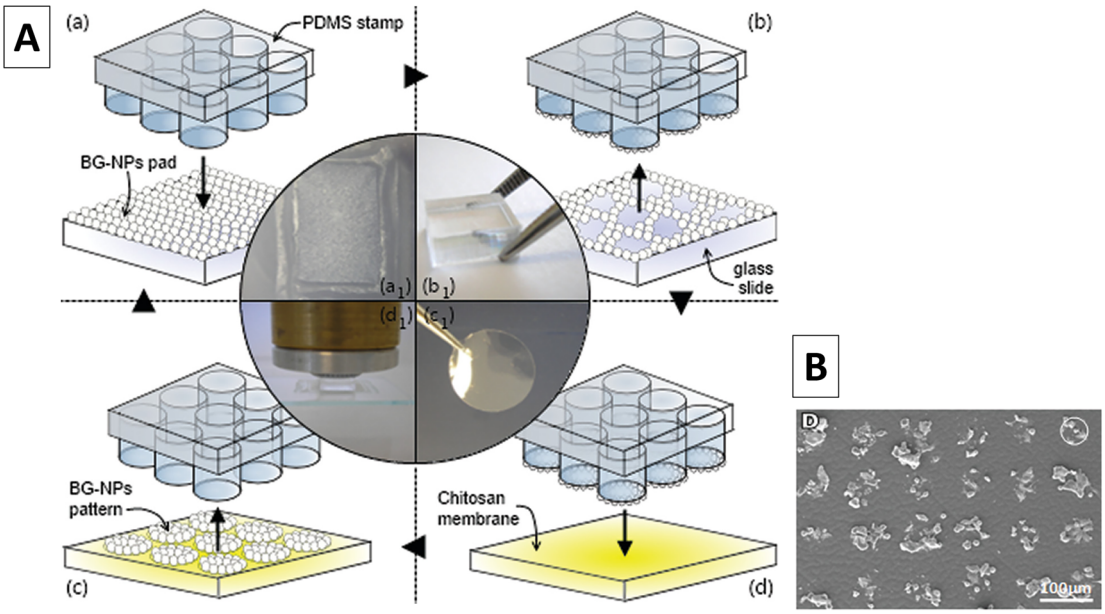

Fig. 5 (A) Schematic illustration and photographs of the fabrication process of the micropatterned bioactive glass deposition on self-standing chitosan membranes: (a) inking of the PDMS stamp in a glass substrate covered with a homogeneous layer of BG-NPs (a1); (b) lift-off of the PDMS stamp carrying the BG-NPs on the base of the features and PDMS stamp (b1); (c) pressing of the PDMS stamp into the chitosan membrane's surface, and the chitosan membrane used as printing substrate (c1); (d) printing of the BG-NPs over the chitosan membrane's surface, and detail of the device used to press the stamp against the substrate (d1). (B) BG-NPs patterned membranes and micropatterned HA formation. Reprinted (adapted) from ref. 355 (Copyright © 2012 American Chemical Society).

composite membranes are believed to be potentially able to guide tissue regeneration for skin, vascular, articular, and bone tissue engineering and in cellular cocultures, or to confine cells in regions with controlled geometry at the cell's length scale.

Up to now, we have described the influence of the external surface micro- and nanotopography, but it is also possible to identify bulk micro- and nanotopography.

Indeed, an internal nanostructure can be observed in the case of porous scaffolds. In a scaffold, three different length-scale structures can be identified: the macrostructure, the microstructure, and the nanostructure.[332] In the case of porous scaffolds, characterized by a porous structure, these three length-scale structures correspond to different porosity levels. At the minimum level, pores below 100 μm impart to the scaffold a specific surface roughness which enhances the cell attachment. The second level (pores of 100–500 μm) is related to bone in-growth and vascularization, but also to a decrease in the mechanical properties, in particular in the Young's modulus (that reduces the stiffness mismatch with the native tissue and the associated risk of stress shielding, in the case of BG scaffolds). The third level of pores, above 500 μm in size, are called giant macropores and can be used for the passage of suture wires to anchor the implant to the host bone.[44] The ideal scaffold should possess a 3D architecture with a morphology that is almost identical to that of natural tissue, with above 50 vol% porosity composed of large interconnecting macro-pores of about 150–200 μm.[286] Three-dimensional structures are preferred in comparison with bi-dimensional ones, because an instructive three-dimensional environment is fundamental for tissue regeneration, as highlighted by Stevens *et al.* in their review.[28] Recently, it has been discovered that cells often show a non-natural behavior when they have moved away from their natural niches and seeded onto flat substrates.[328]

Scaffolds can be fabricated using many different techniques, not here reported because out of the intended aim of this review, but the interested reader can read the following cited reviews and books.[367,369] In particular, in recent years, porous scaffolds have gained much attention and have been produced by lots of research groups, using various materials and applying different fabrication techniques,[41,190,270,370] allowing even the production of hierarchical structures. Furthermore, several hierarchical glass scaffolds have been successfully produced. Hierarchical materials based on bioactive glasses have been reviewed a few years ago by Baino *et al.*[44]

Finally, to be as inclusive and exhaustive as possible, it is important to draw attention to the interaction of nanoparticulate materials with cells. Indeed, not only nanopatterned and nanofibrous surfaces, but also nanoparticles and nanocomposites are considered nanostructured engineered surfaces, as already elucidated in 2008 in a review by Wei *et al.* about nanostructured biomaterials for tissue regeneration.[371] An interesting review of nanoscale HA particles for bone TE applications was published in 2011 by Zhou and Lee,[372] and therefore here we will focus only on nanoscale BG particles and their composites. BG nanoparticles can be synthesized

 This journal is © The Royal Society of Chemistry 2024

Open Access Article. Published on 06 Eost 2024. Downloaded on 2026-06-06 12:45:47.
This article is licensed under a Creative Commons Attribution 3.0 Unported Licence.

using various sol–gel synthesis routes, involving acid and/or basic catalysts, such as traditional acid synthesis,[161,356,373] basic synthesis (*e.g.* Stöber synthesis),[374] and acid/base co-catalyzed methods,[108,375] enabling the fabrication of particles with different shapes (irregular, rod-like, spherical and so on) and size. However, despite the numerous possible synthesis strategies, aggregation of nanoparticles often occurs, resulting in a nanostructured architecture composed of lots of aggregated nanostructured particles (briefly called nanoparticles), as shown by some experimental works.[108,172,375] Thus, because of their size in the nano-range and the nanostructured surfaces created by their aggregation (in other words because of their surface nanostructuring), bioceramic NPs allow improved cellular adhesion, enhanced osteoblast proliferation and differentiation, and increased biomineralization of bone and are attracting increasing interest.[291] Increased osteoblast (bone-forming cells) adhesion on nanograined materials was first reported in 1999.[4] Furthermore, nanodimensional bioceramics have been proved to possess higher bioactive properties due to their larger specific surface area, dissolving more rapidly and accelerating the rate of formation and growth of the HA layer on the glass surface if compared with microsized and bulk bioceramics of the same composition.[376] Experimental studies have also shown that melt-derived multicomponent Co- and Sr-co-doped silicate BG particles with a finer size (9 μm) possess a more effective osteogenic potential and higher cytotoxicity against Saos-2 cells as compared with larger particles (725 μm), due to their higher surface area, associated with higher ion release.

In vivo studies and clinical applications

The first reported clinical application of bioactive glass was the treatment of conductive hearing loss, with the reconstruction of the bony ossicular chain of the middle ear.[377] Nowadays, bioactive glasses are applied for the regeneration of hard tissues, such as bone[59] and teeth.[378] So, their main application fields remain orthopedic and dentistry, with several clinical commercial products to treat diseases in orthopedy and dentistry.[113] However, BGs have also potential applications in cartilage regeneration,[15] wound healing,[131] nerve regeneration,[379] and cancer therapeutics[142,143] and products for the delivery of therapeutic dosages of radiation for cancer treatment, such as TheraSphere™, have been approved for clinical use by global regulatory agencies.[113] On the basis of the author's knowledge, nowadays no formulation of drug-loaded BGs and bioactive glass-ceramics is already available on the market.

BGs (in detail, Bioglass® Ossicular Reconstruction Prosthesis, also known as Middle Ear Prothesis, or MEP®) were first approved in 1985 by the FDA and then by several other international agencies.[113] The MEP® gave its success to its ability to bond with both hard bone and softer tissues such as the eardrum and its manufacturing process using small molds, that allow the fabrication of monoliths with precise dimensions based on the specific needs of each patient. Nowadays, it is not commercially available anymore, because of the dissolution and fragmentation of the implant.[113]

In orthopedics and maxillofacial surgery, 45S5 Bioglass® was firstly clinically used and is still applied as a synthetic bone graft material under two different product names, which are still available on the market: PerioGlas® and NovaBone®, both in particulate form.[113,377] Nowadays, other commercial products based on 45S5 Bioglass® are available, such as Glassbone®, Vitoss® BA,[113] and SIGNAFUSE®.[113]

In dentistry, BGs were firstly used as bone substitutes in dentoalveolar and maxillofacial reconstruction, periodontal regeneration, and implants, using commercial products like Unigraft®, and the already abovementioned PerioGlas®, Novabone® and Glassbone®,[113,377] but many other applications are now available in the dental field.[377] For example, BGs can be used for the fabrication of toothpaste as a hypersensitivity inhibiter (like NovaMin®, based on the 45S5 Bioglass® composition) and dental adhesives made of resin bonding systems containing BG fillers, such as micro-fillers of 45S5 Bioglass® or a Zn-polycarboxylated BG. BGs can be also used for the fabrication of coatings on dental implants;[377] in this context, the addition of therapeutic and/or antibacterial doping ions is of great benefit. Besides the therapeutic and antibacterial effects of the released ions, the pH increase caused by the ion release from BGs can be also beneficial, exploiting a topical endodontic disinfectant effect with no negative impact on dentin stability.[377]

The first commercialized BG to be fabricated from a composition different from 45S5 Bioglass® was S53P4 (BonAlive® Biomaterials), a silicate-BG with the composition of 53% SiO_2, 4% P_2O_5, 23% Na_2O, and 20% CaO (in wt%) and a slower dissolution rate than 45S5 Bioglass®, produced in form of granules and a putty system, for the treatment of bone infections and diabetic foot osteomyelitis, and use in spinal fusions.[113]

In the field of wound dressing and infection fight, several biomedical products based on BGs are already available. An interesting example is the antibacterial Ag-doped resorbable phosphate BG particles Arglaes®, developed by Maersk Medical in the UK and marketed by Medline Industries (since the late 1990s), which can be combined either with a polymeric adhesive or with alginate powder for wound dressing, burn care, topical medication and prolonged controlled antibacterial effects (thanks to the slow release of Ag ions).[215]

A doped BG (named Vitryxx®), based on the composition of the 45S5 Bioglass®, is applied in cosmetics for its anti-odor and anti-oxidant properties and its ability to reduce the visibility of wrinkles.[215]

As anticipated in the "Introduction", one of the main drawbacks of the clinical applications of implanted BGs is the development of infection. A systematic review of the clinical applications of the bioactive glass S53P4 in bone infections was published by Bigoni *et al.* in 2019.[380]

Besides their incredible therapeutic and antibacterial properties, BGs possess some other properties like *in vivo* degradation,[381] ion release,[381] devitrification,[381] and brittleness,

Open Access Article. Published on 06 Eost 2024. Downloaded on 2026-06-06 12:45:47.
This article is licensed under a Creative Commons Attribution 3.0 Unported Licence.

that must be taken into account when planning their clinical use.

However, even before thinking about the clinical use of *ad hoc* designed bioceramics, issues associated with the translation from *in vitro* to *in vivo* studies must be solved.

For example, in the case of ion-doped and drug-loaded biomaterials, the *in vitro* test environment significantly differs from the real *in vivo* environment, where the biomaterial should be implanted and exploit its effects. To briefly cite a few examples of this dissimilarity, the fluid movements in the *in vitro* acellular bioactivity tests and biological assays are quite different from the real movements of the body fluids around an implant. Sometimes, *in vitro* bioactivity tests are, in fact, static,[382] whereas the body fluids are in continuous movement. To simulate the real fluid movement, bioactivity tests are often carried out in an orbital shaker under continuous agitation.[370] However, many *in vitro* tests are carried out without renewal of the test solution.[370] In contrast, *in vivo* body fluids are continuously renewed. In any case, the experimental studies with SBF refreshing[41,382,383] should not be ignored, because they are hints that the research is making progress towards realistic *in vitro* and *in vivo* experiments.

In the case of chemically and physically modified surfaces, like in the case of functionalization, coating, *in situ* deposition of metallic NPs, and surface patterning, it could be difficult to translate the results obtained experimentally *in vitro* to *in vivo* studies and *in vivo* applications, because *in vitro* samples often do not perfectly resemble the size and shape of the real devices that must be implanted.

Preclinical tests *in vitro* and *in vivo* are necessary to determine the properties and possible cytotoxic effects of the novel BG formulations and BG-based devices, and to prove their viability, but they are not sufficient to allow the clinical use of these products.[113] If cell and animal tests show promising results, clinical trials on humans must be carried out, to confirm previous results on the properties of the products and demonstrate their reliability and effectiveness.[113]

Unfortunately, *in vivo* trials using animals are usually expensive and time-consuming.[113] Therefore, they are carried out only for a limited part of the newly synthetized BG formulations, obviously the most promising ones.[113]

Then, clinical trials can be carried out.[113] They generally take from 5 to 10 years and cost several million dollars.[113] Finally, regulatory agencies, such as the Food and Drug Administration (FDA), review the data produced through clinical trials and published in a peer-reviewed journal to determine if the product is safe and effective for medical use in humans.[113] This review of the clinical trial data typically takes 10 months.[113] If the approval is granted, the medical device can be sold on the market.[113]

To monitor the long-term effects, performance, and safety of device usage among the general population, data are still collected.[113] For example, the FDA MedWatch program allows both healthcare professionals and the public to report adverse effects of medical devices and drugs that they have experienced.[113]

Last, but not least, after commercialization approval, the products must be manufactured following guidelines and standardized procedures related to the sanitation and hygiene of personnel and facilities, raw materials, manufacturing operations, storage, and analysis of defects.[113]

In any case, nowadays there are at least 25 BG medical devices already approved for clinical use by global regulatory agencies, as well reviewed in a review published in 2023 by Shearer *et al.*[113] However, this is a very low number compared with the constantly growing number of publications related to BGs.[113] In the abovementioned review, the big gap between literature papers and patents has been highlighted, showing the presence of about 5000 results in a Scopus search of publications referring to "bioactive glass" in the title since 1969, whereas a patent search using The Lens searching "bioactive glass" in the title, abstract, or claims resulted in over 2000 granted patents internationally.[113] Detailed information about the topics, countries, and companies of these patents are also available in that review of Shearer *et al.*,[113] but are out of the scope of the present review.

Conclusions and future challenges

Bioactive glasses and glass-ceramics are very promising materials for TE application, due to their ability to mineralize and degrade *in vivo*, releasing ions. Several therapeutic and/or antibacterial ions can be easily introduced into the glass compositions, modulating the glass properties, such as its bioactivity, or imparting novel properties, such as antigenicity, to the material. Besides doping with ions, other strategies are possible to modulate the glass properties and consequently the interaction between glass and cells, both eukaryotic and bacteria cells. These strategies can be simply divided into two main groups: chemical modification and physical modification. Among the chemical ones, we can list the loading and functionalization with ions, drugs, ECM proteins, vitamins, and polyphenols. Physical modifications of the bioceramics surfaces can be achieved mainly by removing materials from the surface (*e.g.* using laser treatment and etching strategies) or depositing materials on the surface (such as in the case of coatings deposition). Thanks to their intrinsic and imparted properties, BGs and bioactive glass-ceramics can elicit a biological response at the interface between the implant's surface and the surrounding tissues, leading to the formation of a strong bond with the new tissue forming at the interface, the proliferation of tissue cells and their implant colonization, genetic upregulation of several critical proteins, like GFs associated with tissue regeneration, and bacterial killing abilities. A summary of these strategies and their effect on eukaryotic or bacterial cells is reported in Table 4.

It is clear that novel micro- and nanostructured surfaces can overcome the limitations of ion- and drug-releasing systems. For example, antibacterial biomimetic nanostructured surfaces can overcome the limits of antibacterial release-based systems, such as particles containing or scaffolds and coating releasing antibiotics and antibacterial ions,[24] for example, BGs

 This journal is © The Royal Society of Chemistry 2024

Open Access Article. Published on 06 Eost 2024. Downloaded on 2026-06-06 12:45:47.
This article is licensed under a Creative Commons Attribution 3.0 Unported Licence.

Table 4 Tailoring strategies and their effect on cells

Type of cells	Method	Magnitude order of modification	Effect on cells	Advantages	Disadvantages
Eukaryotic cells	Ion incorporation (doping)	Macro	Depends on the added ions (angiogenic or osteogenic, and so on...)	Possibility to modulate cell response by simply varying glass composition	Dose-dependent response
				Influence even on cells that are not in direct contact with the material, various simple methods of doping a bioactive ceramic	Need for replenishment or replacement
	Functionalization	Macro	Depends on the linked moieties (angiogenic or osteogenic, and so on...)	Various simple methods of functionalizing a bioactive ceramic	Dose-dependent response
				Easy variations of material surface When the linked moieties are released from the surface, an influence even on cells that are not in direct contact with the material	Need for replenishment or replacement
	Topological modification through deposition methods	Micro or nano	Stimulation of adhesion, differentiation, and proliferation (through mechano-transduction of external signals)	Most eukaryotic cells are anchorage-dependent	Influence only on cells in direct contact with the material surface
Bacterial cells	Ion incorporation (doping)	Macro	Induction of apoptosis of bacterial cells by hindering some of their metabolic pathways	Various simple methods of doping a bioactive ceramic	Dose-dependent Burst-release kinetics Sublethal background dose Impossibility of killing attached bacterial cells Need for replenishment or replacement
	Functionalization	Macro	Induction of apoptosis of bacterial cells (if antibacterial ions are released) OR anti-fouling behavior	Various simple methods of functionalizing a bioactive ceramic	Impossibility of killing attached bacterial cells
				Easy variations of material surface	Need for replenishment or replacement
	Topological modification	Micro or nano	Contact-killing, anti-adhesive, or entrapment strategies	Ability to kill bacteria that adhere to the surface	If bacteria do not enter into contact with the material, they cannot be killed Still not complete understanding of the mechanisms by which topography influences bacterial behavior Unclear over the influence of dead bacterial cells that remained on the material surface after being killed Variable response depending on the bacterial cell, so that the antibacterial surface must be designed *ad hoc* for the target bacterial strain

doped with antibacterial ions like silver, copper, cerium, or zinc. The main drawbacks of the released-based systems are burst-release kinetics that can make the compound ineffective, insufficient concentrations that reach the target (since diffusion is uncontrolled and directionless), a sublethal background dose that can trigger the development of resistance mechanisms, environmental aspects, and a need for replenishment or replacement.[26,317] Moreover, these materials do not kill bacterial cells that manage to attach to the surface, so these bacteria can still grow and produce biofilms.[26] All these problems could be solved by using antibacterial non-releasing nanostructured devices that can kill bacteria without the release of any chemicals or biocides, but only thanks to the contact between the antibacterial materials and the bacteria.

On the other hand, the advantage of physically-modified patterned surfaces is also their limit, because they can exploit

Open Access Article. Published on 06 Eost 2024. Downloaded on 2026-06-06 12:45:47.
This article is licensed under a Creative Commons Attribution 3.0 Unported Licence.

their antibacterial effect only if bacterial adhesion on the implant has already occurred.[2] Similar conclusions could be stated also in the case of eukaryotic mammalian cells, because it is well known that not only direct stimuli (such as the ones given by cell adhesion on a surface, *e.g.* the roughness and stiffness of the substrate), but also indirect stimuli (such as the paracrine effect[19]) strongly affect cell response.

In addition, in the case of antibacterial contact-killing physically-modified surfaces, the bulk environment surrounding the surface cannot be sterilized and it is not clear how the presence of the dead bacteria adhered to the surface can influence the further adhesion of both bacterial and tissue cells.[326] For example, it was supposed that these dead bacteria could be a nutrient source for other bacteria[384] or, in contrast, the presence of parts of dead bacteria could render the further adhesion of other bacteria less favorable.[385]

Some results have shown that eukaryotic cells can grow and proliferate on previously infected nano-patterned,[386] and Somayaji *et al.*[411] reported that ultraviolet-killed *S. aureus* present on the surface of titanium implants can act as an osteoconductive coating, leading to an enhancement of osteoblast adhesion, expression of osteoblast markers (such as collagen, osteocalcin, and ALP), and formation of mineralized nodules, if compared with surfaces not coated with dead bacteria; the results of Somayaji *et al.*[248] were attributed to increased surface roughness given by the presence of attached dead bacteria.

However, further investigations are necessary to understand the feasibility of long-term benefits.

It is important to bear in mind that there are no bacteria-resistant or bacteria-release surfaces with an efficacy equal to 100%, so some bacterial cells – that succeed in attaching to the implant surface – remain alive.[384]

It is important to remember that nanostructured substrates may promote the cell adhesion of one type of cell but at the same time may discourage another.[352]

An implant inserted into the body will be also subjected to protein adsorption, which can be affected by the nano-topography and compromise the osteoblastic and antibacterial functions of the implant.[10]

In any case, the mechanism that controls the interaction between cells and rough surfaces is still under investigation and continuous upgrade.

As previously discussed in the section "Doping with ions and loading with drugs", another important drawback of doped biomaterials is associated with their potential cytotoxicity, related to the toxicity limits of the doping ions. To cite a few examples, silver, copper, and cobalt are known to be cytotoxic at high concentrations. The limits of cytotoxicity and the probability of cytotoxic effects depend on the used doping ions, *e.g.* between the pro-angiogenic ions copper and cobalt, the second one is more likely to be cytotoxic.[9] To avoid the cytotoxicity of cobalt, a low dopant concentration is necessary, but doses below 4 mol% of this dopant network modifier are too low to cause highly significant changes in the structure.[22] This example helps us to understand the importance of defining a safe therapeutic dosage range for each doping ion and to be sure of the advantages offered by doping over the potential risks based on a scientifically defined cost–benefit ratio.[113] Unfortunately, the effect of inorganic ions on cells is still not completely clear. For example, the positive effect of magnesium on bone cells has been largely demonstrated, but the exact mechanisms of action of this ion are still obscure.[93] A reason for this lack of knowledge is that most experimental studies utilize single doses in a cell culture medium, not mimicking in a realistic way the continual and sustained release of an ion, which may initiate and mediate a completely different response.[54]

The risk of ion accumulation in tissues and organs should also not be ignored, especially in the case of metallic ions. It is well known, in fact, that the release of metallic ions from orthopedic metallic implants can lead to metallosis.[387,388]

In addition, high contents of dopant ions can induce the nucleation of different crystalline phases in the BG, leading to the formation of glass-ceramics.[55] Sometimes, this side effect of doping is not desired, because the crystallinity of the glass-ceramic can reduce its bioactivity.[4]

Regarding the loading with drugs, the main drawback of this strategy in the case of antibacterial applications is the increasing spread of bacterial resistance to antibiotics, which has been, indeed, recently declared as a "global threat" by the World Health Organization.[215] However, this problem could be overcome using doping ions as antibacterial agents against multidrug-resistant bacteria, in the so-called "ion-driven" antimicrobial approach.[215]

For this application, sol–gel derived mesoporous BGs are very promising and widely studied, but nowadays sol–gel BGs are still not dominating the market due to their expensive and cytotoxic precursor materials and the need for a strict quality control to guarantee the removal of any cytotoxic residuals, avoiding the potential for cytotoxic activity.[113]

In recent years, a promising alternative to both synthetic drugs and metallic ions is emerging: natural extracts.[215]

Regarding the chemical approach based on functionalization and coating, they are versatile tools for the modification of the outermost surface layer of biomaterials, allowing a tailoring of the interaction of the implanted materials with the biological environment (which mainly occurs at the interface surface), without any alteration of the bulk properties of the biomaterials.[284] In this way, it is possible to combine the starting features of the biomaterial with the ones added at the surface.[284] However, possible further drawbacks of these strategies could be the issues related to the long-term stability of the functionalization/coating,[251] possible variations of the bioactivity rates,[247,389] and an unwanted physical modification, associated with the deposition of functionalizing molecules and metallic *in situ* synthetized nanoparticles, and related toxicity.[390] In addition, the deposition of BG and bioactive glass-ceramic coatings can alter the wettability of the implant;[391] this wettability modification should be taken into consideration when planning *in vivo* applications, since it is well-known that the hydrophilicity of an implanted material influ-

 This journal is © The Royal Society of Chemistry 2024

Open Access Article. Published on 06 Eost 2024. Downloaded on 2026-06-06 12:45:47.
This article is licensed under a Creative Commons Attribution 3.0 Unported Licence.

ences the attachment of cells, both eukaryotic mammalian and bacterial cells. Moreover, a reliable comparison of the performance of different coatings applied on non-flat substrates (like realistic implants) is not easy, because very often there are no standard methods or procedures for their characterization, like in the case of the measurement of the adhesion strength of the coating to the substrate (in this case, only international recommendations for testing flat samples are available).[251]

As discussed in depth in the section "Influence of topography on cell behaviour – surface and internal nanostructure", another important limit of physically-modified nano- and microstructured bioactive glasses is the difficulty in fabricating them with the desired *ad hoc* nano- and microfeatures. Besides technological limitations, the mechanisms regulating the response of mammalian and bacterial cells are still not completely understood and literature information about parameters affecting this response is controversial.[327] Taking into consideration the promise of these modified surfaces for TE and antibacterial applications, researchers should continue their investigation of both suitable fabrication methods and different surface parameters affecting the cell response. In this context, the development of standardized biological tests could be of great benefit, helping in the critical comparison of different nano- and microstructured surfaces.[392]

Regarding BG nanoparticles and their interactions with cells, the advantages given by their small size (such as a higher surface area, higher bioactivity, faster degradation, and quicker release of therapeutic ions) come immediately to mind;[113] however possible issues related to cytotoxicity caused by their small size and ion release should be properly investigated.

In addition, both in the case of chemically- and physically-modified surfaces, the effects of these modifications on bioactivity and ion release are still under investigation, even though, according to a previous review by Kargozar *et al.*,[284] published in 2019, bioactivity is generally maintained after BG surface functionalization.

In addition, the immobilization of biomolecules, such as drugs and growth factors, is complex, unstable, and more expensive, in comparison with ion doping, which is a relatively simple, stable, and low-cost approach.[135]

Regarding the strategy of doping with ions, up to now, almost all elements of the periodic table have been added to a glass composition. So, the new frontiers of doping are the synthesis of co-doped BGs and the study of the synergic effects of multiple doping ions. As previously discussed, several experimental studies of co-doped BGs are already available, but a comprehensive understanding of their synergic effects is still lacking.

For all these strategies, the modulation of the glass reactivity is a further open issue, because a high surface reactivity can render chemical treatments and etchings more difficult and cause both a too quick release of doping ions, loaded drugs, and grafted molecules and a rapid change of the modified surface, making the chemical and physical modification of the surface ineffective.

To solve all the abovementioned open and challenging issues related to the here-reviewed tailoring strategies and reduce the experimental time, costs, and ethical issues, the synergical implementation of computational strategies, such as computational simulations and machine-learning, could be beneficial.[22,393]

To meet the rising demand for customized BG-based substitutes, 3D processing technologies are needed;[13] they can be used for the fabrication of tridimensional scaffolds with a hierarchical porosity and could also potentially help in the fabrication of BG devices with nano- and microfeatures. However, the 3D additive processing of ceramics still suffers from some limitations, such as:

- the possibility of air-bubble entrapment in the ink (in the case of robocasting),[370]
- suboptimal sintering of the ceramic powders in the case of the direct selective laser sintering (SLS) of ceramic parts,[394]
- reduced resolution, possibility of printing process imprecision, uneven distribution of the filler particles inside the printed structure (resulting from poor dispersion and sedimentation of the ceramic powders), and a limit of ceramic filler concentration equal to 40%, in the case of stereolithography (SLA),[395]
- difficult control over materials' properties at the nanoscale (whereas macro- and microfeatures can be produced with a good degree of control),[396]
- shrinkage[370] and long-lasting optimization of the process parameters[397] in general,

leading to unwanted inner voids and cracking in the case of the filaments of robo-casted scaffolds,[370] poor morphological and mechanical properties in the case of direct SLS and SLA,[394,395] and difficulties in the fabrication of nanostructured materials.[396] The realization of nano- and microfeatures using 3D printing and other additive manufacturing processes is, indeed, still an open challenge.[398] In any case, these methodologies allow a good control of dimensions, macro- and microstructural features, and porosity (*e.g.* pores as small as the ones in the trabecular bone can be obtained).[370,399,400] In addition, it is interesting to point out that some promising composite microspheres and composite porous scaffolds, containing bioceramics, have been already successfully fabricated, overcoming some of the above-reported limitations of additive techniques.[401–405] To fabricate nano- and microfeatured bone scaffolds, a well-defined microfeatured polylactic acid (PLA) scaffold was printed and nano-HA was then conjugated on its surface through post-processing aminolysis.[406] Composite patches with multiscale 3D porosity were produced by combining extrusion 3D printing and electrospinning.[407] In the actual review, we will not add further details, because a detailed discussion about the advantages and open issues of the additive 3D processing of bioceramics is out of the scope of the actual paper, but more info is available in the following reviews.[395,408]

Making a general final consideration about BGs, independently from the used tailoring strategy, in the case of the emerging field of soft TE, in particular for wound healing, the com-

Open Access Article. Published on 06 Eost 2024. Downloaded on 2026-06-06 12:45:47.
This article is licensed under a Creative Commons Attribution 3.0 Unported Licence.

plete dissolution of the BG device and the absence of apatite-forming ability are desirable, allowing the wound site to fully heal with the host tissue, without mineralization of the healing tissues.[113] Besides potentially altering the healing soft tissue and its mechanical properties (making it more rigid), HA formation could inhibit hemostasis, and calcium deposits could delay or even stop the healing of leg ulcers.[113] Thus, the application of soft TE seems to be in contrast with the inherent and typical bioactivity of BGs.[113] The use of BGs for these specific applications is highly challenging, but new BG compositions, that do not lead to the formation of a calcium phosphate layer on the material surface, are actually investigated.[113] In this regard, the term "bioactive" is not referred anymore to the formation of hydroxyapatite but, rather, to the stimulation of a beneficial biological response through ion release.[113]

In this context, novel polymer composite scaffolds and hybrid materials containing doped BGs are showing promising results in both hard and soft TE. Another emerging application in which hybrid BGs are gaining increasing interest is cartilage repair and regeneration.[113]

According to the target application, the connectivity of the BG network, and ultimately the extent of apatite-forming ability, can be properly tailored by adding the proper amount of specific ions,[22] as discussed in depth in "Doping with ions and loading with drugs – Bioactive properties". Indeed, as previously written, while the bioactivity is desirable for bone TE, it is not advisable in contact with soft tissues (*e.g.*, dermal regeneration).

We can conclude that, nowadays, each of the discussed tailoring strategies offers different advantages and disadvantages, on the basis of the intended final use.

The best modulation strategies of the glass properties are still an open issue and multidisciplinary investigation approaches are running to contribute to solving this issue.

In addition, to ensure reproducibility and successful scalability and translation to industrial market and *in vivo* applications, the standardization of the fabrication procedures is necessary.[230]

Author contributions

Piatti Elisa: writing – original draft; Miola Marta: writing – original draft, supervision; Verné Enrica: writing – original draft, supervision; conceptualization.

Conflicts of interest

There are no conflicts to declare.

References

1 L. L. Hench, I. D. Xynos and J. M. Polak, *J. Biomater. Sci., Polym. Ed.*, 2004, **15**, 543–562.
2 M. N. Rahaman, D. E. Day, B. S. Bal, Q. Fu, S. B. Jung, L. F. Bonewald and A. P. Tomsia, *Acta Biomater.*, 2011, **7**, 2355–2373.
3 L. L. Hench, *J. Am. Ceram. Soc.*, 1998, **81**, 1705–1728.
4 A. Hoppe, N. S. Güldal and A. R. Boccaccini, *Biomaterials*, 2011, **32**, 2757–2774.
5 R. S. Katari, A. Peloso and G. Orlando, *Adv. Surg.*, 2014, **48**, 137–154.
6 L. C. Gerhardt and A. R. Boccaccini, *Materials*, 2010, **3**, 3867–3910.
7 M. A. Fernandez-Yague, S. A. Abbah, L. McNamara, D. I. Zeugolis, A. Pandit and M. J. Biggs, *Adv. Drug Delivery Rev.*, 2015, **84**, 1–29.
8 H. Zhou, J. G. Lawrence and S. B. Bhaduri, *Acta Biomater.*, 2012, **8**, 1999–2016.
9 C. Wu and J. Chang, *J. Controlled Release*, 2014, **193**, 282–295.
10 K. G. Neoh, X. Hu, D. Zheng and E. T. Kang, *Biomaterials*, 2012, **33**, 2813–2822.
11 A. Itälä, H. O. Ylnen, J. Yrjans, T. Heino, T. Hentunen, M. Hupa and H. T. Aro, *J. Biomed. Mater. Res.*, 2002, **62**, 404–411.
12 X. Liu, P. K. Chu and C. Ding, in *Materials Science and Engineering R: Reports*, Elsevier B.V., 2010, vol. 70, pp. 275–302.
13 J. Lee, H. Byun, S. K. Madhurakkat Perikamana, S. Lee and H. Shin, *Adv. Healthcare Mater.*, 2019, **8**, 1–20.
14 M. Younesi, V. M. Goldberg and O. Akkus, *Acta Biomater.*, 2016, **30**, 212–221.
15 D. M. Yunos, Z. Ahmad, V. Salih and A. R. Boccaccini, *J. Biomater. Appl.*, 2011, **27**, 537–551.
16 D. Williams, *Mater. Today*, 2004, **7**, 24–29.
17 A. J. Salinas, M. Vallet-Regi and J. Heikkilä, in *Bioactive Glasses*, Elsevier Ltd, 2nd edn, 2018, vol. 1883, pp. 337–364.
18 C. Wu, Y. Zhou, W. Fan, P. Han, J. Chang, J. Yuen, M. Zhang and Y. Xiao, *Biomaterials*, 2012, **33**, 2076–2085.
19 H. Li and J. Chang, *Acta Biomater.*, 2013, **9**, 6981–6991.
20 J. M. Kanczler and R. O. C. Oreffo, *Eur. Cells Mater.*, 2008, **15**, 100–114.
21 S. Kulanthaivel, B. Roy, T. Agarwal, S. Giri, K. Pramanik, K. Pal, S. S. Ray, T. K. Maiti and I. Banerjee, *Mater. Sci. Eng., C*, 2016, **58**, 648–658.
22 F. Baino, M. Montazerian and E. Verné, *Materials*, 2023, **16**, 1–21.
23 M. Wekwejt, M. Dziaduszewska and A. Pałubicka, *Eur. J. Med. Technol.*, 2018, **4**, 19–26.
24 M. K. S. Ballo, S. Rtimi, S. Mancini, J. Kiwi, C. Pulgarin, J. M. Entenza and A. Bizzini, *Appl. Microbiol. Biotechnol.*, 2016, **100**, 5945–5953.
25 A. Cochis, J. Barberi, S. Ferraris, M. Miola, L. Rimondini, E. Verné, S. Yamaguchi and S. Spriano, *Nanomaterials*, 2020, **10**, 1–19.
26 M. Ghasemlou, F. Daver, E. P. Ivanova, J. W. Rhim and B. Adhikari, *ACS Appl. Mater. Interfaces*, 2019, **11**, 22897–22914.

 This journal is © The Royal Society of Chemistry 2024

Open Access Article. Published on 06 Eost 2024. Downloaded on 2026-06-06 12:45:47.
This article is licensed under a Creative Commons Attribution 3.0 Unported Licence.

27 Y. W. Chun and T. J. Webster, *Ann. Biomed. Eng.*, 2009, **37**, 2034–2047.
28 M. M. Stevens and J. H. George, *Science*, 2005, **310**, 1135–1138.
29 H. N. Kim, A. Jiao, N. S. Hwang, M. S. Kim, D. H. Kang, D. H. Kim and K. Y. Suh, *Adv. Drug Delivery Rev.*, 2013, **65**, 536–558.
30 K. Bazaka, R. J. Crawford and E. P. Ivanova, *Biotechnol. J.*, 2011, **6**, 1103–1114.
31 F. Baino, *Ceram. Int.*, 2018, **44**, 14953–14966.
32 M. S. N. Shahrbabak, F. Sharifianjazi, D. Rahban and A. Salimi, *Silicon*, 2019, **11**, 2741–2751.
33 Y. C. Fredholm, N. Karpukhina, R. V. Law and R. G. Hill, in *Journal of Non-Crystalline Solids*, Elsevier B.V., 2010, vol. 356, pp. 2546–2551.
34 A. J. Salinas, S. Shruti, G. Malavasi, L. Menabue and M. Vallet-Regí, *Acta Biomater.*, 2011, **7**, 3452–3458.
35 V. Luginbuehl, L. Meinel, H. P. Merkle and B. Gander, *Eur. J. Pharm. Biopharm.*, 2004, **58**, 197–208.
36 E. Verné, S. Di Nunzio, M. Bosetti, P. Appendino, C. Vitale Brovarone, G. Maina and M. Cannas, *Biomaterials*, 2005, **26**, 5111–5119.
37 R. S. Varma, D. C. Kothari and R. Tewari, *J. Non-Cryst. Solids*, 2009, **355**, 1246–1251.
38 S. M. Rabiee, N. Nazparvar, M. Azizian, D. Vashaee and L. Tayebi, *Ceram. Int.*, 2015, **41**, 7241–7251.
39 A. Moghanian, S. Firoozi and M. Tahriri, *Ceram. Int.*, 2017, **43**, 14880–14890.
40 R. Koohkan, T. Hooshmand, M. Tahriri and D. Mohebbi-Kalhori, *Ceram. Int.*, 2018, **44**, 2390–2399.
41 F. Baino, E. Fiume, M. Miola, F. Leone, B. Onida and E. Verné, *Mater. Lett.*, 2019, **235**, 207–211.
42 K. Rezwan, Q. Z. Chen, J. J. Blaker and A. R. Boccaccini, *Biomaterials*, 2006, **27**, 3413–3431.
43 C. Beer, R. Foldbjerg, Y. Hayashi, D. S. Sutherland and H. Autrup, *Toxicol. Lett.*, 2012, **208**, 286–292.
44 F. Baino, S. Fiorilli and C. Vitale-Brovarone, *Acta Biomater.*, 2016, **42**, 18–32.
45 X. Yan, C. Yu, X. Zhou, J. Tang and D. Zhao, *Angew. Chem., Int. Ed.*, 2004, **43**, 5980–5984.
46 J. Xiao, Y. Wan, F. Yao, Y. Huang, Y. Zhu, Z. Yang and H. Luo, *Mater. Lett.*, 2019, **248**, 201–203.
47 A. Lopez-Noriega, D. Arcos, I. Izquierdp-Barba, Y. Sakamoto, O. Terasaki and M. Vallet-Regí, *Chem. Mater.*, 2006, **18**, 3137–3144.
48 X. Yan, G. Wei, L. Zhao, J. Yi, H. Deng, L. Wang, G. M. Lu and C. Yu, *Microporous Mesoporous Mater.*, 2010, **132**, 282–289.
49 C. Wu, Y. Zhou, M. Xu, P. Han, L. Chen, J. Chang and Y. Xiao, *Biomaterials*, 2013, **34**, 422–433.
50 P. Han, C. Wu, J. Chang and Y. Xiao, *Biomaterials*, 2012, **33**, 6370–6379.
51 C. Wu, Y. Zhou, C. Lin, J. Chang and Y. Xiao, *Acta Biomater.*, 2012, **8**, 3805–3815.
52 S. Zhao, J. Zhang, M. Zhu, Y. Zhang, Z. Liu, C. Tao, Y. Zhu and C. Zhang, *Acta Biomater.*, 2015, **12**, 270–280.
53 Y. Zhu, Y. Zhang, C. Wu, Y. Fang, J. Yang and S. Wang, *Microporous Mesoporous Mater.*, 2011, **143**, 311–319.
54 N. J. Lakhkar, I. H. Lee, H. W. Kim, V. Salih, I. B. Wall and J. C. Knowles, *Adv. Drug Delivery Rev.*, 2013, **65**, 405–420.
55 V. M. Schatkoski, T. Larissa do Amaral Montanheiro, B. R. Canuto de Menezes, R. M. Pereira, K. F. Rodrigues, R. G. Ribas, D. Morais da Silva and G. P. Thim, *Ceram. Int.*, 2021, **47**, 2999–3012.
56 L. Hupa, in *Bioactive Glasses*, Elsevier Ltd, 2nd edn, 2018, pp. 1–35.
57 I. D. Xynos, A. J. Edgar, L. D. K. Buttery, L. L. Hench and J. M. Polak, *J. Biomed. Mater. Res.*, 2001, **55**, 151–157.
58 P. Balasubramanian, T. Büttner, V. Miguez Pacheco and A. R. Boccaccini, *J. Eur. Ceram. Soc.*, 2018, **38**, 855–869.
59 O. Tsigkou, J. R. Jones, J. M. Polak and M. M. Stevens, *Biomaterials*, 2009, **30**, 3542–3550.
60 I. A. Silver and M. Erecinska, in *Materialwissenschaft und Werkstofftechnik*, 2003, vol. 34, pp. 1069–1075.
61 H. Oonishi, L. L. Hench, J. Wilson, F. Sugihara, E. Tsuji, S. Kushitani and H. Iwaki, *J. Biomed. Mater. Res.*, 1999, **44**, 31–43.
62 M. Khorami, S. Hesaraki, A. Behnamghader, H. Nazarian and S. Shahrabi, *Mater. Sci. Eng., C*, 2011, **31**, 1584–1592.
63 M. Blochberger, L. Hupa and D. S. Brauer, *Biomed. Glas.*, 2015, **1**, 93–107.
64 C. Stähli, M. James-Bhasin, A. Hoppe, A. R. Boccaccini and S. N. Nazhat, *Acta Biomater.*, 2015, **19**, 15–22.
65 V. Nicolini, G. Malavasi, L. Menabue, G. Lusvardi, F. Benedetti, S. Valeri and P. Luches, *J. Mater. Sci.*, 2017, **52**, 8845–8857.
66 S. Chen, M. Michálek, D. Galusková, M. Michálková, P. Švančárek, A. Talimian, H. Kaňková, J. Kraxner, K. Zheng, L. Liverani, D. Galusek and A. R. Boccaccini, *Mater. Sci. Eng., C*, 2020, **112**, 1–9.
67 S. I. Schmitz, B. Widholz, C. Essers, M. Becker, D. U. Tulyaganov, A. Moghaddam, I. Gonzalo de Juan and F. Westhauser, *Bioact. Mater.*, 2020, **5**, 55–65.
68 E. J. Kim, S. Y. Bu, M. K. Sung and M. K. Choi, *Biol. Trace Elem. Res.*, 2013, **152**, 105–112.
69 L. J. Robinson, H. C. Blair, J. B. Barnett, M. Zaidi and C. L.-H. Huang, in *Annals of the New York Academy of Sciences*, 2010, vol. 1192, pp. 351–357.
70 M. Bohner, *Biomaterials*, 2009, **30**, 6403–6406.
71 P. Valerio, M. M. Pereira, A. M. Goes and M. F. Leite, *Biomaterials*, 2004, **25**, 2941–2948.
72 S. Maeno, Y. Niki, H. Matsumoto, H. Morioka, T. Yatabe, A. Funayama, Y. Toyama, T. Taguchi and J. Tanaka, *Biomaterials*, 2005, **26**, 4847–4855.
73 L. L. Hench, *J. Eur. Ceram. Soc.*, 2009, **29**, 1257–1265.
74 S. Kargozar, N. Lotfibakhshaiesh, J. Ai, A. Samadikuchaksaraie, R. G. Hill, P. A. Shah, P. B. Milan, M. Mozafari, M. Fathi and M. T. Joghataei, *J. Non-Cryst. Solids*, 2016, **449**, 133–140.
75 P. J. Marie, D. Felsenberg and M. L. Brandi, in *Osteoporosis International*, 2011, vol. 22, pp. 1659–1667.

Open Access Article. Published on 06 Eost 2024. Downloaded on 2026-06-06 12:45:47.
This article is licensed under a Creative Commons Attribution 3.0 Unported Licence.

76 S. Kargozar, N. Lotfibakhshaiesh, J. Ai, M. Mozafari, P. Brouki Milan, S. Hamzehlou, M. Barati, F. Baino, R. G. Hill and M. T. Joghataei, *Acta Biomater.*, 2017, **58**, 502–514.
77 L. Wei, J. Ke, I. Prasadam, R. J. Miron, S. Lin, Y. Xiao, J. Chang, C. Wu and Y. Zhang, *Osteoporosis Int.*, 2014, **25**, 2089–2096.
78 J. Liu, S. C. F. Rawlinson, R. G. Hill and F. Fortune, *Dent. Mater.*, 2016, **32**, 412–422.
79 S. K. Arepalli, H. Tripathi, S. K. Hira, P. P. Manna, R. Pyare and S. P. Singh, *Mater. Sci. Eng., C*, 2016, **69**, 108–116.
80 J. Isaac, J. Nohra, J. Lao, E. Jallot, J.-M. Nedelec, A. Berdal and J. M. Sautier, *Eur. Cells Mater.*, 2011, **21**, 130–143.
81 S. Kargozar, M. Montazerian, E. Fiume and F. Baino, *Front. Bioeng. Biotechnol.*, 2019, **7**, 1–29.
82 M. Julien, S. Khoshniat, A. Lacreusette, M. Gatius, A. Bozec, E. F. Wagner, Y. Wittrant, M. Masson, P. Weiss, L. Beck, D. Magne and J. Guicheux, *J. Bone Miner. Res.*, 2009, **24**, 1856–1868.
83 J. R. Jones, O. Tsigkou, E. E. Coates, M. M. Stevens, J. M. Polak and L. L. Hench, *Biomaterials*, 2007, **28**, 1653–1663.
84 S. L. Hall, H. P. Dimai and J. R. Farley, *Calcif. Tissue Int.*, 1999, **64**, 163–172.
85 W. R. Holloway, F. M. Collier, R. E. Herbst, J. M. Hodge and G. C. Nicholson, *Bone*, 1996, **19**, 137–142.
86 X. Luo, D. Barbieri, N. Davison, Y. Yan, J. D. De Bruijn and H. Yuan, *Acta Biomater.*, 2014, **10**, 477–485.
87 J. P. O'Connor, D. Kanjilal, M. Teitelbaum, S. S. Lin and J. A. Cottrell, *Materials*, 2020, **13**, 1–22.
88 D. Boyd, G. Carroll, M. R. Towler, C. Freeman, P. Farthing and I. M. Brook, *J. Mater. Sci. Mater. Med.*, 2009, **20**, 413–420.
89 M. Huang, R. G. Hill and S. C. F. Rawlinson, *Dent. Mater.*, 2017, **33**, 543–552.
90 Z. Neščáková, K. Zheng, L. Liverani, Q. Nawaz, D. Galusková, H. Kaňková, M. Michálek, D. Galusek and A. R. Boccaccini, *Bioact. Mater.*, 2019, **4**, 312–321.
91 F. Westhauser, S. Wilkesmann, Q. Nawaz, F. Hohenbild, F. Rehder, M. Saur, J. Fellenberg, A. Moghaddam, M. S. Ali, W. Peukert and A. R. Boccaccini, *J. Biomed. Mater. Res., Part A*, 2021, **109**, 1457–1467.
92 A. M. Abdelghany, F. H. ElBatal and H. A. ElBatal, *Process. Appl. Ceram.*, 2014, **8**, 185–193.
93 M. Diba, F. Tapia, A. R. Boccaccini and L. A. Strobel, *Int. J. Appl. Glass Sci.*, 2012, **3**, 221–253.
94 A. Balamurugan, G. Balossier, J. Michel, S. Kannan, H. Benhayoune, A. H. S. Rebelo and J. M. F. Ferreira, *J. Biomed. Mater. Res.*, 2007, **5**, 546–553.
95 S. Kargozar, P. B. Milan, M. Amoupour, F. Kermani, S. Gorgani, S. Nazarnezhad, S. Hooshmand and F. Baino, *Materials*, 2022, **15**, 1–16.
96 J. Zhang, C. Liu, Y. Li, J. Sun, P. Wang, K. Di and Y Zhao, *J. Rare Earths*, 2010, **28**, 138–142.
97 K. Zheng, E. Torre, A. Bari, N. Taccardi, C. Cassinelli, M. Morra, S. Fiorilli, C. Vitale-Brovarone, G. Iviglia and A. R. Boccaccini, *Mater. Today Bio*, 2020, **5**, 1–14.
98 I. Burghardt, F. Lüthen, C. Prinz, B. Kreikemeyer, C. Zietz, H. G. Neumann and J. Rychly, *Biomaterials*, 2015, **44**, 36–44.
99 J. V. Rau, M. Curcio, M. G. Raucci, K. Barbaro, I. Fasolino, R. Teghil, L. Ambrosio, A. De Bonis and A. R. Boccaccini, *ACS Appl. Mater. Interfaces*, 2019, **11**, 5812–5820.
100 Y. Lin, W. Xiao, B. S. Bal and M. N. Rahaman, *Mater. Sci. Eng., C*, 2016, **67**, 440–452.
101 S. Kargozar, M. Mozafari, S. Ghodrat, E. Fiume and F. Baino, *Mater. Sci. Eng., C*, 2021, **121**, 1–18.
102 X. Ying, S. Cheng, W. Wang, Z. Lin, Q. Chen, W. Zhang, D. Kou, Y. Shen, X. Cheng, F. A. Rompis, L. Peng and C. Z. Lu, *Biol. Trace Elem. Res.*, 2011, **144**, 306–315.
103 Y. Gu, W. Huang, M. N. Rahaman and D. E. Day, *Acta Biomater.*, 2013, **9**, 9126–9136.
104 L. Bi, M. N. Rahaman, D. E. Day, Z. Brown, C. Samujh, X. Liu, A. Mohammadkhah, V. Dusevich, J. D. Eick and L. F. Bonewald, *Acta Biomater.*, 2013, **9**, 8015–8026.
105 Y. Gu, G. Wang, X. Zhang, Y. Zhang, C. Zhang, X. Liu, M. N. Rahaman, W. Huang and H. Pan, *Mater. Sci. Eng., C*, 2014, **36**, 294–300.
106 K. O'Connell, C. Pierlot, H. O'Shea, D. Beaudry, M. Chagnon, M. Assad and D. Boyd, *J. Biomed. Mater. Res., Part B*, 2017, **105**, 1818–1827.
107 A. A. Gorustovich, J. M. P. López, M. B. Guglielmotti and R. L. Cabrini, *Biomed. Mater.*, 2006, **1**, 100–105.
108 E. Piatti, E. Verné and M. Miola, *Ceram. Int.*, 2022, **48**, 13706–13718.
109 C. Wu, R. Miron, A. Sculean, S. Kaskel, T. Doert, R. Schulze and Y. Zhang, *Biomaterials*, 2011, **32**, 7068–7078.
110 C. Y. C. Pak, J. E. Zerwekh and P. Antich, *Trends Endocrinol. Metab.*, 1995, **6**, 229–234.
111 L. Bergandi, V. Aina, S. Garetto, G. Malavasi, E. Aldieri, E. Laurenti, L. Matera, C. Morterra and D. Ghigo, *Chem.-Biol. Interact.*, 2010, **183**, 405–415.
112 L. Li, *Crit. Rev. Oral Biol. Med.*, 2003, **14**, 100–114.
113 A. Shearer, M. Montazerian, J. J. Sly, R. G. Hill and J. C. Mauro, *Acta Biomater.*, 2023, **160**, 14–31.
114 L. A. H. Durand, G. E. Vargas, F. Gomez-Gramajo, R. Vera-Mesones, V. Miguez-Pacheco, A. R. Boccaccini and A. Gorustovich, in *Biomedical, Therapeutic and Clinical Applications of Bioactive Glasses*, Elsevier Ltd, 2018, pp. 201–217.
115 M. Miola, C. Vitale-Brovarone, G. Maina, F. Rossi, L. Bergandi, D. Ghigo, S. Saracino, M. Maggiora, R. A. Canuto, G. Muzio and E. Verné, *Mater. Sci. Eng., C*, 2014, **38**, 107–118.
116 G. de Souza Balbinot, F. M. Collares, F. Visioli, P. B. F. Soares, A. S. Takimi, S. M. W. Samuel and V. C. B. Leitune, *Dent. Mater.*, 2018, **34**, 1449–1458.
117 G. de Souza Balbinot, V. C. B. Leitune, D. Ponzoni and F. M. Collares, *Dent. Mater.*, 2019, **35**, 1490–1497.
118 A. A. El-Rashidy, J. A. Roether, L. Harhaus, U. Kneser and A. R. Boccaccini, *Acta Biomater.*, 2017, **62**, 1–28.
119 D. Pradhan, A. W. Wren, S. T. Misture and N. P. Mellott, *Mater. Sci. Eng., C*, 2016, **58**, 918–926.

 This journal is © The Royal Society of Chemistry 2024

Open Access Article. Published on 06 Eost 2024. Downloaded on 2026-06-06 12:45:47.
This article is licensed under a Creative Commons Attribution 3.0 Unported Licence.

120 X. Wang, Y. Zhang, Y. Ma, D. Chen, H. Yang and M. Li, *Ceram. Int.*, 2016, **42**, 3609–3617.
121 M. Hu, J. Fang, Y. Zhang, X. Wang, W. Zhong and Z. Zhou, *J. Colloid Interface Sci.*, 2020, **579**, 654–666.
122 J. Ma, Y. Wang, L. Zhou and S. Zhang, *Mater. Sci. Eng., C*, 2013, **33**, 440–445.
123 L. He, H. Li, X. Chen, T. Xu, T. Sun, H. Huang, M. Lu, Y. Yin, J. Ge, J. Weng, N. Zhuo and K. Duan, *Ceram. Int.*, 2019, **45**, 13787–13798.
124 P. Zhao, M. Li, Y. Chen, C. He, X. Zhang, T. Fan, T. Yang, Y. Lu, R. J. Lee, X. Ma, J. Luo and G. Xiang, *Int. J. Pharm.*, 2019, **570**, 1–7.
125 C. Rodríguez-Valencia, M. Lopez-Álvarez, B. Cochón-Cores, I. Pereiro, J. Serra and P. González, *J. Biomed. Mater. Res., Part A*, 2013, **101 A**, 853–861.
126 Z. Deng, B. Lin, Z. Jiang, W. Huang, J. Li, X. Zeng, H. Wang, D. Wang and Y. Zhang, *Int. J. Biol. Sci.*, 2019, **15**, 1113–1124.
127 S. Kargozar, F. Baino, S. Hamzehlou, R. G. Hill and M. Mozafari, *Trends Biotechnol.*, 2018, **36**, 430–444.
128 S. Chen, Q. Yang, R. K. Brow, K. Liu, K. A. Brow, Y. Ma and H. Shi, *Mater. Sci. Eng., C*, 2017, **73**, 447–455.
129 S. Chen, D. Galusková, H. Kaňková, K. Zheng, M. Michálek, L. Liverani, D. Galusek and A. R. Boccaccini, *Materials*, 2020, **13**, 1–15.
130 H. Oliveira, S. Catros, O. Castano, S. Rey, R. Siadous, D. Clift, J. Marti-Munoz, M. Batista, R. Bareille, J. Planell, E. Engel and J. Amédée, *Acta Biomater.*, 2017, **54**, 377–385.
131 A. M. Deliormanlı, H. Seda Vatansever, H. Yesil and F. Özdal-Kurt, *Ceram. Int.*, 2016, **42**, 11574–11583.
132 M. Dziadek, B. Zagrajczuk, E. Menaszek, K. Dziadek and K. Cholewa-Kowalska, *Mater. Lett.*, 2018, **215**, 87–90.
133 M. Miola and E. Verné, *Materials*, 2016, **9**, 1–16.
134 M. Miola, E. Bertone and E. Verné, *Appl. Surf. Sci.*, 2019, **495**, 2–14.
135 C. Huang, M. Yu, H. Li, X. Wan, Z. Ding, W. Zeng and Z. Zhou, *Adv. Mater. Interfaces*, 2021, **8**, 1–27.
136 W. Zhai, H. Lu, C. Wu, L. Chen, X. Lin, K. Naoki, G. Chen and J. Chang, *Acta Biomater.*, 2013, **9**, 8004–8014.
137 Y. Yu, G. Jin, Y. Xue, D. Wang, X. Liu and J. Sun, *Acta Biomater.*, 2017, **49**, 590–603.
138 L. Mao, L. Xia, J. Chang, J. Liu, L. Jiang, C. Wu and B. Fang, *Acta Biomater.*, 2017, **61**, 217–232.
139 A. Hoppe, A. Brandl, O. Bleiziffer, A. Arkudas, R. E. Horch, B. Jokic, D. Janackovic and A. R. Boccaccini, *Mater. Sci. Eng., C*, 2015, **57**, 157–163.
140 N. Gupta, D. Santhiya, S. Murugavel, A. Kumar, A. Aditya, M. Ganguli and S. Gupta, *Colloids Surf., A*, 2018, **538**, 393–403.
141 E. Verné, M. Miola, S. Ferraris, C. L. Bianchi, A. Naldoni, G. Maina and O. Bretcanu, *Adv. Eng. Mater.*, 2010, **12**, 309–319.
142 M. Miola, Y. Pakzad, S. Banijamali, S. Kargozar, C. Vitale-Brovarone, A. Yazdanpanah, O. Bretcanu, A. Ramedani, E. Vernè and M. Mozafari, *Acta Biomater.*, 2019, **83**, 55–70.
143 O. Sedighi, A. Alaghmandfard, M. Montazerian and F. Baino, *J. Am. Ceram. Soc.*, 2022, **105**, 1723–1747.
144 A. Moeini, T. Hassanzadeh Chinijani, A. Malek Khachatourian, M. Vinicius Lia Fook, F. Baino and M. Montazerian, *Int. J. Appl. Glass Sci.*, 2023, **14**, 69–87.
145 M. Awais, A. Aizaz, A. Nazneen, Q. ul A. Bhatti, M. Akhtar, A. Wadood and M. Atiq Ur Rehman, *Prosthesis*, 2022, **4**, 263–316.
146 F. A. Shah, D. S. Brauer, N. Desai, R. G. Hill and K. A. Hing, *Mater. Lett.*, 2014, **119**, 96–99.
147 J. Liu, S. C. F. Rawlinson, R. G. Hill and F. Fortune, *Dent. Mater.*, 2016, **32**, 221–237.
148 J. Barralet, S. Best and W. Bonfield, *J. Biomed. Mater. Res.*, 1998, **41**, 79–86.
149 A. Al-Noaman, S. C. F. Rawlinson and R. G. Hill, *J. Non-Cryst. Solids*, 2012, **358**, 3019–3027.
150 N. Bai, W. Chen, L. Luo, W. Tong, C. Wen, X. Zhan and B. Sa, *J. Am. Ceram. Soc.*, 2021, **104**, 3058–3072.
151 A. M. Abdelghany, H. A. ElBatal and F. M. Ezzeldin, *Ceram. Int.*, 2012, **38**, 1105–1113.
152 A. M. Abdelghany and H. Kamal, *Ceram. Int.*, 2014, **40**, 8003–8011.
153 F. H. ElBatal, M. A. Ouis and H. A. ElBatal, *Ceram. Int.*, 2016, **42**, 8247–8256.
154 M. A. Marzouk and H. A. ElBatal, *Process. Appl. Ceram.*, 2014, **8**, 167–177.
155 A. M. Deliormanlı, *Mater. Technol.*, 2014, **29**, 358–365.
156 S. B. Jung, Borate based bioactive glass scaffolds for hard and soft tissue engineering, Doctoral Dissertations Missouri University of Science and Technology, 2010, 1–350.
157 K. Zheng, X. Dai, M. Lu, N. Hüser, N. Taccardi and A. R. Boccaccini, *Colloids Surf., B*, 2017, **150**, 159–167.
158 J. Ma, C. Z. Chen, D. G. Wang and J. H. Hu, *Ceram. Int.*, 2011, **37**, 1637–1644.
159 F. Sharifianjazi, M. Moradi, A. Abouchenari, A. H. Pakseresht, A. Esmaeilkhanian, M. Shokouhimehr and M. Shahedi Asl, *Ceram. Int.*, 2020, **46**, 22674–22682.
160 H. Jodati, B. Güner, Z. Evis, D. Keskin and A. Tezcaner, *Ceram. Int.*, 2020, **46**, 10503–10511.
161 V. Aina, C. Morterra, G. Lusvardi, G. Malavasi, L. Menabue, S. Shruti, C. L. Bianchi and V. Bolis, *J. Phys. Chem. C*, 2011, **115**, 22461–22474.
162 H. E. Lundager Madsen, *J. Cryst. Growth*, 2008, **310**, 2602–2612.
163 R. Sergi, V. Cannillo, A. R. Boccaccini and L. Liverani, *Appl. Sci.*, 2020, **10**, 1–19.
164 V. Aina, G. Malavasi, A. Fiorio Pla, L. Munaron and C. Morterra, *Acta Biomater.*, 2009, **5**, 1211–1222.
165 A. Balamurugan, G. Balossier, S. Kannan, J. Michel, A. H. S. S. Rebelo and J. M. F. F. Ferreira, *Acta Biomater.*, 2007, **3**, 255–262.
166 S. Shahrabi, S. Hesaraki, S. Moemeni and M. Khorami, *Ceram. Int.*, 2011, **37**, 2737–2746.
167 R. K. Singh and A. Srinivasan, *Appl. Surf. Sci.*, 2010, **256**, 1725–1730.

Open Access Article. Published on 06 Eost 2024. Downloaded on 2026-06-06 12:45:47.
This article is licensed under a Creative Commons Attribution 3.0 Unported Licence.

168 V. Anand, K. J. Singh and K. Kaur, *J. Non-Cryst. Solids*, 2014, **406**, 88–94.
169 V. K. Vyas, A. S. Kumar, P. Sunil, S. P. Singh and R. Pyare, *Bull. Mater. Sci.*, 2015, **38**, 957–964.
170 B. R. Barrioni, A. G. S. de Laia, T. M. Valverde, T. M. da M. Martins, M. V. Caliari, M. A. de Sá, A. M. de Goes and M. de M. Pereira, *Ceram. Int.*, 2018, **44**, 20337–20347.
171 S. Hesaraki, M. Alizadeh, H. Nazarian and D. Sharifi, *J. Mater. Sci. Mater. Med.*, 2010, **21**, 695–705.
172 A. Hoppe, B. Sarker, R. Detsch, N. Hild, D. Mohn, W. J. Stark and A. R. Boccaccini, *J. Non-Cryst. Solids*, 2014, **387**, 41–46.
173 A. Moghanian, M. Zohourfazeli and M. H. M. Tajer, *J. Non-Cryst. Solids*, 2020, **546**, 1–9.
174 S. Agathopoulos, D. U. Tulyaganov, J. M. G. Ventura, S. Kannan, M. A. Karakassides and J. M. F. Ferreira, *Biomaterials*, 2006, **27**, 1832–1840.
175 W. C. Lepry, S. Smith and S. N. Nazhat, *J. Non-Cryst. Solids*, 2018, **500**, 141–148.
176 A. Moghanian, M. Zohourfazeli, M. H. M. Tajer, Z. Miri, S. M. Hosseini and A. Rashvand, *Ceram. Int.*, 2021, **47**, 23762–23769.
177 S. Mokhtari, E. A. Krull, L. M. Sanders, A. Coughlan, N. P. Mellott, Y. Gong, R. Borges and A. W. Wren, *Mater. Sci. Eng., C*, 2019, **103**, 1–14.
178 A. Obata, Y. Takahashi, T. Miyajima, K. Ueda, T. Narushima and T. Kasuga, *Appl. Mater. Interfaces*, 2012, **4**, 5684–5690.
179 H. Pirayesh and J. A. Nychka, *J. Am. Chem. Soc.*, 2013, **96**, 1643–1650.
180 S. V. Dorozhkin, *J. Mater. Sci. Mater. Med.*, 2013, **24**, 1335–1363.
181 T. Zambanini, R. Borges, P. C. Faria, G. P. Delpino, I. S. Pereira, M. M. Marques and J. Marchi, *Int. J. Appl. Ceram. Technol.*, 2019, **16**, 2028–2039.
182 S. Ouyang, K. Zheng, Q. Huang, Y. Liu and A. R. Boccaccini, *Mater. Lett.*, 2020, **273**, 1–4.
183 X. Wang, Y. Zhang, C. Lin and W. Zhong, *Colloids Surf., B*, 2017, **160**, 406–415.
184 S. K. Arepalli, H. Tripathi, V. K. Vyas, S. Jain, S. K. Suman, R. Pyare and S. P. Singh, *Mater. Sci. Eng., C*, 2015, **49**, 549–559.
185 S. Majumdar, S. K. Hira, H. Tripathi, A. S. Kumar, P. P. Manna, S. P. Singh and S. Krishnamurthy, *Ceram. Int.*, 2021, **47**, 7143–7158.
186 U. Pantulap, M. Arango-Ospina and A. R. Boccaccini, *J. Mater. Sci. Mater. Med.*, 2022, **33**, 1–41.
187 N. Durán, M. Durán, M. B. de Jesus, A. B. Seabra, W. J. Fávaro and G. Nakazato, *Nanomedicine*, 2016, **12**, 789–799.
188 M. Bellantone, H. D. Williams and L. L. Hench, *Antimicrob. Agents Chemother.*, 2002, **46**, 1940–1945.
189 D. Kozon, K. Zheng, E. Boccardi, Y. Liu, L. Liverani and A. R. Boccaccini, *Materials*, 2016, **9**, 1–8.
190 M. Miola, E. Verné, C. Vitale-Brovarone and F. Baino, *Int. J. Appl. Glass Sci.*, 2016, **7**, 238–247.
191 G. Muzio, M. Miola, S. Perero, M. Oraldi, M. Maggiora, S. Ferraris, E. Vernè, V. Festa, F. Festa, R. A. Canuto and M. Ferraris, *Surf. Coat. Technol.*, 2017, **319**, 326–334.
192 M. Rahmani, A. Moghanian and M. S. Yazdi, *Ceram. Int.*, 2021, **47**, 15985–15994.
193 H. Zhu, C. Hu, F. Zhang, X. Feng, J. Li, T. Liu, J. Chen and J. Zhang, *Mater. Sci. Eng., C*, 2014, **42**, 22–30.
194 B. Xue, W. Wang, L. Guo, Z. Zhang, J. Meng, X. Tao, X. Ren, Z. Liu and Y. Qiang, *J. Biomater. Appl.*, 2019, **34**, 86–93.
195 E. A. Abou Neel, I. Ahmed, J. Pratten, S. N. Nazhat and J. C. Knowles, *Biomaterials*, 2005, **26**, 2247–2254.
196 S. P. Valappil, D. Ready, E. A. Abou Neel, D. M. Pickup, W. Chrzanowski, L. A. O'Dell, R. J. Newport, M. E. Smith, M. Wilson and J. C. Knowles, *Adv. Funct. Mater.*, 2008, **18**, 732–741.
197 D. M. Pickup, S. P. Valappil, R. M. Moss, H. L. Twyman, P. Guerry, M. E. Smith, M. Wilson, J. C. Knowles and R. J. Newport, *J. Mater. Sci.*, 2009, **44**, 1858–1867.
198 A. M. Deliormanlı, *Ceram. Int.*, 2016, **42**, 897–906.
199 J. Zhu, G. Jiang, G. Song, T. Liu, C. Cao, Y. Yang, Y. Zhang and W. Hong, *ACS Appl. Bio Mater.*, 2019, **2**, 5042–5052.
200 M. E. Galarraga-Vinueza, B. Passoni, C. A. M. Benfatti, J. Mesquita-Guimarães, B. Henriques, R. S. Magini, M. C. Fredel, B. V. Meerbeek, W. Teughels and J. C. M. Souza, *J. Biomed. Mater. Res., Part A*, 2017, **105**, 1994–2003.
201 F. N. S. Raja, T. Worthington, M. A. Isaacs, L. Forto Chungong, B. Burke, O. Addison and R. A. Martin, *ACS Biomater. Sci. Eng.*, 2019, **5**, 283–293.
202 A. Moghanian, S. Firoozi and M. Tahriri, *Ceram. Int.*, 2017, **43**, 12835–12843.
203 R. Sergi, D. Bellucci, R. Salvatori, G. Maisetta, G. Batoni and V. Cannillo, *Mater. Sci. Eng., C*, 2019, **104**, 1–9.
204 Q. Nawaz, U. A. M. Rehman, A. Burkovski, J. Schmidt, A. M. Beltrán, A. Shahid, N. K. Alber, W. Peukert and A. R. Boccaccini, *J. Mater. Sci. Mater. Med.*, 2018, **5**, 29–64.
205 X. He, Y. Liu, Y. Tan, L. M. Grover, J. Song, S. Duan, D. Zhao and X. Tan, *Mater. Sci. Eng., C*, 2019, **105**, 1–11.
206 Z. Tabia, S. Akhtach, K. El Mabrouk, M. Bricha, K. Nouneh and A. Ballamurugan, *Biomed. Glas.*, 2020, **6**, 10–22.
207 M. Miola, J. Massera, A. Cochis, A. Kumar, L. Rimondini and E. Verné, *Mater. Sci. Eng., C*, 2021, **123**, 1–12.
208 R. Shafaghi, O. Rodriguez, A. W. Wren, L. Chiu, E. H. Schemitsch, P. Zalzal, S. D. Waldman, M. Papini and M. R. Towler, *J. Biomed. Mater. Res., Part A*, 2021, **109**, 146–158.
209 O. Rodriguez, W. Stone, E. H. Schemitsch, P. Zalzal, S. Waldman, M. Papini and M. R. Towler, *Heliyon*, 2017, **3**, 1–21.
210 M. Ferraris, S. Perero, M. Miola, S. Ferraris, G. Gautier, G. Maina, G. Fucale and E. Verné, *Adv. Eng. Mater.*, 2010, **12**, 276–282.
211 S. Pal, Y. K. Tak and J. M. Song, *Appl. Environ. Microbiol.*, 2007, **73**, 1712–1720.
212 L. C. A. da Silva, F. G. Neto, S. S. C. Pimentel, R. da Silva Palácios, F. Sato, K. M. Retamiro, N. S. Fernandes, C. V. Nakamura, F. Pedrochi and A. Steimacher, *J. Non-Cryst. Solids*, 2021, **554**, 1–6.

 This journal is © The Royal Society of Chemistry 2024

Open Access Article. Published on 06 Eost 2024. Downloaded on 2026-06-06 12:45:47.
This article is licensed under a Creative Commons Attribution 3.0 Unported Licence.

213 S. Kargozar, R. K. Singh, H. W. Kim and F. Baino, *Acta Biomater.*, 2020, **115**, 1–28.
214 S. Kargozar, M. Montazerian, S. Hamzehlou, H. W. Kim and F. Baino, *Acta Biomater.*, 2018, **81**, 1–19.
215 S. Kargozar, S. Hamzehlou and F. Baino, *Mater. Sci. Eng., C*, 2019, **97**, 1009–1020.
216 V. Nicolini, G. Malavasi, G. Lusvardi, A. Zambon, F. Benedetti, G. Cerrato, S. Valeri and P. Luches, *Ceram. Int.*, 2019, **45**, 20910–20920.
217 M. Stevanović, N. Filipović, J. Djurdjević, M. Lukić, M. Milenković and A. R. Boccaccini, *Colloids Surf., B*, 2015, **132**, 208–215.
218 A. M. El-Kady, M. M. Ahmed, B. M. Abd El-Hady, A. F. Ali and A. M. Ibrahim, *J. Non-Cryst. Solids*, 2019, **521**, 1–12.
219 H. W. Kim, J. C. Knowles and H. E. Kim, *J. Mater. Sci. Mater. Med.*, 2005, **16**, 189–195.
220 J. Hum and A. R. Boccaccini, *J. Mater. Sci.: Mater. Med.*, 2012, **23**, 2317–2333.
221 A. L. Andrade, D. M. Souza, W. A. Vasconcellos, R. V. Ferreira and R. Z. Domingues, *J. Non-Cryst. Solids*, 2009, **355**, 811–816.
222 Y. Zhu and S. Kaskel, *Microporous Mesoporous Mater.*, 2009, **118**, 176–182.
223 A. López-Noriega, D. Arcos and M. Vallet-Regí, *Chem. – Eur. J.*, 2010, **16**, 10879–10886.
224 W. Li, P. Nooeaid, J. A. Roether, D. W. Schubert and A. R. Boccaccini, *J. Eur. Ceram. Soc.*, 2014, **34**, 505–514.
225 A. M. El-Kady, M. M. Farag and A. M. I. El-Rashedi, *Eur. J. Pharm. Sci.*, 2016, **91**, 243–250.
226 C. Chen, J. Ding, H. Wang and D. Wang, *J. Inorg. Mater.*, 2022, **37**, 1245–1258.
227 A. M. El-Kady and M. M. Farag, *J. Nanomater.*, 2015, **2015**, 1–11.
228 M. S. Ur Rahman, M. A. Tahir, S. Noreen, M. Yasir, I. Ahmad, M. B. Khan, K. W. Ali, M. Shoaib, A. Bahadur and S. Iqbal, *RSC Adv.*, 2020, **10**, 21413–21419.
229 M. E. Galarraga-Vinueza, J. Mesquita-Guimarães, R. S. Magini, J. C. M. Souza, M. C. Fredel and A. R. Boccaccini, *J. Biomed. Mater. Res., Part A*, 2018, **106**, 1614–1625.
230 M. H. Kaou, M. Furkó, K. Balázsi and C. Balázsi, *Nanomaterials*, 2023, **13**, 1–33.
231 M. Erol, A. Özyuğuran, Ö. Özarpat and S. Küçükbayrak, *J. Eur. Ceram. Soc.*, 2012, **32**, 2747–2755.
232 C. Vitale-Brovarone, M. Miola, C. Balagna and E. Verné, *Chem. Eng. J.*, 2008, **137**, 129–136.
233 J. I. Sasaki, W. Kiba, G. L. Abe, C. Katata, M. Hashimoto, H. Kitagawa and S. Imazato, *Dent. Mater.*, 2019, **35**, 780–788.
234 K. Xiong, J. Zhang, Y. Zhu, L. Chen and J. Ye, *Mater. Sci. Eng., C*, 2019, **105**, 1–9.
235 M. Miola, M. Bruno, G. Maina, G. Fucale, G. Lucchetta and E. Vernè, *Mater. Sci. Eng., C*, 2014, **43**, 65–75.
236 M. Miola, G. Fucale, G. Maina and E. Verné, *J. Mater. Sci.*, 2017, **52**, 5133–5146.
237 M. Miola, A. Cochis, A. Kumar, C. R. Arciola, L. Rimondini and E. Verné, *Materials*, 2018, **11**, 1–13.
238 M. R. Syed, M. Khan, F. Sefat, Z. Khurshid, M. S. Zafar and A. S. Khan, in *Biomedical, Therapeutic and Clinical Applications of Bioactive Glasses*, Elsevier Ltd, 2018, pp. 467–495.
239 A. Bistolfi, R. Ferracini, C. Albanese, E. Vernè and M. Miola, *Materials*, 2019, **12**, 1–16.
240 S. P. Sevari, F. Shahnazi, C. Chen, J. C. Mitchell, S. Ansari and A. Moshaverinia, *J. Biomed. Mater. Res., Part A*, 2020, **108**, 557–564.
241 K. Vuornos, M. Ojansivu, J. T. Koivisto, H. Häkkänen, B. Belay, T. Montonen, H. Huhtala, M. Kääriäinen, L. Hupa, M. Kellomäki, J. Hyttinen, J. A. Ihalainen and S. Miettinen, *Mater. Sci. Eng., C*, 2019, **99**, 905–918.
242 J. Wu, K. Zheng, X. Huang, J. Liu, H. Liu, A. R. Boccaccini, Y. Wan, X. Guo and Z. Shao, *Acta Biomater.*, 2019, **91**, 60–71.
243 M. Miola, F. Laviano, R. Gerbaldo, M. Bruno, A. Lombardi, A. Cochis, L. Rimondini and E. Verné, *Ceram. Int.*, 2017, **43**, 4831–4840.
244 J. J. Blaker, S. N. Nazhat and A. R. Boccaccini, *Biomaterials*, 2004, **25**, 1319–1329.
245 G. A. Fielding, M. Roy, A. Bandyopadhyay and S. Bose, *Acta Biomater.*, 2012, **8**, 3144–3152.
246 V. L. Calvo, M. V. Cabedo, E. Bannier, E. C. Recacha, A. R. Boccaccini, L. C. Arias and E. S. Vilches, *J. Mater. Sci.*, 2014, **49**, 7933–7942.
247 M. Miola, E. Verné, F. E. Ciraldo, L. Cordero-Arias and A. R. Boccaccini, *Front. Bioeng. Biotechnol.*, 2015, **3**, 1–13.
248 Y. fan Goh, M. Akram, A. Alshemary and R. Hussain, *Appl. Surf. Sci.*, 2016, **387**, 1–7.
249 G. Molino, A. Bari, F. Baino, S. Fiorilli and C. Vitale-Brovarone, *J. Mater. Sci.*, 2017, **52**, 9103–9114.
250 P. H. Kuo, S. S. Joshi, X. Lu, Y. H. Ho, Y. Xiang, N. B. Dahotre and J. Du, *Int. J. Appl. Glass Sci.*, 2019, **10**, 307–320.
251 F. Baino and E. Verne, *Biomed. Glas.*, 2017, **3**, 1–17.
252 A. Zambon, G. Malavasi, A. Pallini, F. Fraulini and G. Lusvardi, *ACS Biomater. Sci. Eng.*, 2021, **7**, 4388–4401.
253 S. Cui, C. Boussard-plédel, L. Calvez, F. Rojas, K. Chen, H. Ning, M. J. Reece, T. Guizouarn and B. Bureau, *Adv. Appl. Ceram.*, 2015, **114**, 42–47.
254 Y. Zhang, M. Hu, W. Zhang and X. Zhang, *J. Colloid Interface Sci.*, 2022, **610**, 719–730.
255 S. Bano, M. Akhtar, M. Yasir, M. S. Maqbool, A. Niaz, A. Wadood and M. A. U. Rehman, *Gels*, 2021, **7**, 1–15.
256 P. Naruphontjirakul, P. Kanchanadumkerng and P. Ruenraroengsak, *Sci. Rep.*, 2023, **13**, 1–15.
257 M. B. Taye, H. S. Ningsih and S.-J. Shih, *Appl. Sci.*, 2023, **13**, 1–22.
258 K. Schuhladen, X. Wang, L. Hupa and A. R. Boccaccini, *J. Non-Cryst. Solids*, 2018, **502**, 22–34.
259 M. Miola, E. Piatti, P. Sartori and E. Verné, *J. Non-Cryst. Solids*, 2023, **622**, 1–8.
260 S. S. Seyedmomeni, M. Naeimi, M. Raz, J. A. Mohandesi, F. Moztarzadeh, F. Baghbani and M. Tahriri, *Silicon*, 2018, **10**, 197–203.

Open Access Article. Published on 06 Eost 2024. Downloaded on 2026-06-06 12:45:47.
This article is licensed under a Creative Commons Attribution 3.0 Unported Licence.

261 F. N. S. Raja, T. Worthington, L. P. L. De Souza, S. B. Hanaei and R. A. Martin, *ACS Biomater. Sci. Eng.*, 2022, **8**, 1193–1199.
262 Y. Li, V. Ramesh, F. Bider, N. Bradshaw, C. Rehbock, A. R. Boccaccini and S. Barcikowski, *J. Biomed. Mater. Res., Part A*, 2022, **110**, 1537–1550.
263 A. Anand, S. Sengupta, H. Kaňková, A. Švančárková, A. M. Beltrán, D. Galusek, A. R. Boccaccini and D. Galusková, *Gels*, 2022, **8**, 1–19.
264 J. Bejarano, P. Caviedes and H. Palza, *Biomed. Mater.*, 2015, **10**, 1–13.
265 P. K. Khan, A. Mahato, B. Kundu, S. K. Nandi, P. Mukherjee, S. Datta, S. Sarkar, J. Mukherjee, S. Nath, V. K. Balla and C. Mandal, *Sci. Rep.*, 2016, **6**, 1–18.
266 S. Kapoor, A. Goel, A. Tilocca, V. Dhuna, G. Bhatia, K. Dhuna and J. M. F. Ferreira, *Acta Biomater.*, 2014, **10**, 3264–3278.
267 M. N. Vinayak, S. Jana, P. Datta, H. Das, B. Chakraborty, P. Mukherjee, S. Mondal, B. Kundu and S. K. Nandi, *J. Drug Delivery Sci. Technol.*, 2023, **81**, 1–14.
268 S. A. Batool, K. Ahmad, M. Irfan and M. A. Ur Rehman, *J. Funct. Biomater.*, 2022, **13**, 1–24.
269 Y. Zhu, Y. Ouyang, Y. Chang, C. Luo, J. Xu, C. Zhang and W. Huang, *Mol. Med. Rep.*, 2013, **7**, 1129–1136.
270 C. Heras, J. Jiménez-Holguín, A. L. Doadrio, M. Vallet-Regí, S. Sánchez-Salcedo and A. J. Salinas, *Acta Biomater.*, 2020, **114**, 395–406.
271 S. Chitra, P. Bargavi, M. Balasubramaniam, R. R. Chandran and S. Balakumar, *Mater. Sci. Eng., C*, 2020, **109**, 1–14.
272 M. M. Farag and Z. M. Al-Rashidy, *J. Sol-Gel Sci. Technol.*, 2023, **105**, 430–442.
273 S. Huang, X. Kang, Z. Cheng, P. Ma, Y. Jia and J. Lin, *J. Colloid Interface Sci.*, 2012, **387**, 285–291.
274 H. Hu, Y. Tang, L. Pang, C. Lin, W. Huang, D. Wang and W. Jia, *ACS Appl. Mater. Interfaces*, 2018, **10**, 22939–22950.
275 H. Wang, S. Zhao, W. Xiao, J. Xue, Y. Shen, J. Zhou, W. Huang, M. N. Rahaman, C. Zhang and D. Wang, *Mater. Sci. Eng., C*, 2016, **58**, 194–203.
276 O. Access, W. C. Lepry, S. Smith, L. Liverani, A. R. Boccaccini and S. N. Nazhat, *Biomed. Glas.*, 2016, **2**, 88–98.
277 S. Prasad S., S. Datta, T. Adarsh, P. Diwan, K. Annapurna, B. Kundu and K. Biswas, *J. Non-Cryst. Solids*, 2018, **498**, 204–215.
278 M. Shi, Z. Chen, S. Farnaghi, T. Friis, X. Mao, Y. Xiao and C. Wu, *Acta Biomater.*, 2016, **30**, 334–344.
279 A. Tilocca and A. N. Cormack, *J. Phys. Chem. B*, 2007, **111**, 14256–14264.
280 Y. ni Tan, W. juan Chen, W. Wei, Q. li Huang and X. He, *Trans. Nonferrous Met. Soc. China*, 2021, **31**, 521–532.
281 N. Sarin, K. J. Singh, D. Singh, S. Arora, A. P. Singh and H. Mahajan, *Mater. Chem. Phys.*, 2020, **253**, 1–14.
282 X. Wang, Y. Wang, L. Li, Z. Gu, H. Xie and X. Yu, *Ceram. Int.*, 2014, **40**, 6999–7005.
283 R. K. Singh and A. Srinivasan, *J. Magn. Magn. Mater.*, 2011, **323**, 330–333.
284 S. Kargozar, F. Kermani, S. M. Beidokhti, S. Hamzehlou, E. Verné, S. Ferraris and F. Baino, *Materials*, 2019, **12**, 1–18.
285 J. H. Lopes, E. M. B. Fonseca, I. O. Mazali, A. Magalhães, R. Landers and C. A. Bertran, *Mater. Sci. Eng., C*, 2017, **72**, 86–97.
286 S. Ferraris, C. Vitale-Brovarone, O. Bretcanu, C. Cassinelli and E. Vernè, *Appl. Surf. Sci.*, 2013, **271**, 412–420.
287 G. J. Owens, R. K. Singh, F. Foroutan, M. Alqaysi, C.-M. Han, C. Mahapatra, H.-W. Kim and J. C. Knowles, *Prog. Mater. Sci.*, 2016, **77**, 1–79.
288 A. Ansari and P. I. Imoukhuede, *Nano Res.*, 2018, **11**, 5107–5129.
289 L. Azizi, P. Turkki, N. Huynh, J. M. Massera and V. P. Hytönen, *ACS Omega*, 2021, **6**, 22635–22642.
290 E. Verné, S. Ferraris, C. Vitale-Brovarone, S. Spriano, C. L. Bianchi, A. Naldoni, M. Morra and C. Cassinelli, *Acta Biomater.*, 2010, **6**, 229–240.
291 A. Simchi, E. Tamjid, F. Pishbin and A. R. Boccaccini, *Nanomedicine*, 2011, **7**, 22–39.
292 Q. Z. Chen, K. Rezwan, D. Armitage, S. N. Nazhat and A. R. Boccaccini, *J. Mater. Sci. Mater. Med.*, 2006, **17**, 979–987.
293 A. El-Fiqi, J. H. Lee, E. J. Lee and H. W. Kim, *Acta Biomater.*, 2013, **9**, 9508–9521.
294 S. Ferraris, A. Nommeots-Nomm, S. Spriano, E. Vernè and J. Massera, *Appl. Surf. Sci.*, 2019, **475**, 43–55.
295 C. Gruian, A. Vulpoi, E. Vanea, B. Oprea, H. J. Steinhoff and S. Simon, *J. Phys. Chem. B*, 2013, **117**, 16558–16564.
296 E. Vernè, S. Ferraris, C. Cassinelli and A. R. Boccaccini, *Surf. Coat. Technol.*, 2015, **264**, 132–139.
297 M. Ozmen, K. Can, I. Akin, G. Arslan, A. Tor, Y. Cengeloglu and M. Ersoz, *J. Hazard. Mater.*, 2009, **171**, 594–600.
298 K. Schickle, K. Zurlinden, C. Bergmann, M. Lindner, A. Kirsten, M. Laub, R. Telle, H. Jennissen and H. Fischer, *J. Mater. Sci. Mater. Med.*, 2011, **22**, 763–771.
299 J. Hum and A. R. Boccaccini, *Int. J. Mol. Sci.*, 2018, **19**, 1–21.
300 E. Verné, C. Vitale-Brovarone, E. Bui, C. L. Bianchi and A. R. Boccaccini, *J. Biomed. Mater. Res., Part A*, 2009, **90**, 981–992.
301 G. Lusvardi, G. Malavasi, L. Menabue and S. Shruti, *Mater. Sci. Eng., C*, 2013, **33**, 3190–3196.
302 Y. Zhang, J. Luan, S. Jiang, X. Zhou and M. Li, *Composites, Part B*, 2019, **172**, 397–405.
303 V. Aina, T. Marchis, E. Laurenti, E. Diana, G. Lusvardi, G. Malavasi, L. Menabue, G. Cerrato and C. Morterra, *Langmuir*, 2010, **26**, 18600–18605.
304 E. Verné, M. Miola, C. Vitale-Brovarone, M. Cannas, S. Gatti, G. Fucale, G. Maina, A. Massé and S. Di Nunzio, *J. Mater. Sci. Mater. Med.*, 2009, **20**, 733–740.
305 T. Meincke, V. M. Pacheco, D. Hoffmann, A. R. Boccaccini and R. N. K. Taylor, *J. Mater. Sci.*, 2017, **52**, 9082–9090.

 This journal is © The Royal Society of Chemistry 2024

Open Access Article. Published on 06 Eost 2024. Downloaded on 2026-06-06 12:45:47.
This article is licensed under a Creative Commons Attribution 3.0 Unported Licence.

306 A. W. Wren, A. Coughlan, P. Hassanzadeh and M. R. Towler, *J. Mater. Sci. Mater. Med.*, 2012, **23**, 1331–1341.
307 E. Verné, S. Ferraris, M. Miola, G. Fucale, G. Maina, G. Martinasso, R. A. Canuto, S. Di Nunzio and C. Vitale-Brovarone, *Adv. Appl. Ceram.*, 2008, **107**, 234–244.
308 M. Cazzola, I. Corazzari, E. Prenesti, E. Bertone, E. Verné and S. Ferraris, *Appl. Surf. Sci.*, 2016, **367**, 237–248.
309 X. Zhang, S. Ferraris, E. Prenesti and E. Verné, *Appl. Surf. Sci.*, 2013, **287**, 329–340.
310 S. Ferraris, X. Zhang, E. Prenesti, I. Corazzari, F. Turci, M. Tomatis and E. Vernè, *J. Non-Cryst. Solids*, 2016, **432**, 167–175.
311 M. Cazzola, S. Ferraris, F. Boschetto, A. Rondinella, E. Marin, W. Zhu, G. Pezzotti, E. Vernè and S. Spriano, *Int. J. Mol. Sci.*, 2018, **19**, 1–14.
312 A. S. Abdelgeliel, S. Ferraris, A. Cochis, S. Vitalini, M. Iriti, H. Mohammed, A. Kumar, M. Cazzola, W. M. Salem, E. Verné, S. Spriano and L. Rimondini, *Coatings*, 2019, **9**, 1–15.
313 X. Zhang, S. Ferraris, E. Prenesti and E. Verné, *Appl. Surf. Sci.*, 2013, **287**, 341–348.
314 S. Ferraris, M. Miola, A. Cochis, B. Azzimonti, L. Rimondini, E. Prenesti and E. Verné, *Appl. Surf. Sci.*, 2017, **396**, 461–470.
315 E. Vernè, S. Ferraris, C. Vitale-Brovarone, A. Cochis and L. Rimondini, *Appl. Surf. Sci.*, 2014, **313**, 372–381.
316 K. Zheng, M. Kapp and A. R. Boccaccini, *Appl. Mater. Today*, 2019, **15**, 350–371.
317 N. Lin, P. Berton, C. Moraes, R. D. Rogers and N. Tufenkji, *Adv. Colloid Interface Sci.*, 2018, **252**, 55–68.
318 K. S. Parikh, S. S. Rao, H. M. Ansari, L. B. Zimmerman, L. J. Lee, S. A. Akbar and J. O. Winter, *Mater. Sci. Eng., C*, 2012, **32**, 2469–2475.
319 J. Frostevarg, R. Olsson, J. Powell, A. Palmquist and R. Brånemark, *Appl. Surf. Sci.*, 2019, **485**, 158–169.
320 B. Bhushan, *Philos. Trans. R. Soc., A*, 2009, **367**, 1445–1486.
321 A. J. Scardino and R. de Nys, *Biofouling*, 2011, **27**, 73–86.
322 A. Malshe, K. Rajurkar, A. Samant, H. N. Hansen, S. Bapat and W. Jiang, *CIRP Ann. - Manuf. Technol.*, 2013, **62**, 607–628.
323 A. Jaggessar, H. Shahali, A. Mathew and P. K. D. V. Yarlagadda, *J. Nanobiotechnol.*, 2017, **15**, 1–20.
324 T. Ishizaki, N. Saito and O. Takai, *Langmuir*, 2010, **26**, 8147–8154.
325 R. A. Gittens, R. Olivares-Navarrete, A. Cheng, D. M. Anderson, T. McLachlan, I. Stephan, J. Geis-Gerstorfer, K. H. Sandhage, A. G. Fedorov, F. Rupp, B. D. Boyan, R. Tannenbaum and Z. Schwartz, *Acta Biomater.*, 2013, **9**, 6268–6277.
326 K. Modaresifar, S. Azizian, M. Ganjian, L. E. Fratila-Apachitei and A. A. Zadpoor, *Acta Biomater.*, 2019, **83**, 29–36.
327 A. Elbourne, J. Chapman, A. Gelmi, D. Cozzolino, R. J. Crawford and V. K. Truong, *J. Colloid Interface Sci.*, 2019, **546**, 192–210.
328 E. Santos, R. M. Hernández, J. L. Pedraz and G. Orive, *Trends Biotechnol.*, 2012, **30**, 331–341.
329 A. Carvalho, L. Cangueiro, V. Oliveira, R. Vilar, M. H. Fernandes and F. J. Monteiro, *Appl. Surf. Sci.*, 2018, **435**, 1237–1245.
330 S. Dobbenga, L. E. Fratila-Apachitei and A. A. Zadpoor, *Acta Biomater.*, 2016, **46**, 3–14.
331 L. E. McNamara, R. Burchmore, M. O. Riehle, P. Herzyk, M. J. P. Biggs, C. D. W. Wilkinson, A. S. G. Curtis and M. J. Dalby, *Biomaterials*, 2012, **33**, 2835–2847.
332 K. Anselme, P. Davidson, A. M. Popa, M. Giazzon, M. Liley and L. Ploux, *Acta Biomater.*, 2010, **6**, 3824–3846.
333 J. Lee, A. A. Abdeen, X. Tang, T. A. Saif and K. A. Kilian, *Biomaterials*, 2015, **69**, 174–183.
334 P. Slepicka, N. S. Kasalkova, J. Siegel, Z. Kolska, L. Bacakova and V. Svorcik, *Biotechnol. Adv.*, 2015, **33**, 1120–1129.
335 L. Bacakova, E. Filova, M. Parizek, T. Ruml and V. Svorcik, *Biotechnol. Adv.*, 2011, **29**, 739–767.
336 T. J. Kowal, R. Golovchak, T. Chokshi, J. Harms, U. Thamma, H. Jain and M. M. Falk, *J. Mater. Sci. Mater. Med.*, 2017, **28**, 1–16.
337 S. Ferraris, F. Truffa Giachet, M. Miola, E. Bertone, A. Varesano, C. Vineis, A. Cochis, R. Sorrentino, L. Rimondini and S. Spriano, *Mater. Sci. Eng., C*, 2017, **76**, 1–12.
338 B. Pföss, M. Höner, M. Wirth, A. Bührig-Polaczek, H. Fischer and R. Conradt, in *Biomedical Glasses*, 2016, vol. 2, pp. 63–71.
339 D. Karazisis, S. Petronis, H. Agheli, L. Emanuelsson, B. Norlindh, A. Johansson, L. Rasmusson, P. Thomsen and O. Omar, *Acta Biomater.*, 2017, **53**, 559–571.
340 A. Itälä, J. Koort, H. O. Ylänen, M. Hupa and H. T. Aro, *J. Biomed. Mater. Res., Part A*, 2003, **67**, 496–503.
341 G. Wang, Z. Lu, X. Liu, X. Zhou, C. Ding and H. Zreiqat, *J. R. Soc., Interface*, 2011, **8**, 1192–1203.
342 S. Shaikh, S. Kedia, A. K. Singh, K. Sharma and S. Sinha, *J. Laser Appl.*, 2017, **29**, 1–20.
343 L. Qin, H. Wu, J. Guo, X. Feng, G. Dong, J. Shao, Q. Zeng, Y. Zhang and Y. Qin, *Colloids Surf., B*, 2018, **161**, 628–635.
344 S. Shaikh, D. Singh, M. Subramanian, S. Kedia, A. K. Singh, K. Singh, N. Gupta and S. Sinha, *J. Non-Cryst. Solids*, 2018, **482**, 63–72.
345 L. C. Hsu, J. Fang, D. A. Borca-Tasciuc, R. W. Worobo and C. I. Moraru, *Appl. Environ. Microbiol.*, 2013, **79**, 2703–2712.
346 D. Perera-Costa, J. M. Bruque, M. L. González-Martín, A. C. Gómez-García and V. Vadillo-Rodríguez, *Langmuir*, 2014, **30**, 4633–4641.
347 K. Yang, J. Shi, L. Wang, Y. Chen, C. Liang, L. Yang and L. N. Wang, *J. Mater. Sci. Technol.*, 2022, **99**, 82–100.
348 S. Papa, A. Abou Khalil, H. Hamzeh-Cognasse, M. Thomas, M. Maalouf, Y. Di Maio, X. Sedao, A. Guignandon and V. Dumas, *Appl. Surf. Sci.*, 2022, **606**, 1–9.
349 T. Nishitani, K. Masuda, S. Mimura, T. Hirokawa, H. Ishiguro, M. Kumagai and T. Ito, *AMB Express*, 2022, **12**, 1–10.

Open Access Article. Published on 06 Eost 2024. Downloaded on 2026-06-06 12:45:47.
This article is licensed under a Creative Commons Attribution 3.0 Unported Licence.

350 Z. Cao, L. Mi, J. Mendiola, J. R. Ella-Menye, L. Zhang, H. Xue and S. Jiang, *Angew. Chem., Int. Ed.*, 2012, **51**, 2602–2605.
351 I. Izquierdo-Barba, J. M. García-Martín, R. Álvarez, A. Palmero, J. Esteban, C. Pérez-Jorge, D. Arcos and M. Vallet-Regí, *Acta Biomater.*, 2015, **15**, 20–28.
352 P. Premnath, A. Tavangar, B. Tan and K. Venkatakrishnan, *Exp. Cell Res.*, 2015, **337**, 44–52.
353 Y. Xiao, L. Song, X. Liu, Y. Huang, T. Huang, Y. Wu, J. Chen and F. Wu, *Appl. Surf. Sci.*, 2011, **257**, 1898–1905.
354 H. P. Lin and B. R. Li, in *Nanobiomaterials: Nanostructured Materials for Biomedical Applications*, 2018, pp. 319–338.
355 G. M. Luz, L. Boesel, A. Del Campo and J. F. Mano, *Langmuir*, 2012, **28**, 6970–6977.
356 B. Lei, X. Chen, Y. Wang, N. Zhao, C. Du and L. Fang, *J. Biomed. Mater. Res., Part A*, 2010, **94**, 1091–1099.
357 G. E. Jellison, T. Aytug, A. R. Lupini, M. P. Paranthaman and P. C. Joshi, *Thin Solid Films*, 2016, **617**, 38–43.
358 H. Jain and H. M. M. Moawad, Nano/macroporous bioactive glasses made by melt-quench methods, USOO8389018B2, 2008.
359 H. M. M. Moawad and H. Jain, *J. Am. Ceram. Soc.*, 2007, **90**, 1934–1936.
360 A. Kumar, K. Kashyap, K. W. Liao, M. T. Hou and J. A. Yeh, in *9th IEEE International Conference on Nano/Micro Engineered and Molecular Systems, IEEE-NEMS 2014*, IEEE, 2014, pp. 113–116.
361 D. Tulli, S. D. Hart, P. Mazumder, A. Carrilero, L. Tian, K. W. Koch, R. Yongsunthon, G. A. Piech and V. Pruneri, *ACS Appl. Mater. Interfaces*, 2014, **6**, 11198–11203.
362 E. Yu, S. C. Kim, H. J. Lee, K. H. Oh and M. W. Moon, *Sci. Rep.*, 2015, **5**, 1–6.
363 T. Sato, K. Nagato, J. Choi, T. Hamaguchi and M. Nakao, in *Proceedings of the IEEE Conference on Nanotechnology*, IEEE, 2011, pp. 1–4.
364 E. Marin, S. Horiguchi, M. Zanocco, F. Boschetto, A. Rondinella, W. Zhu, R. M. Bock, B. J. McEntire, T. Adachi, B. S. Bal and G. Pezzotti, *Heliyon*, 2018, **4**, 1–24.
365 L. K. Verma, M. Sakhuja, J. Son, A. J. Danner, H. Yang, H. C. Zeng and C. S. Bhatia, *Renewable Energy*, 2011, **36**, 2489–2493.
366 Y. Hirai, K. Kanakugi, T. Yamaguchi, K. Yao, S. Kitagawa and Y. Tanaka, in *Microelectronic Engineering*, 2003, vol. 67–68, pp. 237–244.
367 D. Meng, M. Erol and A. R. Boccaccini, *Adv. Eng. Mater.*, 2010, **12**, B467–B487.
368 A. Itl, E. G. Nordstrm, H. Ylnen, H. T. Aro and M. Hupa, *J. Biomed. Mater. Res.*, 2001, **56**, 282–288.
369 F. Baino, in *Biomedical, Therapeutic and Clinical Applications of Bioactive Glasses*, Elsevier Ltd, 2018, pp. 443–466.
370 J. Barberi, F. Baino, E. Fiume, G. Orlygsson, A. Nommeots-Nomm, J. Massera and E. Verné, *Materials*, 2019, **12**, 1–16.
371 G. Wei and P. X. Ma, *Adv. Funct. Mater.*, 2008, **18**, 3568–3582.
372 H. Zhou and J. Lee, *Acta Biomater.*, 2011, **7**, 2769–2781.
373 F. Bonino, A. Damin, V. Aina, M. Miola, E. Verné, O. Bretcanu, S. Bordiga, A. Zecchina and C. Morterra, *J. Raman Spectrosc.*, 2008, **39**, 260–264.
374 Y. Takeuchi, *J. Phys. Ther. Sci.*, 2017, **29**, 112–114.
375 G. M. Luz and J. F. Mano, *J. Nanopart. Res.*, 2013, **15**, 1–11.
376 M. Erol-Taygun, K. Zheng and A. R. Boccaccini, *Int. J. Appl. Glass Sci.*, 2013, **4**, 136–148.
377 S. Ali, I. Farooq and K. Iqbal, *Saudi Dent. J.*, 2014, **26**, 1–5.
378 J. C. Mitchell, L. Musanje and J. L. Ferracane, *Dent. Mater.*, 2011, **27**, 386–393.
379 B. Gupta, J. B. Papke, A. Mohammadkhah, D. E. Day and A. B. Harkins, *Ann. Biomed. Eng.*, 2016, **44**, 3468–3477.
380 M. Bigoni, M. Turati, N. Zanchi, A. S. Lombardo, J. Graci, R. J. Omeljaniuk, G. Zatti and D. Gaddi, *Eur. Rev. Med. Pharmacol. Sci.*, 2019, **23**, 240–251.
381 D. S. Brauer and L. Hupa, *C. R. Geosci.*, 2022, **354**, 185–197.
382 E. Fiume, G. Serino, C. Bignardi, E. Verné and F. Baino, *Molecules*, 2019, **24**, 1–13.
383 P. Gentile, V. Chiono, F. Boccafoschi, F. Baino, C. Vitale-Brovarone, E. Vernè, N. Barbani and G. Ciardelli, *J. Biomater. Sci., Polym. Ed.*, 2010, **21**, 1207–1226.
384 Q. Yu, Z. Wu and H. Chen, *Acta Biomater.*, 2015, **16**, 1–13.
385 M. Ganjian, K. Modaresifar, M. R. O. Ligeon, L. B. Kunkels, N. Tümer, L. Angeloni, C. W. Hagen, L. G. Otten, P. L. Hagedoorn, I. Apachitei, L. E. Fratila-Apachitei and A. A. Zadpoor, *Adv. Mater. Interfaces*, 2019, **6**, 1–10.
386 S. H. T. Nguyen, H. K. Webb, J. Hasan, M. J. Tobin, R. J. Crawford and E. P. Ivanova, *Colloids Surf., B*, 2013, **106**, 126–134.
387 C. C. Ude, C. J. Esdaille, K. S. Ogueri, H. M. Kan, S. J. Laurencin, L. S. Nair and C. T. Laurencin, *Regener. Eng. Transl. Med.*, 2021, **7**, 247–261.
388 J. Toledano-Serrabona, O. Camps-Font, D. P. de Moraes, M. Corte-Rodríguez, M. Montes-Bayón, E. Valmaseda-Castellón, C. Gay-Escoda and M. Á. Sánchez-Garcés, *J. Periodontol.*, 2023, **94**, 119–129.
389 M. Miola, L. Cordero-Arias, G. Ferlenda, A. Cochis, S. Virtanen, L. Rimondini, E. Verné and A. R. Boccaccini, *Surf. Coat. Technol.*, 2021, **418**, 1–11.
390 S. Ferraris, S. Spriano, M. Miola, E. Bertone, V. Allizond, A. M. Cuffini and G. Banche, *Surf. Coat. Technol.*, 2018, **344**, 177–189.
391 K. Huang, S. Cai, G. Xu, X. Ye, Y. Dou, M. Ren and X. Wanga, *J. Alloys Compd.*, 2013, **580**, 290–297.
392 S. Rigo, C. Cai, G. Gunkel-Grabole, L. Maurizi, X. Zhang, J. Xu and C. G. Palivan, *Adv. Sci.*, 2018, **5**, 1–13.
393 M. Montazerian, E. D. Zanotto and J. C. Mauro, *Int. Mater. Rev.*, 2020, **65**, 297–321.
394 E. M. Fayed, A. S. Elmesalamy, M. Sobih and Y. Elshaer, *Int. J. Adv. Des. Manuf. Technol.*, 2018, **94**, 2333–2341.
395 S. Simorgh, N. Alasvand, M. Khodadadi, F. Ghobadi, M. M. Kebria, P. B. Milan, S. Kargozar, F. Baino, A. Mobasheri and M. Mozafari, *Methods*, 2022, 75–91.

 This journal is © The Royal Society of Chemistry 2024

Open Access Article. Published on 06 Eost 2024. Downloaded on 2026-06-06 12:45:47.
This article is licensed under a Creative Commons Attribution 3.0 Unported Licence.

396 V. A. Bobrin, K. Lee, J. Zhang, N. Corrigan and C. Boyer, *Adv. Mater.*, 2022, **34**, 1–8.
397 W. Y. Zhou, S. H. Lee, M. Wang, W. L. Cheung and W. Y. Ip, *J. Mater. Sci. Mater. Med.*, 2008, **19**, 2535–2540.
398 A. Zocca, P. Colombo, C. M. Gomes and J. Günster, *J. Am. Ceram. Soc.*, 2015, **98**, 1983–2001.
399 R. Bento, A. Gaddam, P. Oskoei, H. Oliveira and J. M. F. Ferreira, *Materials*, 2021, **14**, 1–16.
400 D. U. Tulyaganov, E. Fiume, A. Akbarov, N. Ziyadullaeva, S. Murtazaev, A. Rahdar, J. Massera, E. Verné and F. Baino, *J. Funct. Biomater.*, 2022, **13**, 1–14.
401 C. Gayer, J. Ritter, M. Bullemer, S. Grom, L. Jauer, W. Meiners, A. Pfister, F. Reinauer, M. Vučak, K. Wissenbach, H. Fischer, R. Poprawe and J. H. Schleifenbaum, *Mater. Sci. Eng., C*, 2019, **101**, 660–673.
402 D. Karl, B. Jastram, P. H. Kamm, H. Schwandt, A. Gurlo and F. Schmidt, *Powder Technol.*, 2019, **354**, 289–300.
403 A. Fathi, F. Kermani, A. Behnamghader, S. Banijamali, M. Mozafari, F. Baino and S. Kargozar, *Biomed. Glas.*, 2021, **6**, 57–69.
404 J. Han, J. Wu, X. Xiang, L. Xie, R. Chen, L. Li, K. Ma, Q. Sun, R. Yang, T. Huang, L. Tong, L. Zhu, H. Wang, C. Wen, Y. Zhao and J. Wang, *Mater. Des.*, 2023, **225**, 111543.
405 S. Ahmed, R. Hussain, A. Khan, S. A. Batool, A. Mughal, M. H. Nawaz, M. Irfan, A. Wadood, E. Avcu and M. A. U. Rehman, *ACS Appl. Bio Mater.*, 2023, **6**, 5052–5066.
406 B. Holmes, K. Bulusu, M. Plesniak and L. Zhang, *Adv. Mater. - TechConnect Briefs 2016*, 2016, **3**, 39–42.
407 A. B. R. Touré, E. Mele and J. K. Christie, *Nanomaterials*, 2020, **10**, 1–16.
408 F. Baino and E. Fiume, *Materials*, 2020, **13**, 1–19.
409 W. C. Vrouwenvelder, C. G. Groot and K. de Groot, *Biomaterials*, 1994, **15**, 97–106.
410 Q. Dai, Q. Li, H. Gao, L. Yao, Z. Lin, D. Li, S. Zhu, C. Liu, Z. Yang, W. Gang, D. Chen, X. Chen and X. Cao, *Biomater. Sci.*, 2021, **9**, 5519–5532.
411 S. N. Somayaji, Y. M. Huet, H. E. Gruber and M. C. Hudson, *J. Biomed. Mater. Res., Part A*, 2010, **95 A**, 574–579.